

Renormalization Group Studies of Quantum Theories of Gravity and Matter

Dissertation

zur Erlangung des akademischen Grades
doctor rerum naturalium (Dr. rer. nat.)



**FRIEDRICH-SCHILLER-
UNIVERSITÄT
JENA**

vorgelegt dem Rat der Physikalisch-Astronomischen Fakultät der
Friedrich-Schiller-Universität Jena

von M. Sc. Abdol Sabor Salek
geboren am 01.01.1994 in Kabul, Afghanistan

Gutachter:innen

1. Prof. Dr. Holger Gies (Friedrich-Schiller-Universität Jena)
2. Prof. Dr. Astrid Eichhorn (University of Southern Denmark)
3. Prof. Dr. Frank Saueressig (Radboud University Nijmegen)

Datum der Disputation: 17.01.2023

In dedication to the stranger who struggles for a better future. May the dead rest in peace and never be forgotten, may the survivors find a future in which they prosper, and may the spectators be reminded of the inconvenient reality that inaction is a form of action.

Abstract

In this thesis, we study quantum theories of gravity and matter in the Renormalization Group approach.

We observe light fermions in our universe which feature a remnant of chiral symmetry. While chiral symmetry appears to remain intact along the Renormalization Group flow of asymptotically safe approaches to quantum gravity, these computations are performed on a flat background. Mean field studies performed on negatively curved backgrounds however indicate chiral symmetry breaking in the form of gravitational catalysis. The study of the mean field RG flow on negatively curved spacetime leads to an upper bound for the ratio of curvature of local patches of spacetime to the RG scale. If this ratio does not exceed said bound, gravitational catalysis does not trigger chiral symmetry breaking. We extend these calculations to finite temperature and study how thermal fluctuations affect this bound from gravitational catalysis. Applying this thermal extension of the curvature bound to the asymptotic safety scenario of quantum gravity, it translates into an upper bound of numbers of fermion species allowed in our universe for asymptotically safe quantum gravity to be compatible with the existence of light fermions.

Most approaches towards a UV complete quantum theory of gravity start with General Relativity as its classical theory. Einstein's formulation of gravity can be summarized as pseudo-Riemannian geometry on a manifold equipped with a metric and a connection. While this connection is restricted to the Levi-Cevita connection in Einstein gravity (which is torsionless and compatible with the metric) and therefore is fully determined by the metric, there is a priori no fundamental reason to not use a general connection. This formalism, in which the metric and the general connection are treated as independent degrees of freedom, is referred to as Hilbert-Palatini gravity. In this thesis, we compute the most general solution to the connection for the Einstein-Hilbert-Palatini action and use it in an on-shell reduction scheme to compute the RG flow for the subsequent order in the truncation. We find a UV-attractive fixed point similar to the Reuter fixed point in quantum Einstein gravity that is connected to the Gaussian fixed-point in the IR through an RG trajectory. Our scenario therefore provides evidence for the existence of a corresponding UV complete quantum theory of Hilbert-Palatini gravity that has a long-range limit compatible with classical Einstein gravity.

Zusammenfassung

In dieser Promotionsschrift untersuchen wir Quantentheorien der Gravitation und Materie im Renormierungsgruppenansatz.

Wir beobachten leichte Fermionen in unserem Universum, die ein Überbleibsel der chiralen Symmetrie darstellen. Die chirale Symmetrie scheint zwar im Renormierungsgruppenfluss von asymptotisch sicheren Herangehensweisen der Quantengravitation erhalten zu bleiben, jedoch werden diese Berechnungen auf einem flachen Hintergrund durchgeführt. Studien im Mean Field Formalismus auf negativ gekrümmten Hintergründen deuten jedoch eine Brechung der chiralen Symmetrie in Form der Gravitationskatalyse an. Die Untersuchung des Mean Field Renormierungsgruppenflusses auf einer negativ gekrümmten Raumzeit führt zu einer oberen Schranke für das Verhältnis der Krümmung lokaler Raumzeitflecken zur Renormierungsgruppenskala. Falls dieses Verhältnis die besagte Schranke nicht überschreitet, wird die chirale Symmetriebrechung durch die Gravitationskatalyse nicht ausgelöst. Wir erweitern diese Berechnungen auf endliche Temperaturen und untersuchen, wie sich thermische Fluktuationen auf diese Schranke der Gravitationskatalyse auswirken. Wenn wir diese thermische Erweiterung der Krümmungsschranke auf die asymptotisch sichere Herangehensweise der Quantengravitation anwenden, lässt sie sich in eine obere Schranke der Anzahl der Fermionenarten übersetzen, die in unserem Universum erlaubt sind, damit asymptotisch sichere Quantengravitation kompatibel mit der Existenz leichter Fermionen ist.

Die meisten Herangehensweisen an eine UV-vervollständigte Quantentheorie der Gravitation starten mit der Allgemeinen Relativitätstheorie als klassische Theorie. Einsteins Formulierung der Gravitation kann als eine pseudo-riemannsche Geometrie auf einer Mannigfaltigkeit aufgefasst werden, die mit einer Metrik und einem Zusammenhang ausgestattet ist. Zwar ist dieser Zusammenhang in der einsteinschen Formulierung der Gravitation auf den Levi-Cevita-Zusammenhang eingeschränkt und folglich durch die Metrik vollständig bestimmt, gibt es jedoch a priori keinen fundamentalen Grund, keinen allgemeinen Zusammenhang zu wählen. Dieser Formalismus, in dem die Metrik und der Zusammenhang als unabhängige Freiheitsgrade behandelt werden, wird als Hilbert-Palatini-Gravitation bezeichnet. In dieser Promotionsschrift berechnen wir die allgemeinste Lösung des Zusammenhangs für die Einstein-Hilbert-Palatini-Wirkung und nutzen sie in einem Bewegungsgleichungsreduktionsschema, um den Renormierungsgruppenfluss der nächsthöheren Ordnung in der Trunkierung zu berechnen. Wir finden einen UV-attraktiven Fixpunkt, der dem Reuterfixpunkt der einsteinschen Gravitation ähnelt und mit dem gaußschen Fixpunkt im IR durch eine Renormierungsgruppentrajektorie verbunden ist. Unser Szenario liefert daher einen Nachweis für die Existenz einer entsprechenden UV-vervollständigten Quantentheorie der Hilbert-Palatini-Gravitation, die einen langreichweitigen Limes besitzt, welcher mit der klassischen, einsteinschen Gravitation kompatibel ist.

Contents

1. Introduction	3
2. Non-perturbative Quantum Field Theory	9
2.1. Functional Integral Formulation	9
2.2. Thermal Quantum Field Theory	10
2.3. Treatment of Gauge Fields	12
2.4. Generating Functionals	14
2.5. Wilsonian Interpretation of Renormalization	17
2.6. Functional Renormalization Group	19
2.7. Truncation Ansatz	23
2.8. Asymptotic Safety	26
3. From Classical to Quantum Gravity	31
3.1. General Relativity	31
3.2. Fermions in Curved Spacetime	33
3.3. Heat Kernel Techniques	34
3.4. Gravity as a Gauge Theory	37
3.5. Asymptotically Safe Quantum Gravity	40
4. Symmetries and Phase Transitions	45
4.1. Spontaneous Symmetry Breaking	45
4.2. $\mathcal{O}(N)$ Scalar Model	48
4.3. Chiral Symmetry and Fermion Mass Generation	53
5. Gravitational Catalysis in Thermal Backgrounds	59
5.1. Chiral Channel and Effective Potential	61
5.2. Heat Kernels at Finite Temperature	63
5.3. Curvature Bounds	65
5.3.1. Curvature Bounds at Zero Temperature	65
5.3.2. Curvature Bounds at Finite Temperature	69
5.4. Asymptotically Safe Gravity: from Curvature Bound to Matter Bound	72

6. Asymptotically Safe Hilbert-Palatini Gravity	79
6.1. Classical Hilbert-Palatini Gravity	80
6.1.1. General Connection on Smooth Manifolds	81
6.1.2. Einstein-Hilbert-Palatini Action	82
6.1.3. Geodesic Trajectory in Hilbert-Palatini Gravity	85
6.2. Quantum Hilbert-Palatini Gravity	87
6.2.1. Renormalization Flow of Hilbert-Palatini Gravity	88
6.2.2. Results	91
7. Conclusions	95
A. Flow Equations for Hilbert-Palatini Gravity	I
Bibliography	VII

1. Introduction

In our current understanding of physics, all phenomena in the universe underlie four fundamental forces: the electromagnetic interaction that we feel when our hands are too close to the TV, the weak interaction that is involved in radioactive decay, the strong interaction that binds the particles in an atomic nucleus together and the gravitational interaction that chains us to the surface of this very Earth. On a macroscopic level, we use field theories to accurately model these interactions, e.g. the electric and magnetic field in the Maxwell equations for electrodynamics, and the metric tensor (which represents spacetime itself as a field) in the Einstein field equations in General Relativity (GR). Since the effects of the weak and the strong interaction are not directly observable in our day-to-day life, a classical field theoretical description of these two interactions was initially not formulated.

As we went to smaller and smaller length scales, new phenomena emerged that could not be explained by classical field theories, like the spontaneous emission in which an electron within an atomic shell moves from an excited state to the ground state and emits a photon. Instead, a quantized version of electrodynamics was formulated, coined Quantum Electrodynamics (QED) and the classical field theory was instead substituted by its Quantum Field Theory (QFT) version to accurately describe the effects of the electromagnetic interaction at smaller length scales with great success [1]. As a result, the effects observable at smaller length scales of the weak and the strong interaction could also be well understood through a description of a Quantum Field Theory with the quantum fields exhibiting a local gauge symmetry (an abelian one for QED and a non-abelian one for the latter two).

In the computation of observables within these theories divergences appeared, that had to be removed by hand through the introduction of counter terms. The idea was that the couplings (like the gauge couplings g for the interactions of the gauge fields) appearing in the Lagrangian of the QFT were not the actually measurable couplings, but instead just some bare couplings that can be split into the real, actually measurable parameters (called renormalized couplings) and a counter term that cancels the appearing divergence [1]. While this method of perturbative renormalization was mathematically successful in removing the divergences, it was initially deeply unsatisfactory on a fundamental physics level, as the physical understanding of this renormalization procedure was not well developed.

This led to the Wilsonian interpretation of renormalization [2], in which the couplings of the theory were a priori not treated as constant-valued couplings but instead as running couplings that could change their values depending on the length scale at which one observes

the corresponding interaction. Using this Renormalization Group (RG) technique, only interactions up to a certain length scale (inversely related to the coarse-graining scale k of the RG) were considered and a cutoff was naturally introduced to the integrals one would have to take to compute observables in the QFT formulation. The introduction of the RG not only got rid of the divergences appearing in QFTs, but its foundation in the Wilsonian approach to renormalization also delivered a satisfactory interpretation that could be verified in experiments, as the couplings indeed seemed to change their values depending on the energy scale (inversely related to the length scale) at which the interaction was considered.

While the formulation of a QFT within perturbative renormalization was successful in quantizing three of the four fundamental interactions, it failed for the case of gravity, rendering the gravitational interaction at the lowest order (Einstein-Hilbert action which classically leads to the Einstein field equations) perturbatively non-renormalizable [3]. As a result, other attempts at quantizing gravity were formulated, most notably String Theory [4] and Loop Quantum Gravity [5].

The physicist Steven Weinberg suggested the idea that while gravity may be perturbatively non-renormalizable, we might find a non-perturbative formulation of gravity in which it would be renormalizable [6]. He coined this scenario *asymptotic safety*.

With the introduction of the Functional Renormalization Group (FRG) a non-perturbative approach to renormalization was formulated and initially applied to the Quark-Meson model (a low energy effective model for QCD, the QFT of the strong interaction) to study the chiral phase transition in QCD [7]. Applying this new formulation to gravity yielded a UV-attractive fixed-point in the RG flow, rendering the theory non-perturbatively renormalizable and therefore asymptotically safe [8]. Finally, a QFT description of gravity was formulated.

Further studies on the Asymptotic Safety (AS) approach to Quantum Gravity (QG) were performed to include higher order gravitational interactions (beyond the Einstein-Hilbert action) to great success [9–11] (though there still are open questions, especially regarding unitarity in Quantum Gravity, see [12–14] for more information).

Since the Asymptotic Safety approach to Quantum Gravity is a QFT formulation, the inclusion of matter degrees of freedom to study its effects on the gravitational sector is a rather straightforward task as we can use the preexisting quantum field theory formulations of matter degrees of freedom and extend them to curved spacetime. Studies on asymptotically safe gravity and matter have shown that the Einstein-Hilbert action exhibits a UV-attractive fixed-point in the presence of matter, even so for the types and numbers of particles that are contained in the Standard Model of particle physics [15].

Additionally, the effects of asymptotically safe quantum gravity on the matter sector of the Standard Model have been studied. An issue of concern that the Standard Model has is that the abelian sector contains a Landau pole in its gauge coupling and it therefore diverges at a certain energy scale. With the inclusion of gravitational interactions, a UV-attractive fixed-point was found, rendering QED in a scenario of quantized gravity asymptotically safe

and therefore UV-complete [16].

The interplay between quantum gravity and matter and its phenomenological applications to our universe are of great interest. One of those cases of an interplay is gravitational catalysis [17]. It is a mechanism that is triggered by negatively curved backgrounds and induces chiral symmetry breaking, which would generate fermionic masses on the order of the curvature scale. If the high energy-regime of gravity was characterized by such an average curvature, we would expect all fermions to have Planck scale mass. Since we do not observe these types of massive fermions in our universe, we have to prevent this scenario of gravitational catalysis emerging in our theories.

Studies of the RG flow of fermionic interactions on a negatively curved background indicate that chiral symmetry is intact if the ratio of the curvature of local patches of spacetime does not exceed a certain bound [18]. Any UV-complete quantum theory of gravity has to obey this curvature bound from gravitational catalysis to be compatible with the existence of light fermions in our universe. This bound can henceforth be used as a litmus test to constrain various approaches to quantum gravity.

In this thesis, we are interested in how thermal fluctuations might affect this bound and study the effects of gravitational catalysis on a manifold that is curved in its spatial components and compactified in the temporal direction. This ensures that the negative curvature is included, which would trigger gravitational catalysis, while also allowing thermal fluctuations according to the Matsubara formalism.

We then apply this result phenomenologically to the Asymptotic Safety scenario of quantum gravity. The thermal bound from gravitational catalysis is translated into an upper bound on the absolute value of the cosmological constant in the UV through the Einstein field equations. Matter degrees of freedom cause the absolute value of the cosmological constant in the UV to increase. At a certain critical number of fermion species, the cosmological constant will exceed this thermal bound and gravitational catalysis may be triggered.

To avoid this scenario, the number of fermion species in our universe should not surpass this critical value for our theory to be compatible with the existence of light fermions. Therefore, this bound on the curvature can be translated into a bound on the maximal number of fermion species. Even in the limit of infinitely high temperature, we obtain a finite number for the maximum number of fermion species allowed in our universe to prevent gravitational catalysis. We find that the particle content of the standard model (SM) is compatible with an asymptotic safety approach to quantum gravity and matter that allows light fermions to exist in our universe.

Another field of interest of this thesis is Hilbert-Palatini gravity [19, 20]. General Relativity (GR) is formulated as pseudo-Riemannian geometry on a manifold equipped with a metric and a connection. While in Einstein's formulation of gravity, this connection is set to the Levi-Cevita connection (which is torsionless and compatible with the metric), there is a priori no particular reason to restrict oneself to such a case. In the Hilbert-Palatini formulation

of gravity, the metric and the connection are treated as independent degrees of freedom, similar to how the connection of a non-abelian gauge theory is treated as an independent degree of freedom from the metric in Yang-Mills theories. This causes the connection in the Hilbert-Palatini formalism to have additional contributions to Levi-Cevita which introduce torsion and non-metricity to the manifold.

The most general case of the connection that is constrained by the equations of motion of the Einstein-Hilbert-Palatini action contains an abelian gauge field in addition to the Levi-Cevita connection [21]. With this solution, Palatini curvature tensors can be expressed in terms of ordinary curvature tensors and an additional field strength tensor emerging from the abelian sector of the connection. This additional contribution vanishes at the level of the Einstein-Hilbert-Palatini action.

Additionally, the geodesic equation in this formulation of Hilbert-Palatini gravity can be mapped onto the geodesic equation of Einstein gravity by the introduction of a modified eigentime parameter [22]. This means that the geodesic trajectory in Hilbert-Palatini gravity does not differ from the one in Einstein gravity. The velocity along the trajectory is changed by a scaling parameter though. Therefore, the time it takes for a test particle to move along a geodesic trajectory varies from Hilbert-Palatini gravity to Einstein gravity. This is a possible scenario through which one could observe and even measure the effects of classical Hilbert-Palatini gravity in nature.

To obtain a quantum theory of this formulation of gravity, we therefore study the RG flow of the subsequent order in the truncation of the Hilbert-Palatini gravity in an on-shell reduction scheme using the Functional Renormalization Group. We observe a UV-attractive fixed point of Reuter type with more stabilized critical exponents at a smaller value of the Newton coupling G compared to the same order in truncation in Einstein gravity. It is connected to the Gaussian fixed-point in the IR through an RG trajectory. Our scenario therefore provides evidence for the existence of a corresponding UV complete quantum theory of Hilbert-Palatini gravity that has a long-range limit compatible with classical Einstein gravity

This thesis is structured as followed: Chapter 2 explains the methods of non-perturbative quantum field theories we use. It starts with a description of functional integrals for fermions and bosons – including gauge fields – and also illustrates how to include thermal fluctuations in a quantum field theory approach. After discussing various generating functionals and the Wilsonian interpretation of renormalization, we introduce the Functional Renormalization Group and how to compute flow equations through a truncation ansatz. We conclude with an explanation of the Asymptotic Safety scenario. Chapter 3 starts with a summary of General Relativity and a description of fermions in curved spacetime. After the formulation of gravity as a gauge theory, we quantize it with the Asymptotic Safety approach to quantum gravity. Chapter 4 discusses spontaneous chiral symmetry breaking and fermion mass generation through an interplay with a scalar field theory. We study the effects of

thermal fluctuations on the curvature bound from gravitational catalysis in Chapter 5 and apply it to the Asymptotic Safety approach to quantum gravity. In Chapter 6, we discuss the Hilbert-Palatini formulation of gravity and quantize it in the Asymptotic Safety scenario via an on-shell reduction scheme.

The compilation of this thesis is solely due to the author. However, parts of this work have been developed in collaboration with members of the Theoretical Physical Institute in Jena. The study of the thermal influence on the curvature bound from gravitational catalysis described in Chapter 5 and concluded in Chapter 7 and the study on asymptotically safe Hilbert-Palatini gravity described in Chapter 6 and concluded in Chapter 7 have been elaborated together with H. Gies and published in [23] and [24], respectively.

2. Non-perturbative Quantum Field Theory

In this chapter, we discuss the mathematical techniques we use to include quantum and thermal fluctuations for fermions and bosons including gauge bosons and study quantum fields non-perturbatively with means of the Functional Renormalization Group [25]. Parts of this introductory chapter follow the introduction to the Functional Renormalization Group presented in [26].

2.1. Functional Integral Formulation

The approach to quantum field theories in the path integral formalism is based on the idea of performing a functional integral defined by the classical action over all possible field configurations [27]. It portrays an alternative approach to canonical quantization in which the classical fields are substituted by generically non-commutable operators.

For a better understanding of the general idea of a path integral, we start with a test particle at the initial time t_i . It propagates through spacetime and eventually arrives at a different point at the eventual time t_f . In quantum mechanics, the dynamics of the test particle from the state $|t_i\rangle$ to the state $|t_f\rangle$ can be described by the time evolution operator $\hat{U}(t_f, t_i)$,

$$\begin{aligned} |t_f\rangle &= \hat{U}(t_f, t_i) |t_i\rangle \\ &= e^{-i \int_{t_i}^{t_f} dt \hat{H}} |t_i\rangle, \end{aligned} \tag{2.1}$$

where \hat{H} is the Hamiltonian of the system. In a QFT approach however, this evolution is described by a functional integral $\mathcal{D}[\bar{\Psi}, \Psi]$, in which we integrate over all physically possible field configurations of Ψ and its adjoint $\bar{\Psi}$ from $t_i = 0$ to $t_f = \infty$,

$$\mathcal{Z} = \int \mathcal{D}[\bar{\Psi}, \Psi] e^{iS[\bar{\Psi}(x), \Psi(x)]}. \tag{2.2}$$

$S[\bar{\Psi}(x), \Psi(x)]$ represents the action of the classical field theory in a metric with a Lorentzian

signature,

$$S[\bar{\Psi}(x), \Psi(x)] = \int_0^\infty dt \int d^3x \mathcal{L}(\bar{\Psi}(x), \Psi(x)), \quad (2.3)$$

and is expressed in terms of the Lagrangian density $\mathcal{L}(\bar{\Psi}(x), \Psi(x))$ of the classical field theory. The path integral measure reads

$$\mathcal{D}[\bar{\Psi}, \Psi] = \prod_\alpha \int d\bar{\Psi}_\alpha \Psi_\alpha \quad (2.4)$$

The label α collects all continuous and discrete degrees of freedom of our fields, like their spacetime coordinate, flavor, internal spin (in case of fermions), etc. Each value of the amplitude of each label (even the continuous spacetime coordinates) represents a different field configuration in the path integral, which is integrated out and then encoded in the kernel \mathcal{Z} .

Since path integrals with complex densities e^{iS} are difficult to define rigorously, we perform an analytical continuation of the time coordinate into the complex plane and proceed with an imaginary time,

$$t \rightarrow i\tau. \quad (2.5)$$

Our metric now receives a Euclidean signature and our coordinates are now expressed in terms of Euclidean ones,

$$x_E = (\tau, \vec{x}). \quad (2.6)$$

The path integral in its final form reads

$$\mathcal{Z} = \int \mathcal{D}[\bar{\Psi}, \Psi] e^{-\int d\tau \int d^3x \mathcal{L}_E(\bar{\Psi}(x_E), \Psi(x_E))}, \quad (2.7)$$

with \mathcal{L}_E being the Lagrangian that uses the metric with the Euclidean signature. From now on, we omit the subscript that indicates the Euclidean signature of the metric and – unless stated otherwise – always assume our path integral to be in the Euclidean setting.

2.2. Thermal Quantum Field Theory

If we are interested in the effects of finite temperature on a system within the path integral formulation of quantum field theory, we can include thermal fluctuations through the Matsubara formalism [28].

We start with an approach from quantum statistical mechanics (similarly to how we started

with quantum mechanics in the case of the functional integral). Suppose we have a Hamiltonian operator \hat{H} that describes our system at finite temperature T . The partition function \mathcal{Z}_{th} that includes all possible configurations of our system in a canonical ensemble reads

$$\mathcal{Z}_{\text{th}} = \text{tr} e^{-\beta\hat{H}}, \quad (2.8)$$

with the trace going over all possible states of the system and $\beta = 1/T$ being the inverse temperature.

A trivial introduction of integration through a new parameter τ of Eq. (2.8),

$$e^{-\beta\hat{H}} = e^{-\int_0^\beta d\tau \hat{H}}, \quad (2.9)$$

shows the similarity of this expression to the time evolution operator of Eq. (2.1), with the newly introduced parameter τ interpreted as an imaginary time.

We can now proceed from a quantum statistical mechanics approach to a quantum field theory approach similar to Sec. 2.1 with the introduction of a path integral, and obtain the expression,

$$\mathcal{Z}_{\text{th}} = \int \mathcal{D}[\bar{\Psi}, \Psi] e^{-\int_0^\beta d\tau \int d^3x \mathcal{L}_E(\bar{\Psi}(\tau, \vec{x}), \Psi(\tau, \vec{x}))}. \quad (2.10)$$

Eq. (2.10) resembles Eq. (2.7) with the difference at finite temperature being that the integral of the imaginary time is restricted to the region $[0, \beta]$.

What needs to be taken into consideration though, is that the initial expression within a quantum statistical mechanics approach in Eq. (2.8) contains a trace. This results in a compactification of the temporal direction of our theory in a thermal quantum field theory approach and our fields now obey the following constraints,

$$\Psi(\tau + \beta, \vec{x}) = \zeta \Psi(\tau, \vec{x}). \quad (2.11)$$

Bosonic fields ($\zeta = 1$) are constrained by periodic boundary conditions and fermionic fields ($\zeta = -1$) by anti-periodic boundary conditions. This compactification also leads to the energy spectrum of our theory to be discretized into so-called Matsubara frequencies,

$$\omega_n = \begin{cases} 2\pi T n & \text{if } \Psi \text{ is bosonic,} \\ 2\pi T(n + 1/2) & \text{if } \Psi \text{ is fermionic.} \end{cases} \quad (2.12)$$

In $D = 1 + d$ spacetime dimensions, integrals over the energy spectrum are now transformed into a summation of discrete Matsubara frequencies,

$$\int \frac{d^D p}{(2\pi)^D} f(p_0, \vec{p}) \quad \rightarrow \quad T \sum_n \int \frac{d^d p}{(2\pi)^d} f(\omega_n, \vec{p}). \quad (2.13)$$

In conclusion, this implies that if we want to describe a system at finite temperature within a quantum field theory approach, we compactify the temporal direction of our original quantum field theory to a sphere with circumference β ,

$$\tau \in \mathbb{R}^+ \quad \rightarrow \quad \tau \in S^1, \quad (2.14)$$

and thereby constrain our quantum fields to the boundary conditions of Eq. (2.11).

2.3. Treatment of Gauge Fields

Suppose we have a gauge theory with an action $S[A_\mu]$, that depends on the gauge field A_μ and is therefore invariant under the (infinitesimal) gauge transformation

$$A_\mu \rightarrow A_\mu + \delta A_\mu, \quad (2.15)$$

$$S[A_\mu] \rightarrow S[A_\mu + \delta A_\mu] = S[A_\mu]. \quad (2.16)$$

A quantization of this theory via the above introduced path integral approach yields the difficulty that one would integrate over different configurations of gauge fields that yield the same physical configurations, e.g. one overcounts the redundant degrees of freedom originating from the gauge symmetry.

One now has to efficiently extract those redundant degrees of freedom (also referred to as gauge orbits) from the path integral $\mathcal{D}A_\mu$ by choosing physically unique configurations of gauge fields. To do so, we insert a gauge-fixing condition $\mathcal{G}[(A)]$ into the path integral and use the Faddeev-Popov procedure [1, 29],

$$1 = \int \mathcal{D}[\mathcal{G}] \delta[\mathcal{G}(A)] = \int \mathcal{D}[\alpha] \delta[\mathcal{G}(A^\alpha)] \text{Det} \left[\frac{\delta \mathcal{G}(A^\alpha)}{\delta \alpha} \right], \quad (2.17)$$

to reparameterize our newly introduced path integral $\int \mathcal{D}[\mathcal{G}]$ in terms of an auxiliary field α , which gives rise to the Jacobian in the form of a functional determinant $\text{Det}[\dots]$. This auxiliary field α parameterizes all gauge fields that are physically equivalent by means of a gauge transformation and therefore characterizes our gauge transformation,

$$\delta A_\mu = \delta A_\mu^\alpha. \quad (2.18)$$

We now have constrained our path integral over the gauge fields A_μ to those of physically distinct gauge field configurations A_μ^α and extracted the redundant degrees of freedom in the form of the gauge orbits in the additional path integral $\mathcal{D}[\alpha]$.

Since we introduce these gauge-fixing terms in the path integral over an exponentiated action, it would be useful to express them in a similar manner. For the first expression,

we use the representation of a functional delta distribution as a limit of a Gaussian with decreasing width ξ ,

$$\delta [\mathcal{G}(A^\alpha)] = \lim_{\xi \rightarrow 0} e^{-S_{\text{gf}}}, \quad (2.19)$$

to identify the so-called action S_{gf} for the gauge-fixing term,

$$S_{\text{gf}} = \frac{1}{2\xi} \mathcal{G}(A^\alpha)^2. \quad (2.20)$$

Said action includes the gauge-fixing condition $\mathcal{G}(A^\alpha)$ and the gauge-fixing parameter ξ , which corresponds to various gauges one could chose. Typical choices are the Landau gauge ($\xi \rightarrow 0$), which strictly enforces the gauge fixing condition $\mathcal{G}(A^\alpha)$, or the Feynman gauge ($\xi = 1$).

The second expression in Eq. 2.17 is a functional determinant in the numerator and can therefore be expressed as a result of a path integral over newly introduced Grassmann fields c and \bar{c} ,

$$\text{Det} \left[\frac{\delta \mathcal{G}(A^\alpha)}{\delta \alpha} \right] = \int \mathcal{D} [\bar{c}, c] e^{-S_{\text{gh}}}, \quad (2.21)$$

with the new action

$$S_{\text{gh}} = \bar{c} \frac{\delta \mathcal{G}(A^\alpha)}{\delta \alpha} c. \quad (2.22)$$

The auxiliary fields c and \bar{c} are spin-0 fields, e.g. transform like a scalar under Lorentz transformation, but are Grassmannian bosons. They do not satisfy the spin-statistics theorem, rendering these fields unphysical. Because of this, they are called *ghosts* and not treated as real, physical particles but instead as just auxiliary fields that adequately treat the redundant degrees of freedom of gauge fields during the quantization procedure.

We can now combine all of these results to properly compute the path integral over gauge fields and obtain

$$\int \mathcal{D} [A_\mu] e^{-S[A_\mu]} = \int \mathcal{D} [\alpha] \left\{ \int \mathcal{D} [\bar{c}, c, A_\mu^\alpha] e^{-S[A_\mu^\alpha] - S_{\text{gf}}[A_\mu^\alpha] - S_{\text{gh}}[\bar{c}, c]} \right\}. \quad (2.23)$$

The path integral over the redundant degrees of freedom $\mathcal{D}[\alpha]$ which yields the gauge orbits is now properly extracted and can now be omitted for the correct computation of the path integral without any overcounting of the field configurations occurring. From now on, gauge fields in the path integral are understood as physically unique trajectories and the explicit marking of that is omitted in the notation,

$$A_\mu^\alpha \rightarrow A_\mu. \quad (2.24)$$

This gives rise to the final expression for the path integral of gauge fields,

$$\int \mathcal{D}[\bar{c}, c, A_\mu] e^{-S[A_\mu] - S_{\text{gf}}[A_\mu] - S_{\text{gh}}[\bar{c}, c]}. \quad (2.25)$$

As an example for an abelian gauge theory with the action

$$S[A_\mu] = -\frac{1}{4} F^{\mu\nu} F_{\mu\nu}, \quad F^{\mu\nu} = \partial_\mu A_\nu - \partial_\nu A_\mu, \quad (2.26)$$

we introduce the gauge-fixing condition

$$\mathcal{G}(A_\mu) = \partial^\mu A_\mu, \quad (2.27)$$

which classically corresponds to a Lorenz gauge ($\partial^\mu A_\mu = 0$). The gauge transformation parameterized by the redundant degree of freedom α reads

$$\delta A_\mu^\alpha = \partial_\mu \alpha, \quad (2.28)$$

and the operator in the ghost sector

$$\frac{\delta \mathcal{G}(A_\mu^\alpha)}{\delta \alpha} = \partial^\mu \partial_\mu, \quad (2.29)$$

directly yielding the final expression for the gauge-fixing and ghost action, respectively,

$$S_{\text{gf}}[A_\mu] = \frac{1}{2\xi} (\partial^\mu A_\mu)^2, \quad S_{\text{gh}}[\bar{c}, c] = \bar{c} \partial^\mu \partial_\mu c. \quad (2.30)$$

While this Faddeev-Popov technique is a useful tool for the quantization of gauge theories through the introduction of ghosts, its validity in the most general case is contested. Due to the Gribov ambiguity, one does not restrict the path integral to physically unique configurations in this way [30]. While this issue is not relevant in perturbative settings, non-perturbative continuum formulations addressing this problem are an active field of research [31].

2.4. Generating Functionals

With the formulation of the functional integral in Sec. 2.1, we can compute correlation functions of quantum fields [1, 25, 32], like the propagator,

$$\langle \phi_\alpha \phi_\beta \rangle = \frac{1}{\mathcal{Z}} \int \mathcal{D}[\phi] \phi_\alpha \phi_\beta e^{-S[\phi]}, \quad (2.31)$$

which characterizes how the "points" α and β are correlated by virtue of the quantum theory. The superlabel α collects all continuous and discrete degrees of freedom of the field, like the spacetime position, the flavor, the spin etc. A computation of higher order correlation functions is done accordingly,

$$\langle \phi_{\alpha_1} \dots \phi_{\alpha_n} \rangle = \frac{1}{\mathcal{Z}} \int \mathcal{D}[\phi] \phi_{\alpha_1} \dots \phi_{\alpha_n} e^{-S[\phi]}, \quad (2.32)$$

but the functional integration for each case becomes rather tedious. Instead, we compute the correlation functions by means of differentiation.

We introduce a source term J for our functional integral and define the generating functional

$$\mathcal{Z}[J] := \int \mathcal{D}[\phi] e^{-S[\phi] + \int_{\alpha} J_{\alpha} \phi_{\alpha}}. \quad (2.33)$$

The operation \int_{α} integrates over the continuous degrees of freedom of the superlabel and sums over the discrete ones. Using the Feynman trick of differentiation under an integral, we obtain

$$\begin{aligned} & \langle \phi_{\alpha_1} \dots \phi_{\alpha_n} \rangle \\ &= \frac{1}{\mathcal{Z}[0]} \int \mathcal{D}[\phi] \phi_{\alpha_1} \dots \phi_{\alpha_n} e^{-S[\phi] + \int_{\alpha} J_{\alpha} \phi_{\alpha}} \Big|_{J=0} \\ &= \frac{1}{\mathcal{Z}[0]} \int \mathcal{D}[\phi] \frac{\delta}{\delta J_{\alpha_1}} \dots \frac{\delta}{\delta J_{\alpha_n}} e^{-S[\phi] + \int_{\alpha} J_{\alpha} \phi_{\alpha}} \Big|_{J=0} \\ &= \frac{1}{\mathcal{Z}[0]} \frac{\delta}{\delta J_{\alpha_1}} \dots \frac{\delta}{\delta J_{\alpha_n}} \mathcal{Z}[J] \Big|_{J=0} \\ &=: \mathcal{Z}_{\alpha_1 \dots \alpha_n}^{(n)}. \end{aligned} \quad (2.34)$$

We now have an expression for the computation of higher order correlation functions, $\mathcal{Z}_{\alpha_1, \dots, \alpha_n}^{(n)}$, by taking functional derivatives of the generating functional with respect to the source term J . The issue with this formalism is that the correlation functions derived by the generating functional also include disconnected diagrams and even vacuum bubbles. But if we are interested in the propagation of a particle from point A to point B , we want to analyze correlation functions with connected diagrams. To derive a formalism for the computation of connected diagrams, we first remark that the generating functional can be written as a summation over connected diagrams,

$$\mathcal{Z}[J] = \sum_n \frac{1}{n!} (W[J])^n = e^{W[J]}, \quad (2.35)$$

with $W[J]$ being the Schwinger functional that represents the generating functional for con-

nected diagrams and can be inversely expressed through

$$W[J] := \log(\mathcal{Z}[J]). \quad (2.36)$$

We can now similarly compute connected diagrams by taking the derivatives of the Schwinger functional with respect to the source terms J ,

$$\begin{aligned} & \langle \phi_{\alpha_1} \dots \phi_{\alpha_n} \rangle_c \\ &= \left. \frac{\delta}{\delta J_{\alpha_1}} \dots \frac{\delta}{\delta J_{\alpha_n}} W[J] \right|_{J=0} \\ &=: W_{\alpha_1 \dots \alpha_n}^{(n)}. \end{aligned} \quad (2.37)$$

For example, the connected 2-point function reads

$$\begin{aligned} \langle \phi_\alpha \phi_\beta \rangle_c &= W_{\alpha\beta}^{(2)} = \left. \frac{\delta}{\delta J_\alpha} \frac{\delta}{\delta J_\beta} W[J] \right|_{J=0} = \left. \frac{\delta}{\delta J_\alpha} \frac{\delta}{\delta J_\beta} \log(\mathcal{Z}[J]) \right|_{J=0} \\ &= \left. \frac{1}{\mathcal{Z}[J]} \frac{\delta^2 \mathcal{Z}[J]}{\delta J_\alpha \delta J_\beta} \right|_{J=0} - \left. \frac{1}{(\mathcal{Z}[J])^2} \frac{\delta \mathcal{Z}[J]}{\delta J_\alpha} \frac{\delta \mathcal{Z}[J]}{\delta J_\beta} \right|_{J=0} \\ &= \mathcal{Z}_{\alpha\beta}^{(2)} - \mathcal{Z}_\alpha^{(1)} \mathcal{Z}_\beta^{(1)} \\ &= \langle \phi_\alpha \phi_\beta \rangle - \langle \phi_\alpha \rangle \langle \phi_\beta \rangle, \end{aligned} \quad (2.38)$$

illustrating how the vacuum bubbles have been extracted from the disconnected diagram to obtain the connected one.

Later on, we want to compute flow equations within the Functional Renormalization Group to describe certain physical phenomena at different scales. As it turns out, using connected diagrams can lead to some technical issues depending on the choice of regulator [33]. This problem can be circumvented by using irreducible diagrams generated from the effective action Γ .

For this, we want to express our generating functionals in terms of fields instead of sources. Let us define

$$\Phi_\alpha = \frac{\delta W[J]}{\delta J_\alpha} = \langle \phi_\alpha \rangle_J, \quad (2.39)$$

which can be understood as the expectation value of the field ϕ in the presence of the source J . We perform the Legendre-transformation of $W[J[\Phi]]$,

$$\Gamma[\Phi] = \int_\alpha \Phi_\alpha J_\alpha[\Phi] - W[J[\Phi]]. \quad (2.40)$$

and compute correlation functions by taking derivatives with respect to the fields Φ ,

$$\Gamma_{\alpha_1 \dots \alpha_n}^{(n)} = \left. \frac{\delta^n \Gamma[\Phi]}{\delta \Phi_{\alpha_1} \dots \delta \Phi_{\alpha_n}} \right|_{\Phi=0}. \quad (2.41)$$

This way, only 1PI-diagrams can emerge from the computations. They have the advantage, that if one cuts one internal line off, the resulting diagram is still connected, gifting the 1PI-diagrams with a loop-like structure that is advantageous for the calculation of flow equations through the effective action $\Gamma[\Phi]$ compared to the computation with the Schwinger functional $W[J]$ [33].

2.5. Wilsonian Interpretation of Renormalization

The computation of diagrams through the correlation functions introduced in the previous section faces the problem, that some of the contributions might diverge, depending on the system and underlying types of interactions one wants to study. Early historic attempts to solve this problem introduced the concept of perturbative renormalization [1].

The idea is, that the couplings g_i appearing in the action are not the real, actually physically measurable couplings, but instead just some bare parameter $g_{b,i}$, that can be split into a renormalized coupling $g_{r,i}$ and a counter term Δg_i ,

$$g_{b,i} = g_{r,i} + \Delta g_i. \quad (2.42)$$

The counter terms adequately treat the divergences, rendering them obsolete. Thus, the remaining renormalized couplings $g_{r,i}$ represent the final result for the couplings that could actually be measured in experiments.

While this procedure of perturbative renormalization would mathematically solve the issue, it was a deeply unsatisfying approach from a fundamental physics point of view, as the physical meaning of this renormalization procedure was not well understood. This changed with the Wilsonian interpretation of renormalization [2] which is based on Kadanoff's idea of a block-spin transformation [34] (see Fig. 2.1).

We start with a squared lattice in two dimensions with lattice spacing a . Each lattice site contains a spin that interacts with its neighboring lattice site spin. We only consider nearest-neighbor interactions here, rendering direct long-range interactions obsolete. The strength of the interaction is characterized by the coupling g . In the next step, we coarse-grain the lattice and combine a block of 4 lattice sites into one effective lattice site with lattice spacing $a' = 2a$. The nearest-neighbor interaction between the spins on the new lattice sites are now characterized by the new coupling $g' = g'(g)$ that depends on the initial coupling g of the previous lattice space a . Although we still just consider nearest-neighbor

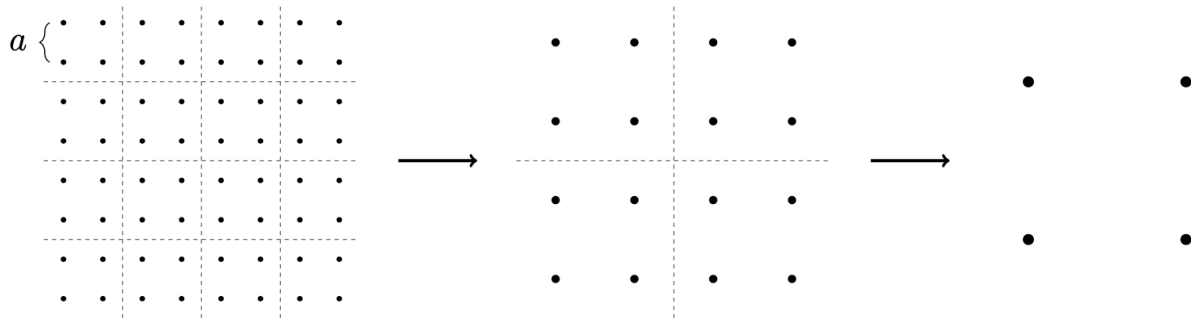


Fig. 2.1.: Schematic illustration of the Kadanoff block-spin transformation on a two-dimensional square lattice, taken from [35].

interactions, the effective range of the interaction has increased from a to $a' = 2a$. If we now perform this procedure of coarse-graining iteratively, we can include interactions at larger and larger ranges, effectively gaining a macroscopic understanding of the system, even though we started from a microscopic model.

Wilson applied this idea of coarse-graining to the path integral, but interpreted it in momentum space. Kadanoff's idea of effectively increasing the range of the interaction translates into a successive integration of momenta in the path integral, effectively introducing a momentum-shell cutoff Λ up to which interactions are considered. For a better illustration, we split our field ϕ into modes of high and low momenta [25],

$$\begin{aligned}\phi &= \theta(\Lambda - p)\phi + \theta(p - \Lambda)\phi \\ &= \phi_{p < \Lambda} + \phi_{p > \Lambda}.\end{aligned}\tag{2.43}$$

The measure in the path integral can now be split into those two contributions,

$$\begin{aligned}\mathcal{Z} &= \int \mathcal{D}[\phi] e^{-S[\phi]} = \int \mathcal{D}[\phi_{p < \Lambda}] \int \mathcal{D}[\phi_{p > \Lambda}] e^{-S[\phi_{p < \Lambda} + \phi_{p > \Lambda}]} \\ &= \int \mathcal{D}[\phi_{p < \Lambda}] e^{-S_\Lambda[\phi_{p < \Lambda}]}.\end{aligned}\tag{2.44}$$

If we perform the integration over the higher momentum modes, we obtain a term $S_\Lambda[\phi_{p < \Lambda}]$ in which the information of the high momentum modes is encoded. The expression $S_\Lambda[\phi_{p < \Lambda}]$ acts as an effective action at the coarse-grained scale Λ . The bare couplings $g_{b,i}$, that previously appeared in the bare action $S[\phi]$, also transform into new couplings at the coarse-grained scale Λ ,

$$g_{b,i} \quad \rightarrow \quad g_{\Lambda,i} = g_{\Lambda,i}(g_{b,i}),\tag{2.45}$$

and depend on the bare couplings. We can now perform another step of coarse-graining at

the scale $\Lambda' < \Lambda$

$$\mathcal{Z} = \int \mathcal{D}[\phi_{p < \Lambda'}] e^{-S_{\Lambda'}[\phi_{p < \Lambda'}]} \quad (2.46)$$

and obtain a new effective action $S_{\Lambda'}[\phi_{p < \Lambda'}]$ at scale Λ' with new couplings

$$g_{\Lambda,i} \quad \rightarrow \quad g_{\Lambda',i} = g_{\Lambda',i}(g_{\Lambda,i}). \quad (2.47)$$

This procedure of coarse-graining can be performed successively until one arrives at $\Lambda = 0$ and has effectively integrated out all momentum-shells, therefore reaching a description of the theory at infinitely large distances.

The transformation of the couplings at each step of coarse-graining can be described in terms of a (semi) group, which is now referred to as Renormalization Group (RG). The couplings in the theory are not some bare parameters anymore that treat the divergences of the diagrams, but are instead referred to as running couplings that change their values with the Renormalization Group scale up to which interactions are considered.

2.6. Functional Renormalization Group

The Functional Renormalization Group introduces a so-called regulator function \mathcal{R}_k that depends on an infrared regulator scale k and controls the flow of the underlying system [25]. We define a regulator term,

$$\Delta S_k[\phi] = \frac{1}{2} \int_{\alpha} \int_{\beta} \phi_{\alpha} \mathcal{R}_k^{\alpha\beta} \phi_{\beta}, \quad (2.48)$$

in which the regulator \mathcal{R}_k effectively acts as a mass term. The generating functionals of Sec. 2.4 are modified accordingly [32],

$$\mathcal{Z}_k[J] := \int \mathcal{D}[\phi] e^{-S[\phi] - \Delta S_k[\phi] + \int_{\alpha} J_{\alpha} \phi_{\alpha}}, \quad (2.49)$$

$$W_k[J] := \log(\mathcal{Z}_k[J]), \quad (2.50)$$

$$\Gamma_k[\Phi] := -W_k[J[\Phi]] + \int_{\alpha} J_{\alpha} \Phi_{\alpha} - \Delta S_k[\Phi], \quad (2.51)$$

and now also depend on the RG scale k .

The regulator function \mathcal{R}_k has several useful traits that can be best demonstrated in momentum space (in practical calculations we either do that or use the heat kernel techniques

discussed in Sec. 3.3). For instance, it has the following high and low energy behavior,

$$\mathcal{R}_k(p) = \begin{cases} 0 & \text{for } p^2 \gg k^2 \\ k^2 & \text{for } p^2 \ll k^2 \end{cases}, \quad (2.52)$$

which ensures that the high energy modes are integrated out in the path integral, while the low energy modes are suppressed, with the regulator function effectively acting as a mass. The limit

$$\lim_{k \rightarrow 0} \mathcal{R}_k = 0 \quad (2.53)$$

ensures that the effective average action, Γ_k , reaches the effective action, Γ . On the other hand, the limit

$$\lim_{k \rightarrow \Lambda \rightarrow \infty} \mathcal{R}_k = \infty \quad (2.54)$$

ensures that the effective average action coincides with the bare action in the UV, S_Λ (see Fig. 2.2). The boundary conditions of the regulator function \mathcal{R}_k constrain the effective average action Γ_k such that it interpolates between the bare action in the UV and the effective action in the IR,

$$\Gamma \xleftarrow{k \rightarrow 0} \Gamma_k \xrightarrow{k \rightarrow \Lambda} S_\Lambda, \quad (2.55)$$

with the exact shape of the trajectory of the flow depending on the specific choice of the regulator function.

Since we are interested in the behavior of systems at different RG scales, we want to study the RG flow of our action. For this, we define a slightly modified action,

$$\begin{aligned} \tilde{\Gamma}_k[\Phi] &:= \Gamma_k[\Phi] + \Delta S_k[\Phi], \\ &= -W_k[J[\Phi]] + \int_\alpha J_\alpha \Phi_\alpha \end{aligned} \quad (2.56)$$

and compute its flow equation,

$$\begin{aligned} \partial_k \tilde{\Gamma}_k[\Phi] &= -\partial_k W_k[J] = -\frac{\partial_k \mathcal{Z}_k[J]}{\mathcal{Z}_k[J]} \\ &= \frac{1}{\mathcal{Z}_k[J]} \int \mathcal{D}[\phi] (\partial_k \Delta S_k[\phi]) e^{-S[\phi] + \int_\alpha J_\alpha \phi_\alpha - \Delta S_k[\phi]} \\ &= \langle \partial_k \Delta S_k[\phi] \rangle \\ &= \frac{1}{2} \int_\alpha \int_\beta \partial_k \mathcal{R}_k^{\alpha\beta} \langle \phi_\alpha \phi_\beta \rangle. \end{aligned} \quad (2.57)$$

The second line of Eq. (2.57) can be expressed in terms of the expectation value of the

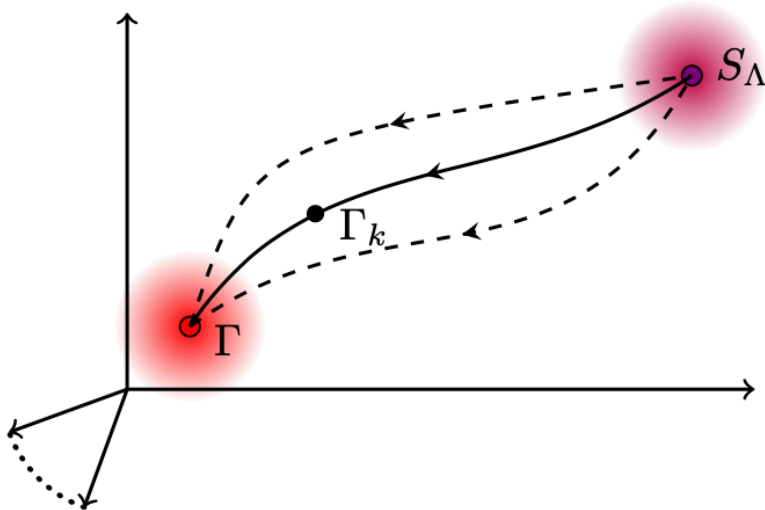


Fig. 2.2.: Schematic sketch of the flow of the effective average action Γ_k in the theory space spanned by the couplings. The flow starts from the bare action S_Λ (pink circle) in the UV and ends at the effective action Γ (red circle) in the IR. Taken from Ref. [35].

regulator term $S_k[\phi]$ and the last line as a two-point correlation function. We can write this expression in terms of a connected two-points function,

$$\begin{aligned} \langle \phi_\alpha \phi_\beta \rangle &= \langle \phi_\alpha \phi_\beta \rangle_c + \langle \phi_\alpha \rangle \langle \phi_\beta \rangle \\ &= W_{k,\alpha\beta}^{(2)} + \Phi_\alpha \Phi_\beta. \end{aligned} \quad (2.58)$$

Inserting this term into Eq. (2.57) yields

$$\partial_k \tilde{\Gamma}_k[\Phi] = \frac{1}{2} \int_\alpha \int_\beta \partial_k \mathcal{R}_k^{\alpha\beta} W_{k,\alpha\beta}^{(2)} + \partial_k \Delta S_k[\Phi]. \quad (2.59)$$

The second expression in Eq. (2.59) exactly cancels the difference between Γ_k and $\tilde{\Gamma}_k$ and we obtain for the flow of the effective average action

$$\partial_k \Gamma_k[\Phi] = \frac{1}{2} \int_\alpha \int_\beta \partial_k \mathcal{R}_k^{\alpha\beta} W_{k,\alpha\beta}^{(2)}. \quad (2.60)$$

For the final step, we express $W_{k,\alpha\beta}^{(2)}$ in terms of $\Gamma_{k,\alpha\beta}^{(2)}$. Since we also want to include the case of fermionic fields, we have to distinguish between derivatives taken from the right and the

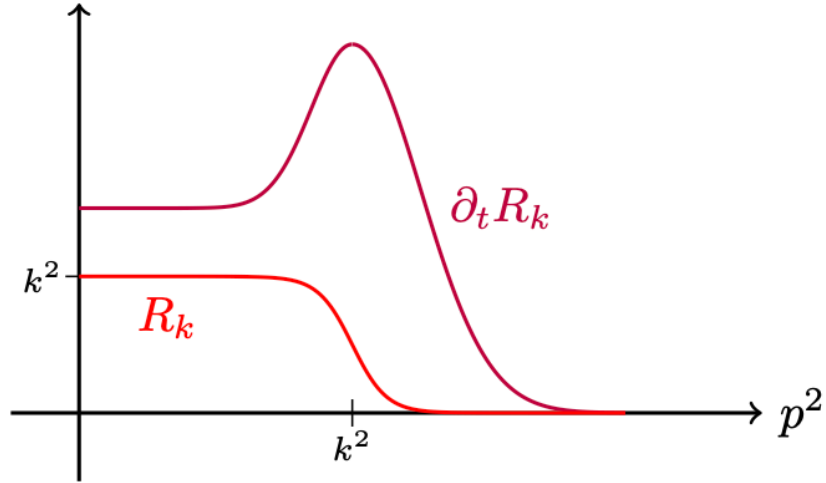


Fig. 2.3.: Schematic sketch of the regulator function \mathcal{R}_k (red) and its derivative $\partial_t \mathcal{R}_k$ (purple). Taken from Ref. [35]

ones taken from the left,

$$\begin{aligned}
 W_{k,\alpha\beta}^{(2)} &= \frac{\vec{\delta}}{\delta J_\alpha} W_k[J] \frac{\vec{\delta}}{\delta J_\beta} = \left(\frac{\vec{\delta}}{\delta J_\alpha} W_k[J] \right) \frac{\vec{\delta}}{\delta J_\beta} \\
 &= \Phi_\alpha \frac{\vec{\delta}}{\delta J_\beta} = \frac{1}{\left(\Phi_\alpha \frac{\vec{\delta}}{\delta J_\beta} \right)^{-1}} \\
 &= \frac{1}{\frac{\vec{\delta}}{\delta \Phi_\alpha} J_\beta} = \frac{1}{\frac{\vec{\delta}}{\delta \Phi_\alpha} \tilde{\Gamma}_k[\Phi] \frac{\vec{\delta}}{\delta \Phi_\beta}} \\
 &= \frac{1}{\tilde{\Gamma}_{k,\alpha\beta}^{(2)}} = \frac{1}{\Gamma_{k,\alpha\beta}^{(2)} + \mathcal{R}_{k,\alpha\beta}}.
 \end{aligned} \tag{2.61}$$

Inserting this into Eq. (2.60), we obtain the final form of our flow equation,

$$\begin{aligned}
 \partial_k \Gamma_k &= \frac{1}{2} \int_\alpha \int_\beta \frac{\partial_k \mathcal{R}_k^{\alpha\beta}}{\Gamma_{k,\alpha\beta}^{(2)} + \mathcal{R}_{k,\alpha\beta}} \\
 &= \frac{1}{2} \int_\alpha \int_\beta \left(\frac{1}{\Gamma_k^{(2)} + \mathcal{R}_k} \right)_{\alpha\beta} \partial_k \mathcal{R}_k^{\alpha\beta} \\
 &= \frac{1}{2} \int_\alpha \int_\beta \zeta_{\alpha\beta} \left(\frac{1}{\Gamma_k^{(2)} + \mathcal{R}_k} \right)_{\beta\alpha} \partial_k \mathcal{R}_k^{\alpha\beta} \\
 &= \frac{1}{2} \text{STr} \left(\frac{1}{\Gamma_k^{(2)} + \mathcal{R}_k} \partial_k \mathcal{R}_k \right)
 \end{aligned} \tag{2.62}$$

The switch of the indices in the second to last line of Eq. (2.62) has to be taken with caution, as fermionic fields receive an additional negative sign in this step. This is manifested in the statistical operator

$$\zeta_{\alpha\beta} = \delta_{\alpha\beta}\zeta_{\alpha}, \quad (2.63)$$

with

$$\zeta_{\alpha} = \begin{cases} +1 & \text{if } \alpha \text{ is a bosonic label,} \\ -1 & \text{if } \alpha \text{ is a fermionic label,} \end{cases} \quad (2.64)$$

that emerges from the switch of indices. If we suppress all internal indices, we can also use the operator STr to sum over all discrete internal labels and integrate over the continuous internal ones, with fermionic labels contributing with a negative prefactor.

Eq. (2.62) is referred to as the Wetterich equation [7] and is an exact evolution equation for the RG flow of the effective average action. It is usually written in terms of a logarithmic scale,

$$t = \log(k) \quad \rightarrow \quad \partial_t = k\partial_k. \quad (2.65)$$

The controlled flow of the effective average action Γ_k can best be shown through the sharp cutoff regulator [36] with the shape function $r_k(p)$,

$$\mathcal{R}_k(p) \sim r_k(p) = (k^2 - p^2)\theta(k^2 - p^2), \quad (2.66)$$

and $\theta(x)$ being the Heaviside step function. On one hand, the derivative of the regulator function in the numerator of the Wetterich equation effectively acts as a cutoff function and takes care of the UV divergences. On the other hand, the regulator in the denominator of the Wetterich equation effectively acts as a mass term and adequately treats IR divergences. Thus, the RG flow of the effective average action is well defined and can be used to compute the flow equations of running couplings within the Functional Renormalization Group.

2.7. Truncation Ansatz

While the Wetterich flow equation, Eq. (2.62), is an exact functional differential equation, its treatment in applications to physical systems requires some approximations [25]. The flow of the effective average action Γ_k is characterized by the second functional derivative of said action with respect to the underlying quantum fields of the system $\Gamma_k^{(2)}$. To properly solve the flow equation, one now has to formulate a functional differential equation for $\Gamma_k^{(2)}$ as well. This can be obtained by taking the second functional derivative of the above mentioned

Wetterich equation, yielding

$$\begin{aligned} \partial_t \Gamma_{k,\sigma\rho}^{(2)} = & \frac{1}{2} \int_{\alpha,\beta,\gamma,\delta,\mu,\nu} \zeta_{\nu\alpha} G_{k,\alpha\beta} \Gamma_{k,\beta\gamma\sigma}^{(3)} G_{k,\gamma\delta} \Gamma_{k,\delta\mu\rho}^{(3)} G_{k,\mu\nu} \partial_t R_{k,\nu\alpha} + \sigma \leftrightarrow \rho \\ & - \frac{1}{2} \int_{\alpha,\beta,\gamma,\delta} \zeta_{\delta\alpha} G_{k,\alpha\beta} \Gamma_{k,\beta\gamma\sigma\rho}^{(4)} G_{k,\gamma\delta} \partial_t R_{k,\delta\alpha}. \end{aligned} \quad (2.67)$$

The flow equation for $\Gamma_k^{(2)}$ includes the higher order vertices $\Gamma_k^{(3)}$ and $\Gamma_k^{(4)}$, demonstrating that in order to solve that functional differential equation, we have to formulate additional ones for $\Gamma_k^{(3)}$ and $\Gamma_k^{(4)}$. It becomes obvious that this is an endless endeavor in which the flow equation for $\Gamma_k^{(n)}$ includes expressions up to order $\Gamma_k^{(n+2)}$, resulting in an infinite tower of functional differential equations which - in practice - cannot be solved analytically exactly. Due to this, one truncates the number of operators \mathcal{O}_i with canonical mass dimension

$$d_i = \dim [\mathcal{O}_i[\Phi]], \quad (2.68)$$

appearing in the action at an finite order n ,

$$\Gamma_k[\Phi] = \int d^D x \sum_{i=1}^n \tilde{u}_{i,k} \mathcal{O}_i[\Phi], \quad (2.69)$$

rendering all remaining vertices of order higher than n unconsidered. This effectively breaks down the infinite number of flow equations to a finite number of n ones. Those operators $\mathcal{O}_i[\Phi]$ can appear in various forms, one of them being a power series of the quantum fields Φ^i as a possible ansatz.

Each operator appears in the action with an independent dimensional running coupling $\tilde{u}_{i,k}$ that determines the underlying interaction of the operator \mathcal{O}_i . To compute the flow equations for each $\tilde{u}_{i,k}$, we have to adequately project them out of the action using appropriate projectors \mathcal{P}_i for their corresponding interaction operators \mathcal{O}_i ,

$$\tilde{u}_{i,k} = \mathcal{P}_i \{ \Gamma_k[\Phi] \}. \quad (2.70)$$

If the operators \mathcal{O}_i are a power series of quantum fields Φ , functional derivatives with respect to said quantum fields would be a suitable choice as a projector to properly extract the running couplings from the action.

We can apply the appropriate projector to the Wetterich equation to compute the flow equation of the corresponding running coupling,

$$\begin{aligned} \partial_t \tilde{u}_{i,k} &= \mathcal{P}_i \{ \partial_t \Gamma_k[\Phi] \} \\ &= \frac{1}{2} \mathcal{P}_i \left\{ \text{STr} \left(\frac{1}{\Gamma_k^{(2)} + R_k} \partial_k R_k \right) \right\}. \end{aligned} \quad (2.71)$$

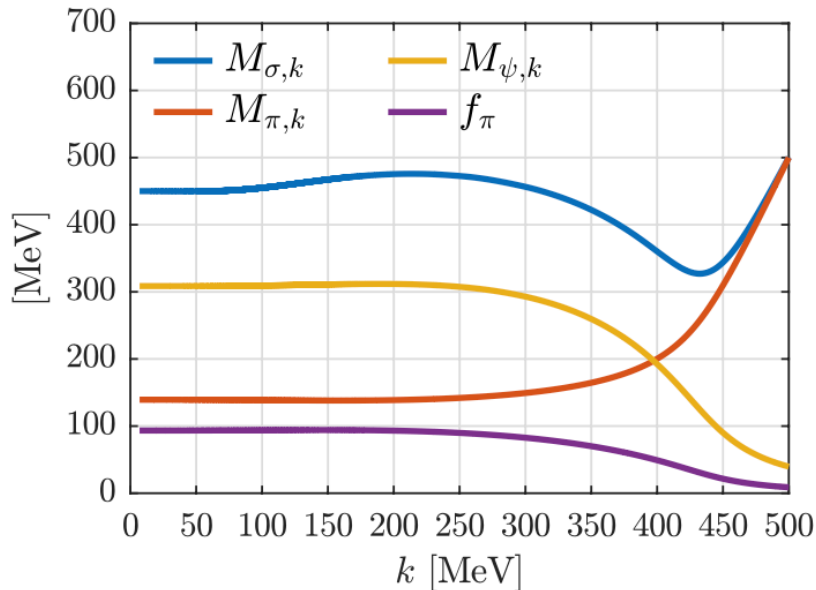


Fig. 2.4.: Schematic sketch of the flow of the meson masses $M_{\sigma,k}$ (blue) and $M_{\pi,k}$ (red), the quark mass $M_{\psi,k}$ (yellow) and the pion decay constant f_{π} (purple). Taken from [37].

Defining dimensionless running couplings in D -dimensional spacetime

$$u_{i,k} = k^{-(D-d_i)} \tilde{u}_{i,k}, \quad (2.72)$$

we can now compute the flow equations for the dimensionless couplings $u_{i,k}$,

$$\partial_t u_{i,k} = \beta_i(u_{1,k}, \dots, u_{n,k}), \quad (2.73)$$

also referred to as beta functions. In addition to the dimensional rescaling in Eq. (2.72), also field rescalings are often included.

The flow equations characterize the RG scale evolution of our running couplings and determine how strong or weak various interaction channels become at certain scales. Once the flow equations of a system are computed, one could potentially solve them analytically or numerically starting with some initial condition at a reference scale k_0 and observing their behavior with varying RG scale k .

For example, this could be the initial strength of the couplings in the UV, at small length scales, if one starts with a microscopic theory. With increasing renormalization scale k , one would now include fluctuations with larger and larger length scales and determine the effective interaction at larger ranges to eventually have a macroscopic understanding of the theory in the IR. Through the Renormalization Group one could then describe macroscopic phenomena like magnetization [25], superconductivity [25], or even fermionic mass generation [37] through a coarse-graining of microscopic degrees of freedom (see Fig. 2.4 for an example of a low-energy model of QCD).

It should be noted though that a general recipe for truncations of arbitrary theories does not exist and one does not a priori know, how many orders of interaction operators one has to include in their truncation to adequately describe the underlying theory. It is a process that can at least be systemized, where one starts with a certain truncation in an expansion scheme, computes the flow equations, applies them to a specific physical system - and then repeats this procedure with higher order operators in the truncation. If the results do not meaningfully change, this signals at least apparent convergence indicating that the initial truncation already describes the system well enough. If the results however meaningfully change, one has to include higher and higher order of operators, until the system "stabilizes" and an inclusion of further truncations does not drastically change the results (see [9–11] as possible examples in the case of asymptotically safe quantum gravity), or use a different expansion scheme.

2.8. Asymptotic Safety

An important question within the renormalization group study of field theories is whether or not a theory can be accurately described to arbitrarily large RG scales k , e.g. do the couplings of the theory remain finite along the RG flow, even in the limit of infinitely large k . If that is the case, said theory is UV complete and can be *asymptotically safe* [6]. For a theory to be asymptotically safe, the running couplings therefore have to converge towards a point of finite values in the UV, \vec{u}_* (ignoring scenarios of strictly oscillating couplings). This means, that if we set our couplings \vec{u}_k to these specific values of the point \vec{u}_* at an initial reference scale k_0 , the running couplings would remain constant along the RG flow. We have therefore discovered a so-called fixed point of the RG flow, that represents a specific configuration of our couplings for which our theory is scale invariant.

For the sake of a more convenient visualization, we collect the dimensionless running couplings and their corresponding beta-functions into two separate vectors,

$$\vec{u}_k = (u_{1,k}, \dots, u_{n,k})^T, \quad \vec{\beta} = (\beta_1(\vec{u}_k), \dots, \beta_n(\vec{u}_k))^T. \quad (2.74)$$

A fixed point \vec{u}_* is defined as the root of the beta functions,

$$\vec{\beta}(\vec{u}_*) = 0. \quad (2.75)$$

A trivial solution for the fixed point of the beta functions, e.g. $\vec{u}_* = 0$, is a Gaussian fixed point. If we describe our theory in the vicinity of a Gaussian fixed point, an approach within perturbative renormalization is possible. For a so-called non-Gaussian fixed point, e.g. $\vec{u}_* \neq 0$, a perturbative approach is generically not possible.

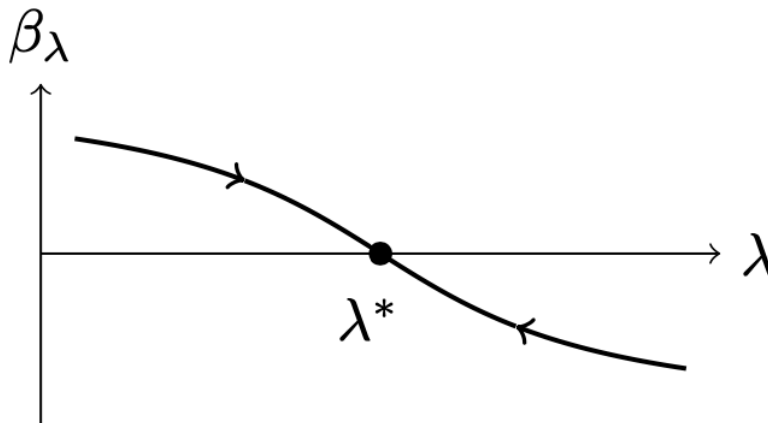


Fig. 2.5.: Schematic sketch of a beta function β_λ in dependence of its coupling λ with the root being at the fixed point λ_* . The arrows point towards the UV. Taken from [35].

While our theory is scale invariant at the fixed point, it is a priori not clear how the flow behaves in the vicinity of the fixed point, e.g. does it move towards or away from it. We therefore make a stability analysis and expand the flow equations up to linear order in the couplings,

$$\beta_i(\vec{u}) = \mathcal{M}_{ij} \cdot (u_{j,k} - u_{j,*}) + \mathcal{O}((u_{j,k} - u_{j,*})^2), \quad \text{with} \quad \mathcal{M}_{ij} = \left. \frac{\partial \beta_i(\vec{u}_k)}{\partial u_{j,k}} \right|_{\vec{u}_k = \vec{u}_*}. \quad (2.76)$$

\mathcal{M} is the stability matrix of the flow around the fixed point,

$$\{\theta_1, \dots, \theta_n\} = -\text{eig}(\mathcal{M}), \quad \mathcal{M}V_i = \theta_i V_i, \quad (2.77)$$

θ_i are its eigenvalues and V_i its right-eigenvectors. We now formulate a set of couplings $\hat{u}_{i,k} = u_{i,k} - u_{i,*}$ with respect to a basis spanned by the right-eigenvectors of \mathcal{M} that are centered around the fixed point \vec{u}_* and are constrained by the flow equations

$$\partial_t \hat{u}_{i,k} = -\theta_i \hat{u}_{i,k}. \quad (2.78)$$

Directly solving them to obtain the behavior of the running couplings around the fixed point yields

$$\hat{u}_{i,k} = \hat{u}_{i,*} + c_i \left(\frac{k}{k_0} \right)^{-\theta_i}, \quad (2.79)$$

with the parameters c_i being degrees of freedom in the form of a constant of integration and the eigenvalues of the stability matrix θ_i appearing in the form of a so-called critical exponent. We can use this to solve the linearized flow equations for the original couplings

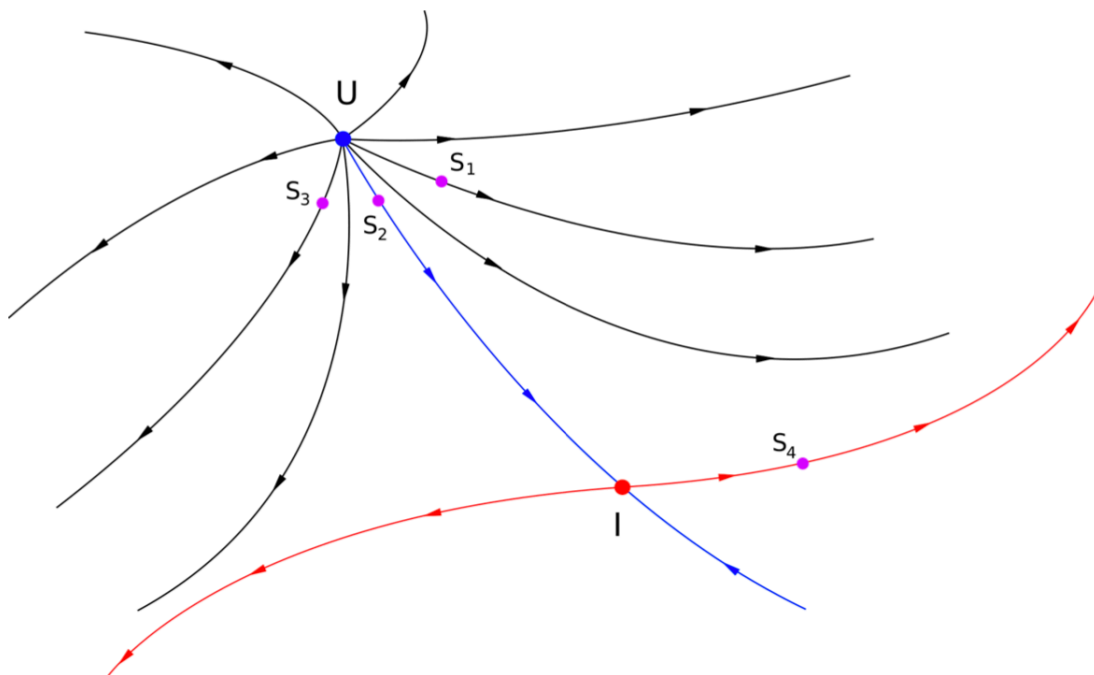


Fig. 2.6.: Schematic illustration of an RG flow in a theory space spanned by two couplings with the flow pointing towards the IR, taken from [38]. U represents a fixed point with two relevant directions, I represents a fixed point with one relevant and one irrelevant direction. The points S_1 to S_4 represent different positions in the theory space along their corresponding RG trajectories.

$u_{i,k}$ and obtain

$$u_{i,k} = u_{i,\star} + \sum_{j=1}^n c_j (V_j)_i \left(\frac{k}{k_0} \right)^{-\theta_j}. \quad (2.80)$$

Here, $(V_j)_i$ denotes the i -th component of the eigenvector V_j to each critical exponent θ_j .

If we want our theory to be asymptotically safe and therefore UV complete, the running couplings of the system have to approach the fixed point for increasing k . For a positive real part of the critical exponent $\text{Re}\{\theta_i\} > 0$, the second expression in Eq. (2.79) vanishes for decreasing k and the flow approaches the fixed point value from this specific direction. This happens independently of the value of c_i , making it a free parameter of our theory that needs to be fixed by experiments. For a negative real part of the critical exponent however, $\text{Re}\{\theta_i\} < 0$, the second expression in Eq. (2.79) grows exponentially for increasing k , causing the flow to divert from the fixed point. For the flow to emanate from the fixed point, the parameter c_i has to be zero for that specific direction. The resulting flow then remains on a so-called UV critical hypersurface (see Fig. 2.7) within the theory space of running couplings in which the asymptotically safe fixed point is located. The directions that span this critical surface are the UV-attractive ones with positive critical exponents (so-called relevant directions), whereas the UV-repulsive directions with negative critical exponents

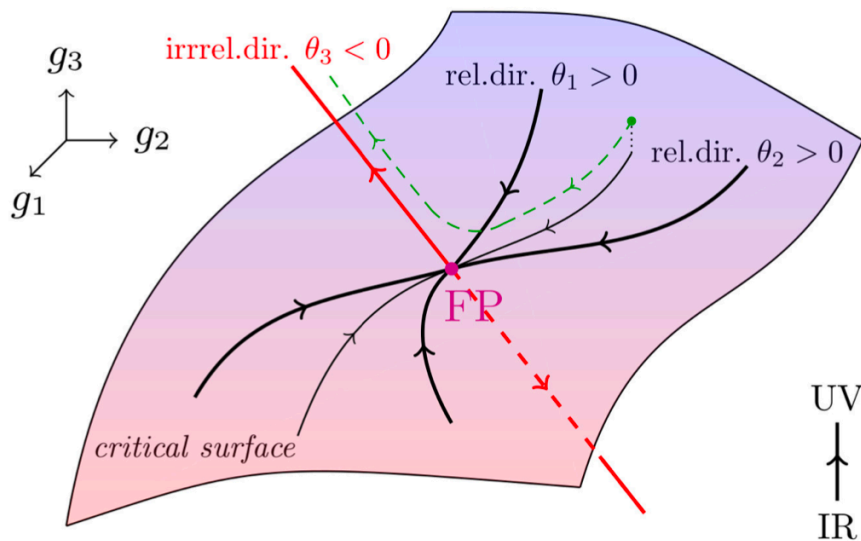


Fig. 2.7.: Schematic illustration of a UV critical surface in a theory space spanned by the three couplings g_1 , g_2 , and g_3 , taken from [35]. FP (red dot) represents a fixed point, θ_1 and θ_2 represent relevant directions, and θ_3 an irrelevant direction. The arrows point towards the UV.

(so-called irrelevant directions) are orthogonal to this hypersurface. The parameters c_i of the UV-attractive directions are free parameters of our theory, whereas the ones from the the UV-repulsive directions are fixed ones if one demands the theory to be asymptotically safe. This is a feature of asymptotic safety to predict the values of supposedly free parameters of a system. This means that if we have a theory with even infinitely many couplings, and therefore seemingly infinitely free parameters, only the relevant directions (the UV-attractive ones), of which there might be just finitely many ones for a given theory, deliver actually free parameters.

If those free parameters were to be fixed by experimental data, we would find the exact RG trajectory of our system in the theory space spanned by the couplings and could accurately describe the system at any given RG scale k .

3. From Classical to Quantum Gravity

The gravitational force of the day-to-day life is well described by Newtonian dynamics, yet it is still just a weak-field approximation of General Relativity (GR). While GR is a good description of the gravitational interaction in the IR, a quantum theory of gravity is needed to describe the theory at smaller scales, possibly even beyond the Planck scale.

In this chapter, we will use the non-perturbative approach of the Functional Renormalization Group introduced in Chapter 2 to formulate a quantum field theory of gravity.

3.1. General Relativity

General relativity is a geometric interpretation of gravity relying on the idea that the curvature of spacetime is the underlying origin of what we observe as an gravitational force [39]. In curved spacetime, we have to distinguish between covariant and contravariant vector fields V_α and V^α , respectively, which live on a tangent space or its dual of a manifold \mathcal{M} and can be translated into one another using the metric tensor g ,

$$V_\mu = g_{\mu\nu} V^\nu. \quad (3.1)$$

The metric tensor, as its name suggests, is used as a metric to compute the norm of a vector,

$$|V|^2 = V_\mu V^\mu = g_{\mu\nu} V^\mu V^\nu. \quad (3.2)$$

In addition to the metric tensor, our manifold is equipped with a connection Γ that translates vectors of a tangent space at one point on the manifold to vectors of a different tangent space at another point on the manifold. While this connection can have a general form (see Ch. 6), we will restrict ourselves to the Levi-Cevita connection for now,

$$\Gamma_{\mu\nu}^\alpha = \frac{1}{2} g^{\alpha\sigma} (\partial_\mu g_{\sigma\nu} + \partial_\nu g_{\mu\sigma} - \partial_\sigma g_{\nu\mu}), \quad (3.3)$$

which is the most commonly used one in general relativity. It is torsion-free

$$T_{\mu\nu}^\alpha := \Gamma_{\mu\nu}^\alpha - \Gamma_{\nu\mu}^\alpha = 0, \quad (3.4)$$

and compatible with the metric

$$Q_{\alpha\mu\nu} := \nabla_\alpha g_{\mu\nu} = 0. \quad (3.5)$$

To properly describe the dynamics in curved spacetime (for which one moves from the tangent space at one point of the manifold to the tangent space at another point of the manifold) one has to use the covariant derivative instead of the partial derivative,

$$\partial_\mu \rightarrow \nabla_\mu, \quad (3.6)$$

which adequately encodes the connection for this specific purpose,

$$\nabla_\mu V^\alpha = \partial_\mu V^\alpha + \Gamma_{\mu\nu}^\alpha V^\nu. \quad (3.7)$$

The covariant derivative of a tensor adds contributions to the dynamics for each tensorial degree of freedom,

$$\begin{aligned} \nabla_\mu T_{\beta_1, \dots, \beta_m}^{\alpha_1, \dots, \alpha_n} = & \partial_\mu T_{\beta_1, \dots, \beta_m}^{\alpha_1, \dots, \alpha_n} + \Gamma_{\mu\nu}^{\alpha_1} T_{\beta_1, \dots, \beta_m}^{\nu, \dots, \alpha_n} + \dots + \Gamma_{\mu\nu}^{\alpha_n} T_{\beta_1, \dots, \beta_m}^{\alpha_1, \dots, \nu} \\ & - \Gamma_{\mu\beta_1}^\nu T_{\nu, \dots, \beta_m}^{\alpha_1, \dots, \alpha_n} - \dots - \Gamma_{\mu\beta_m}^\nu T_{\beta_1, \dots, \nu}^{\alpha_1, \dots, \alpha_n}, \end{aligned} \quad (3.8)$$

with the most trivial case being that of a tensor of rank 0, a scalar,

$$\nabla_\mu \phi = \partial_\mu \phi. \quad (3.9)$$

Parameterizing a trajectory x^α through its eigentime τ , the dynamic on a manifold

$$u^\alpha := \dot{x}^\alpha(\tau) = \frac{dx^\alpha(\tau)}{d\tau} \quad (3.10)$$

is given by geodesics, which are trajectories of covariantly constant motion,

$$u^\mu \nabla_\mu u^\alpha = 0 \quad \Rightarrow \quad \frac{du^\alpha}{d\tau} + \Gamma_{\mu\nu}^\alpha u^\mu u^\nu = 0. \quad (3.11)$$

Rewriting Eq. (3.11) into a form that is more analogous to Newtonian mechanics,

$$\frac{d^2 x^\alpha(\tau)}{d\tau^2} = -\Gamma_{\mu\nu}^\alpha u^\mu u^\nu, \quad (3.12)$$

it becomes clear that the trajectory of a test particle moving alongside the parameterized curve $x^\alpha(\tau)$ is determined by the structure of spacetime encoded in the right-hand side of Eq. (3.12). In Newtonian mechanics, one would interpret the right-hand side as a force acting on a test particle of mass m , while in general relativity neither a force is acting nor a mass is needed for the test particle to move along the trajectory. What we intuitively observe as

a gravitational force is therefore just a consequence of the curved nature of spacetime.

To analyze the exact structure of spacetime, we define the Riemann curvature tensor given by a commutator of covariant derivatives,

$$[\nabla_\mu, \nabla_\nu]V^\alpha =: R^\alpha{}_{\beta\mu\nu}V^\beta, \quad (3.13)$$

which can be contracted into lower rank curvature tensors, namely the Ricci tensor and the Ricci scalar, respectively,

$$R_{\mu\nu} = R^\alpha{}_{\mu\alpha\nu}, \quad R = R^\mu{}_\mu. \quad (3.14)$$

These tensors are needed for the Einstein field equations (at vanishing cosmological constant Λ , for simplicity),

$$R_{\mu\nu} - \frac{1}{2}Rg_{\mu\nu} = \kappa T_{\mu\nu}, \quad \kappa = 8\pi G. \quad (3.15)$$

The left-hand side of Eq. (3.15) is a purely geometric quantity and depends on the metric tensor, while the right-hand side consists of the energy-momentum tensor $T_{\mu\nu}$ (with G being the Newton coupling). Eq. (3.15) therefore illustrates how the specific structure of spacetime is determined by the energy in the universe.

3.2. Fermions in Curved Spacetime

For an adequate description of the dynamics of fermions in curved spacetime, we need to express the proper form of the covariant derivative ∇ acting on a spinor ψ (similar to how we formulated the covariant derivative for scalars, vector fields, and higher rank tensors in general).

It is important to understand that in curved spacetime, the gamma matrices that span the internal space of spin degrees of freedom now depend on spacetime,

$$\gamma_\mu \rightarrow \gamma_\mu(x). \quad (3.16)$$

This is because the Clifford algebra connects the Dirac structure with the spacetime-dependent metric tensor g , instead of the flat-spacetime metric η ,

$$\{\gamma_\mu, \gamma_\nu\} = 2g_{\mu\nu}\mathbb{1}. \quad (3.17)$$

One can now formulate a map between the local general coordinate frame (characterized by Greek indices) and the locally inertial frame (characterized by Latin indices) through the

introduction of tetrads [40],

$$g_{\mu\nu} = e_{\mu}^a e_{\nu}^b \eta_{ab}. \quad (3.18)$$

Through these tetrads, we can formulate the curved spacetime Dirac matrices in terms of the well-known flat-spacetime ones,

$$\gamma_{\mu}(x) = e_{\mu}^a \gamma_a, \quad \{\gamma_a, \gamma_b\} = 2\eta_{ab} \mathbb{1}. \quad (3.19)$$

The covariant derivative acting on a spinor now receives a so-called spin connection, ω ,

$$\nabla \psi^a = \gamma^{\mu}(x) \nabla_{\mu} \psi^a = \gamma^{\mu}(x) (\partial_{\mu} \psi^a + \omega_{\mu}^a{}_b \psi^b) \quad (3.20)$$

that can be expressed in terms of the above introduced tetrads and the Levi-Civita connection Γ ,

$$\omega_{\mu}^a{}_b = -e^{\nu}{}_b \partial_{\mu} e_{\nu}^a + \Gamma_{\mu\nu}^{\lambda} e_{\lambda}^a e^{\nu}{}_b. \quad (3.21)$$

We can properly describe the dynamics of fermions in curved spacetime by substituting the partial derivative with the covariant one,

$$\not{\partial} \psi^a \rightarrow \nabla \psi^a. \quad (3.22)$$

While we use the formulation of fermions in curved spacetime through the introduction of tetrads, there are alternative ways of doing so, one of them being the spin-base invariant formulation in which not only general coordinate invariance, but also invariance under local spin-base transformations is considered [41, 42].

3.3. Heat Kernel Techniques

The computation of flow equations through the Functional Renormalization Group requires the evaluation of functional traces over an operator \mathcal{O} . In the case of dynamical theories, this operator is a kinetic one in the form of the Laplacian in D -dimensional spacetime,

$$\mathcal{O} = \Delta, \quad (3.23)$$

and occasionally contains an additional endomorphism (for instance, if dynamical fermions in curved spacetime are included).

In flat spacetime, the covariant Laplacian boils down to a product of partial derivatives,

$$\mathcal{O} = \Delta = -\partial^\mu \partial_\mu, \quad (3.24)$$

with the plane wave being its eigenfunction and the four-momentum p_μ containing its spectrum,

$$-\partial^\mu \partial_\mu e^{ipx} = p^2 e^{ipx}. \quad (3.25)$$

The computation of the functional trace in this case becomes straightforward through a Fourier transformation (as the kernel of the Fourier transformation consists of a plane wave e^{-ipx})

$$\text{Tr} [f(\Delta)] = \int \frac{d^D p}{(2\pi)^D} f(p^2). \quad (3.26)$$

In curved spacetime though, an analogous treatment of functional traces is not straightforward, as a general solution for the eigenfunctions and the spectrum of a covariant Laplacian with arbitrary spacetime structure does not exist. Due to this, alternative methods need to be considered, among them being the heat kernel techniques [43].

We assume a set of orthogonal eigenfunctions ξ_a of our operator \mathcal{O} with eigenspectrum λ_a ,

$$\mathcal{O}\xi_a = \lambda_a \xi_a \quad (3.27)$$

and perform a spectral decomposition of a general function of said Operator [38],

$$f(\mathcal{O}) = \int d\mu(\lambda_a) f(\lambda_a) \mathbb{P}_a. \quad (3.28)$$

Here, $\mu(\lambda_a)$ represents the spectral measure and \mathbb{P}_a is a projection operator for the appropriate subspace of the eigenspectrum. Introducing the Laplace transformation,

$$f(t) = \int_0^\infty ds \mathcal{L}^{-1}\{f\}(s) e^{-ts}, \quad (3.29)$$

with $\mathcal{L}^{-1}\{f\}(s)$ being the inverse Laplace transformation of f evaluated at s , we can apply

it to the spectral decomposition in Eq. (3.28),

$$\begin{aligned}
 f(\mathcal{O}) &= \int d\mu(\lambda_a) \int_0^\infty ds \mathcal{L}^{-1}\{f\}(s) e^{-\lambda_a s} \mathbb{P}_a \\
 &= \int_0^\infty ds \mathcal{L}^{-1}\{f\}(s) \int d\mu(\lambda_a) e^{-\lambda_a s} \mathbb{P}_a \\
 &= \int_0^\infty ds \mathcal{L}^{-1}\{f\}(s) e^{-\mathcal{O}s}.
 \end{aligned} \tag{3.30}$$

Taking the trace on both sides of Eq. (3.30), we obtain

$$\text{Tr}[f(\mathcal{O})] = \int_0^\infty ds \mathcal{L}^{-1}\{f\}(s) \text{Tr}[e^{-\mathcal{O}s}]. \tag{3.31}$$

This means, that if we want to compute the trace of a general function of an operator, we just have to compute the trace of one specific function of the operator, namely $e^{-\mathcal{O}s}$. That function is a solution to the equation

$$\left(\frac{d}{ds} + \mathcal{O} \right) e^{-\mathcal{O}s} = 0, \tag{3.32}$$

which has the form of a modified heat flow equation (with s being interpreted as a time parameter). The expression is therefore coined as a heat kernel trace, defined as

$$K_{\mathcal{O}}(s) := \text{Tr}[e^{-\mathcal{O}s}]. \tag{3.33}$$

Solving the modified heat flow equation, Eq. (3.32), for the heat kernel and afterwards applying it to Eq. (3.30), yields the result for the trace of a general function of an operator.

For our purposes, the underlying operator of interest would be the Laplacian in D -dimensional curved spacetime (occasionally with an additional endomorphism),

$$\mathcal{O} = \Delta = -\nabla^\mu \nabla_\mu. \tag{3.34}$$

The corresponding heat kernel one has to compute is

$$K_\Delta(s) = \text{Tr}[e^{-\Delta s}]. \tag{3.35}$$

While an exact solution of this heat kernel exists for specific spacetime structures (like the spinor heat kernel in 3-dimensional hyperbolic spacetime [44]), a so-called early time expansion of the heat kernel is usually performed to obtain an expression in successive orders of the curvature using the Seeley-deWitt coefficients [43],

$$K_\Delta(s) = \frac{1}{(4\pi s)^{D/2}} \left(1 + \frac{R}{6}s + \dots \right). \tag{3.36}$$

The coefficients themselves depend on the fields the Laplacian acted on in the original action (scalars, fermions, (transversal) vectors, (transversal) tensors etc.) and are listed in [45, 46].

While the approximation of the heat kernel in the form of an early time expansion may seem unsatisfactory at first, it turns out to be quite useful in the Asymptotic Safety approach to Quantum Gravity. Since we have to make a truncation ansatz to properly use the Functional Renormalization Group in practice, we expand our effective average action Γ_k in powers of the curvature operators, qualitatively illustrated as

$$\Gamma_k = \sum_{i=1}^n \frac{\alpha_{i,k}}{i!} R^i. \quad (3.37)$$

For simplicity, we constrain ourselves to the Ricci scalar R and omit additional curvature invariants that start to appear from the second order in the expansion. We then use the order of the curvature to properly project the corresponding running coupling from the action and compute its flow equations,

$$\alpha_{i,k} = \left. \frac{\partial^i}{\partial R^i} \Gamma_k \right|_{R=0}. \quad (3.38)$$

This implies, that even if we were to have an exact expression as a solution to the heat kernel of the covariant Laplacian for general spacetime structures, we would have to expand it in powers of the curvature anyway to obtain its contribution to the flow equation for each running coupling. The heat kernel expansion is therefore well suited to be an efficient and accurate method to compute flow equations in Asymptotic Safety approaches to Quantum Gravity in an operator expansion.

3.4. Gravity as a Gauge Theory

The description of gravity in terms of General Relativity can also be understood as a gauge theory of gravity with diffeomorphism invariance as its gauge symmetry [39].

For a better understanding of this, we start with the so-called Einstein-Hilbert action in $D = 4$,

$$S[g] = \int d^4x \sqrt{g} \frac{1}{16\pi G} (R - 2\Lambda), \quad (3.39)$$

that depends on the metric tensor g with a Euclidean signature. Here, $g = \det(g_{\mu\nu})$ is part of the integration measure, R is the Ricci scalar, G the Newton coupling and Λ the cosmological constant. With a variation of the action with respect to the metric, we can

derive the equations of motion that classically constrain our action,

$$\frac{\delta S[g]}{\delta g_{\mu\nu}} \stackrel{!}{=} 0. \quad (3.40)$$

In the case of the Einstein Hilbert action this leads to

$$R_{\mu\nu} - \frac{1}{2}Rg_{\mu\nu} + \Lambda g_{\mu\nu} = 0, \quad (3.41)$$

which are the Einstein field equations. We can therefore derive the dynamics of General Relativity through a Lagrangian Field Theory approach of gravity in the form of the Einstein-Hilbert action.

In General Relativity, one can perform a so-called general coordinate transformation,

$$x^\mu \rightarrow x^\mu + \epsilon^\mu(x) \quad \Rightarrow \quad \delta x^\mu = \epsilon^\mu(x), \quad (3.42)$$

that does not change the description of physics in the new coordinates compared to the old ones. This invariance under the general coordinate transformation is referred to as diffeomorphism invariance and can be understood as a gauge symmetry. To check whether this gauge symmetry is also encoded in our action, we have to analyze how general tensorial quantities change under this transformation.

Luckily for us, this change is characterized by a so-called Lie-derivative of the tensorial quantity along the direction ϵ^μ of the infinitesimal general coordinate transformation [39],

$$\delta(\dots) = \mathcal{L}_\epsilon(\dots), \quad (3.43)$$

with the Lie-derivative on manifolds without torsion, e.g. $T_{\mu\nu}^\alpha = 0$, being defined as,

$$\begin{aligned} \mathcal{L}_\epsilon T_{\beta_1, \dots, \beta_m}^{\alpha_1, \dots, \alpha_n} = & \epsilon^\nu \nabla_\nu T_{\beta_1, \dots, \beta_m}^{\alpha_1, \dots, \alpha_n} - (\nabla_\nu \epsilon^{\alpha_1}) T_{\beta_1, \dots, \beta_m}^{\nu, \dots, \alpha_n} - \dots - (\nabla_\nu \epsilon^{\alpha_n}) T_{\beta_1, \dots, \beta_m}^{\alpha_1, \dots, \nu} \\ & + (\nabla_{\beta_1} \epsilon^\nu) T_{\nu, \dots, \beta_m}^{\alpha_1, \dots, \alpha_n} + \dots + (\nabla_{\beta_m} \epsilon^\nu) T_{\beta_1, \dots, \nu}^{\alpha_1, \dots, \alpha_n}. \end{aligned} \quad (3.44)$$

The expression \sqrt{g} of the integration measure transforms like a density under general coordinate transformation. Under the integral, it remains invariant,

$$\delta \left(\int d^4x \sqrt{g} \right) = 0 \quad \Rightarrow \quad \int d^4x \sqrt{g} \rightarrow \int d^4x \sqrt{g}. \quad (3.45)$$

The Ricci scalar also is invariant under this general coordinate transformation,

$$\delta R = 0 \quad \Rightarrow \quad R \rightarrow R. \quad (3.46)$$

Thus, the Einstein-Hilbert action also remains invariant under this transformation,

$$\delta S = 0 \quad \Rightarrow \quad S \rightarrow S. \quad (3.47)$$

What needs to be taken into consideration here, though, is that the metric tensor g is not invariant under this transformation,

$$\begin{aligned} \delta g_{\mu\nu} &= \mathcal{L}_\epsilon(g_{\mu\nu}) \\ &= \epsilon^\alpha \nabla_\alpha g_{\mu\nu} + (\nabla_\mu \epsilon^\alpha) g_{\alpha\nu} + (\nabla_\nu \epsilon^\alpha) g_{\mu\alpha} \\ &= \nabla_\mu \epsilon_\nu + \nabla_\nu \epsilon_\mu \\ &\neq 0, \end{aligned} \quad (3.48)$$

where we used the metric compatibility condition, $\nabla_\alpha g_{\mu\nu} = 0$, in the second to last line of the equation and contracted the indices of the covariant derivative and the parameter ϵ for infinitesimal general coordinate transformation with the metric. This implies that two different metric tensors g and g' that can be mapped onto one another via a general coordinate transformation along the infinitesimal direction ϵ^μ ,

$$\begin{aligned} g'_{\mu\nu} &= g_{\mu\nu} + \delta g_{\mu\nu} \\ &= g_{\mu\nu} + \nabla_\mu \epsilon_\nu + \nabla_\nu \epsilon_\mu, \end{aligned} \quad (3.49)$$

could characterize the same manifold and describe the same physical system, as the action is invariant under this transformation.

This symmetry of diffeomorphism invariance can be interpreted as a gauge symmetry and its quantization through a functional integral approach,

$$\mathcal{Z} = \int \mathcal{D}[g] e^{-S[g]}, \quad (3.50)$$

contains redundant degrees of freedom in the path integral measure that need to be treated according to the Faddeev-Popov quantization method discussed in Sec. 2.3. As we discuss the approach of asymptotically safe quantum gravity in Sec 3.5, we will perform our calculations over all possible physically distinct field configurations of the metric g by computing the metric fluctuations h around a background field \bar{g} which will from now on be treated as a background metric tensor. This split is performed according to

$$g_{\mu\nu} = \bar{g}_{\mu\nu} + h_{\mu\nu}. \quad (3.51)$$

The indices are now raised and lowered by the fixed background metric \bar{g} and the path

integral measure is now reparameterized in terms of the the fluctuations h ,

$$\int \mathcal{D}[g] = \int \mathcal{D}[h]. \quad (3.52)$$

For the background metric \bar{g} to be fixed and the fluctuations h to carry over all of the information of g , including its symmetries, both quantities need to transform in the following way under a quantum general coordinate transformation,

$$\delta \bar{g}_{\mu\nu} = 0 \quad (3.53)$$

$$\delta h_{\mu\nu} = \delta g = \mathcal{L}_\epsilon(g_{\mu\nu}) = \mathcal{L}_\epsilon(\bar{g}_{\mu\nu}) + \mathcal{L}_\epsilon(h_{\mu\nu}). \quad (3.54)$$

This ensures that no information is lost during the quantization procedure with the split into the background \bar{g} and the metric fluctuations h .

3.5. Asymptotically Safe Quantum Gravity

We now formulate a quantum field theory of the gauge field formulation of General Relativity [8, 47] according to the non-perturbative techniques we outlined in Chapter 2 and verify that it indeed satisfies the conditions for Asymptotic Safety according to Sec. 2.8.

We start with the effective average action Γ_k for the Einstein-Hilbert truncation (which goes to linear order in the curvature) in $D = 4$ spacetime dimensions,

$$\Gamma_{\text{EH},k}[g] = \int d^4x \sqrt{g} \frac{1}{16\pi \bar{G}_k} (R - 2\bar{\Lambda}_k). \quad (3.55)$$

Here, \sqrt{g} is part of the integration measure with $g = \det(g_{\mu\nu})$, R the Ricci scalar, \bar{G}_k the Newton coupling and $\bar{\Lambda}_k$ the cosmological coupling. The two couplings now dependent on the RG scale k and are therefore running couplings. The bar on top of them emphasizes that they are dimensional couplings and yet have to be rescaled accordingly to make them dimensionless for a convenient study of their RG flow. As discussed in Sec 3.4, we now split our metric field into a background metric \bar{g} , which is fixed and from now on represents the metric tensor to raise and lower indices, and fluctuations around the background h that are quantized and contain all of the information of the metric field g ,

$$g_{\mu\nu} = \bar{g}_{\mu\nu} + h_{\mu\nu}. \quad (3.56)$$

We want to stress that this does not indicate a perturbative expansion, in which h were to be assumed small compared to the background \bar{g} , but instead just a split into a background and fluctuations with the fluctuations being arbitrarily large.

To properly treat the redundant gauge degrees of freedom tracing back to the diffeomorphism invariance discussed in Sec. 3.4, we introduce a gauge-fixing and a ghost term as suggested in Sec. 2.3. The gauge-fixing condition reads

$$\mathcal{G}_\mu = \sqrt{\frac{1}{16\pi\bar{G}_k}} \left(\bar{\nabla}^\alpha h_{\alpha\mu} - \frac{1+\beta}{4} \bar{\nabla}_\mu h^\alpha_\alpha \right), \quad (3.57)$$

and is contained in the gauge-fixing action

$$\Gamma_{\text{gf},k} = \frac{1}{2\alpha} \int d^4x \sqrt{\bar{g}} \bar{g}^{\mu\nu} \mathcal{G}_\mu \mathcal{G}_\nu. \quad (3.58)$$

Here, α and β are gauge-fixing parameters that can later on be set to certain values to choose the appropriate gauge. Additionally, we obtain an action containing ghosts through the Faddeev-Popov gauge-fixing procedure,

$$\Gamma_{\text{gh}} = - \int d^4x \sqrt{\bar{g}} \bar{c}_\mu \left(\bar{\nabla}^\alpha \bar{g}^{\mu\sigma} g_{\sigma\nu} \nabla_\alpha + \bar{\nabla}^\alpha \bar{g}^{\mu\sigma} g_{\alpha\nu} \nabla_\sigma - \frac{1+\beta}{2} \bar{\nabla}^\mu \bar{g}^{\alpha\rho} g_{\alpha\nu} \nabla_\rho \right) c^\nu. \quad (3.59)$$

Combining all of these contributions leads us to the effective average action of this theory,

$$\Gamma_k[\bar{g}, h, \bar{c}, c] = \Gamma_{\text{EH},k} + \Gamma_{\text{gf},k} + \Gamma_{\text{gh}}. \quad (3.60)$$

To compute the RG flow of the couplings \bar{G}_k and $\bar{\Lambda}_k$, we use the Wetterich flow equation derived in Sec. 2.6,

$$\partial_t \Gamma_k[\bar{g}, h, \bar{c}, c] = \frac{1}{2} \text{STr} \left(\frac{1}{\Gamma_k^{(2)} + \mathcal{R}_k} \partial_t \mathcal{R}_k \right). \quad (3.61)$$

Here, \mathcal{R}_k is the regulator function that controls the RG flow and $\Gamma_k^{(2)}$ is a matrix spanned by all possible combinations of second derivatives of the effective average action with respect to the fields h , \bar{c} and c . All internal labels in the expression are suppressed and are understood to be summed over or integrated out by the operator STr . If both internal labels in an entry are fermionic, said contribution to the flow equation receives a negative sign. We perform the computations of the flow equations on a spherical background, on which the expressions for the curvature tensors simplify to

$$\bar{R}_{\mu\nu\rho\sigma} = \frac{\bar{R}}{12} (\bar{g}_{\mu\rho} \bar{g}_{\nu\sigma} - \bar{g}_{\mu\sigma} \bar{g}_{\rho\nu}), \quad \bar{R}_{\mu\nu} = \frac{\bar{R}}{4} g_{\mu\nu}. \quad (3.62)$$

For a better understanding of the metric contributions to the flow equations, we split the

metric fluctuation h into separate modes according to the York decomposition [48],

$$h_{\mu\nu} = h_{\mu\nu}^{\text{TT}} + \bar{\nabla}^\mu \xi_\nu^{\text{T}} + \bar{\nabla}_\nu \xi_\mu^{\text{T}} + \left(\nabla_\mu \nabla_\nu + \nabla_\nu \nabla_\mu - \frac{1}{2} \bar{g}_{\mu\nu} \bar{\nabla}^2 \right) \sigma + \frac{1}{4} \bar{g}_{\mu\nu} h_{\text{Tr}}. \quad (3.63)$$

h^{TT} represents the transverse, traceless tensor modes of the original metric fluctuation tensor h , ξ^{T} the transverse vector modes, σ the conformal scalar mode and h_{Tr} the scalar trace mode. The constraints

$$\bar{\nabla}^\mu h_{\mu\nu}^{\text{TT}} = 0, \quad \bar{g}^{\mu\nu} h_{\mu\nu}^{\text{TT}} = 0, \quad \bar{\nabla}^\mu \xi_\mu^{\text{T}} = 0, \quad (3.64)$$

ensure, that we adequately distributed the modes of the original degrees of freedom of the metric fluctuation h onto the fields generated by the York decomposition. Since this split generates Jacobians, we have to redefine our fields of the decomposition according to

$$\sqrt{\Delta - \frac{\bar{R}}{4}} \xi_\mu^{\text{T}} \rightarrow \xi_\mu^{\text{T}}, \quad (3.65)$$

$$\sqrt{\Delta^2 - \frac{1}{3} \bar{R} \Delta} \sigma \rightarrow \sigma, \quad (3.66)$$

to cancel the contributions from the Jacobians [48]. We expand our right-hand side of the Wetterich equation in powers of the curvature and then use the powers of the Ricci scalar (in our case, R^0 and R^1) to project the flow equations for the dimensionless couplings

$$G_k = k^2 \bar{G}_k \quad \text{and} \quad \Lambda_k = \frac{\bar{\Lambda}_k}{k^2}. \quad (3.67)$$

We set the gauge parameters to

$$\alpha \rightarrow 0, \quad \beta = 0. \quad (3.68)$$

The Landau gauge ($\alpha \rightarrow 0$) strictly enforces the gauge fixing condition and omits any contributions from the transverse vector modes ξ_μ^{T} , illustrating that those modes were pure gauge contributions [49]. The second gauge fixing condition ($\beta = 0$) omits the contribution of the scalar mode σ [49]. Thus, only the contributions of the transverse, traceless tensor modes $h_{\mu\nu}^{\text{TT}}$ and the scalar trace mode h_{Tr} remain in the flow equations. At last, we use the regulator shape function

$$r_k(z) = (k^2 - z)\theta(k^2 - z) \quad (3.69)$$

to compute the flow equations for G and Λ in the same manner as Ref. [49] using the above

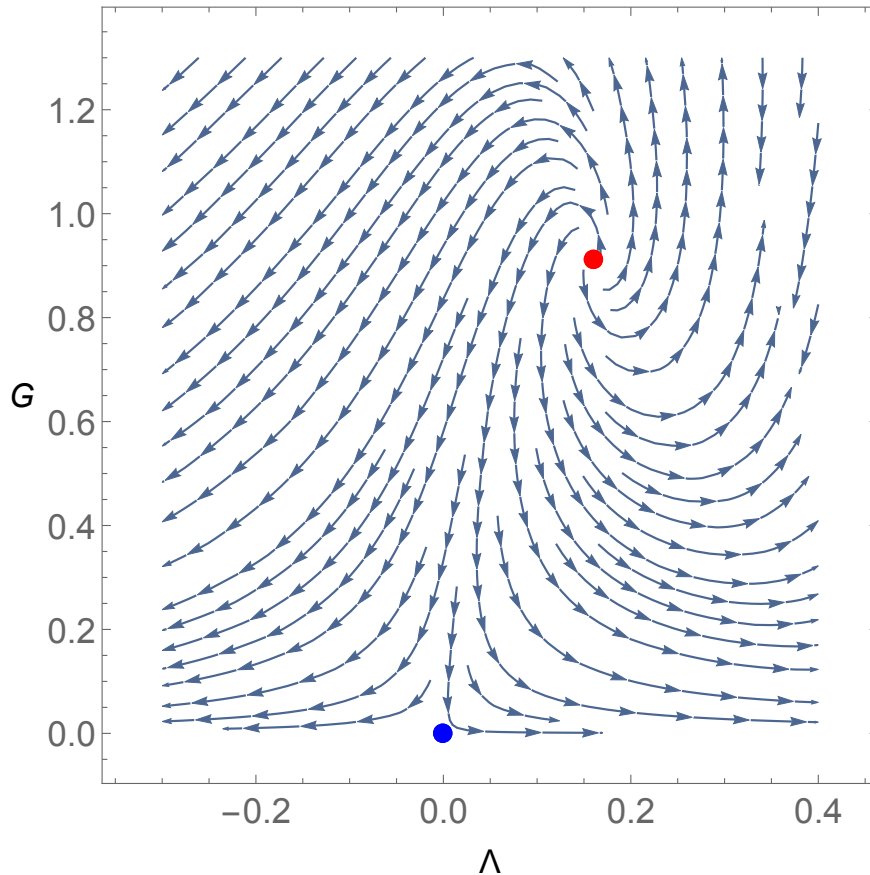


Fig. 3.1.: Flow diagram in the theory space spanned by the couplings Λ and G . The red dot represents the non-Gaussian UV fixed-point and the blue dot the Gaussian IR fixed-point. The arrows flow towards the IR.

mentioned heat kernel techniques,

$$\beta_G = -\frac{G(G(656\Lambda^3 - 1652\Lambda^2 + 1980\Lambda - 819) - 144\pi(1 - 2\Lambda)^2(4\Lambda - 3))}{G(224\Lambda^3 - 308\Lambda^2 + 30\Lambda + 54) + 72\pi(4\Lambda - 3)(1 - 2\Lambda)^2}, \quad (3.70)$$

$$\beta_\Lambda = \frac{\left(-576\pi^2\Lambda(8\Lambda^2 - 10\Lambda + 3)^2 + G^2 f_G^{(2)} - 4\pi G f_G^{(1)}\right)}{8\pi(4\Lambda - 3)(G(112\Lambda^3 - 154\Lambda^2 + 15\Lambda + 27) + 36\pi(4\Lambda - 3)(1 - 2\Lambda)^2)}, \quad (3.71)$$

with the abbreviations

$$f_G^{(1)} = 6208\Lambda^5 - 11584\Lambda^4 + 9276\Lambda^3 - 5328\Lambda^2 + 2133\Lambda - 324, \quad (3.72)$$

$$f_G^{(2)} = -640\Lambda^4 - 5944\Lambda^3 + 15738\Lambda^2 - 12495\Lambda + 3231. \quad (3.73)$$

The system of flow equations exhibits a non-Gaussian fixed point (Reuter fixed point) at

$$G_\star = 0.911, \quad \Lambda_\star = 0.161, \quad (3.74)$$

with critical exponents

$$\theta_1 = 2.132 \pm i \cdot 2.700. \quad (3.75)$$

The real part of both critical exponents is larger than zero, rendering this Gaussian fixed point UV-attractive with both directions being relevant. This means, that the Functional Renormalization Group applied to the Einstein-Hilbert action shows that the theory is asymptotically safe in the universality class of the Reuter fixed point and therefore non-perturbatively renormalizable. Thus, we have found a UV-complete quantum theory of gravity. Upon further inspection, we find an additional Gaussian fixed point at

$$G_\star = 0, \quad \Lambda_\star = 0, \quad (3.76)$$

with critical exponents

$$\theta_1 = 2, \quad \theta_2 = -2. \quad (3.77)$$

The physics near the Gaussian fixed point describes the weak gravitational interaction at large length scales with the critical exponents being the canonical mass dimension of the couplings in the IR. The Gaussian fixed point in the IR is connected with the non-Gaussian fixed point in the UV through a certain RG trajectory, see Fig. 3.1. Thus the weak long-range interactions of General Relativity emerge from the quantum theory of gravity at the UV-attractive fixed point.

While this calculation has been performed for the Einstein-Hilbert truncations, studies on higher order truncations also detect a UV-attractive fixed-point with finitely many relevant directions [9–11].

4. Symmetries and Phase Transitions

A material can have several attributes that characterize its state of phase. It can be a liquid and freeze if the temperature decreases beyond a certain value, it can become magnetic itself after being exposed to an external magnetic field or it can become – if we consider more exotic phases – superfluid with no viscosity whatsoever if the temperature is low enough and the pressure high enough.

In this chapter, we discuss how a phase transition can be described within a quantum field theory, how phases relate to the symmetries they exhibit and how fermionic masses are dynamically generated through the spontaneous breaking of chiral symmetry [50].

4.1. Spontaneous Symmetry Breaking

Macroscopically, a phase is characterized by a so-called order parameter, that changes its value depending on the current state of phase. The magnetization of a system for example is the order parameter for whether the system is in a magnetic state. Its density tells us, if we are dealing with a liquid or a solid. And for more exotic phases, like a superconductor, the order parameter may be formed from a collective behavior of bound states such as a Cooper pair condensate in the case of a superconductor, which is a bound state of electrons [51].

Different phases can often be characterized by different realizations of a symmetry groups they exhibit. For a liquid for example, the symmetry would be a continuous translation invariance, whereas for a solid, the symmetry breaks down into a discrete translation invariance [25]. For a superconductor, the symmetry breaks down from a $U(1)$ gauge symmetry in the non-superconducting phase to a \mathbb{Z}_2 symmetry in the superconducting phase [52].

A phase transition is therefore characterized not only by a change in the value of the order parameter, but also in the change of the residual symmetry group of the system considered. The symmetry group generically breaks down in the phase transition from a group of higher symmetry to one of lower symmetry or even no residual symmetry [1].

An interesting observation is, that the breaking of symmetries may not only be a feature of a phase transition, but even strongly tied to the underlying mechanism of the transition [53]. As an example, we consider an effective potential $U(\phi)$ that depends on a bosonic field

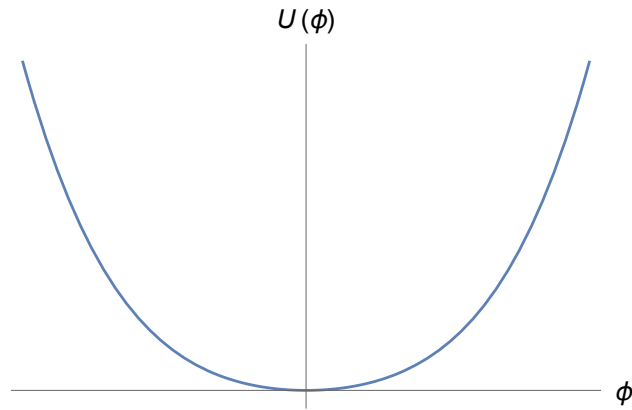


Fig. 4.1.: Schematic sketch of the potential $U(\phi)$ in the symmetric phase with the ground state at the origin, $\phi_0 = 0$.

ϕ ,

$$U(\phi) = \frac{\alpha}{2}\phi^2 + \frac{\lambda}{4!}\phi^4, \quad \alpha, \lambda > 0. \quad (4.1)$$

It features a \mathbb{Z}_2 symmetry around the origin $\phi = 0$,

$$U(-\phi) = U(\phi), \quad (4.2)$$

and the global minimum ϕ_0 of the potential also lies at said origin, see Fig. 4.1. It represents the ground state of our system in which physical quantities are evaluated, like the curvature mass

$$M^2(\phi_0) = \left. \frac{\delta^2 U(\phi)}{\delta \phi^2} \right|_{\phi=\phi_0}. \quad (4.3)$$

In this particular case, where the ground state is located at the origin, $\phi_0 = 0$, and the system is symmetric around the ground state, the curvature mass yields

$$M^2(0) = \alpha. \quad (4.4)$$

The couplings α and λ may depend on external parameters like the RG scale k , the temperature T , the pressure p , an external magnetic field h , the chemical potential μ , the curvature of spacetime κ and many more. If those parameters are changed, the values of the couplings α and λ may also change such that the conditions of Eq. (4.1) may not be valid anymore. One of those cases of particular interest to us is if the coupling α becomes negative,

$$U(\phi) = \frac{\alpha}{2}\phi^2 + \frac{\lambda}{4!}\phi^4, \quad \lambda > 0, \quad \alpha < 0. \quad (4.5)$$

The qualitative shape of the potential now drastically changes, see Fig. 4.2, and the global

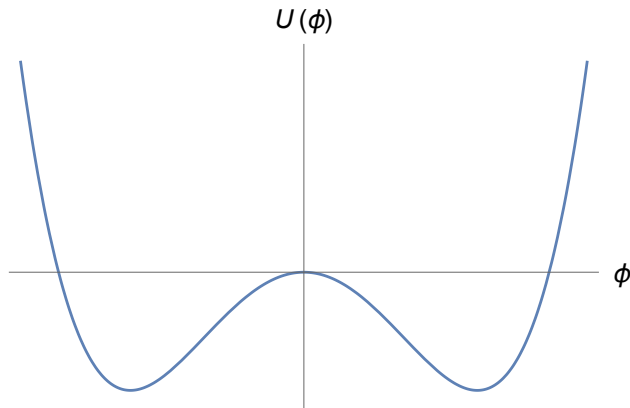


Fig. 4.2.: Schematic sketch of the potential $U(\phi)$ in the phase of broken symmetry with the ground state $\phi_0 \neq 0$.

minimum of the potential shifts from the the origin to

$$\phi_0 = \pm \sqrt{-\frac{6\alpha}{\lambda}} \neq 0. \quad (4.6)$$

The prior ground state at the origin is not a stable state anymore and a small perturbation through quantum fluctuations is sufficient to move the system to one of the two new local minimums. Thus, we now have a new stable ground state, in which physical quantities like the curvature mass are evaluated,

$$M^2(\phi_0) = -2\alpha > 0. \quad (4.7)$$

This means that quantum fluctuations of our field ϕ are now also considered from the perspective of the ground state,

$$\phi = \phi_0 + \varphi. \quad (4.8)$$

Here, φ is the new quantum field that we consider and the effective potential expressed in terms of it reads

$$U(\phi) = U(\phi_0 + \varphi) = \frac{\alpha}{2}(\phi_0 + \varphi)^2 + \frac{\lambda}{4!}(\phi_0 + \varphi)^4 =: U_{\phi_0}(\varphi). \quad (4.9)$$

As we can see, our new effective potential $U_{\phi_0}(\varphi)$ is not symmetric with respect to the ground state anymore

$$U_{\phi_0}(-\varphi) \neq U_{\phi_0}(\varphi). \quad (4.10)$$

Thus, the previous \mathbb{Z}_2 symmetry was spontaneously broken when the change in the shape of the potential forced our system to abandon the now unstable state at the origin and instead move to one of the two new stable ground states. We can interpret the ground state of our

potential as an order parameter for the phase with the corresponding symmetry it exhibits,

$$\phi_0 \begin{cases} = 0 & \text{if the symmetry is intact,} \\ \neq 0 & \text{if the symmetry is broken.} \end{cases} \quad (4.11)$$

With the spontaneous breaking of the symmetry (in this case, the \mathbb{Z}_2 symmetry), a phase transition occurs and changes the macroscopic properties of the system (like the mass of the field). If the change in the parameters (like the temperature T or the curvature κ) causes the coupling α to suddenly change from a positive to a negative value without smoothly crossing the value $\alpha_{\text{crit}} = 0$, the order parameter ϕ_0 also exhibits a jump to a finite value. This type of a transition is labeled a 1st order or discontinuous phase transition and occurs for potentials with a higher leading power than ϕ^4 such that we have several competing minima. If though the change of the parameters causes the coupling α to smoothly transition to a negative value while crossing $\alpha_{\text{crit}} = 0$, the order parameter ϕ_0 also smoothly changes from a non-finite to a finite value. This type of a transition is coined a 2nd order or continuous phase transition. It is responsible for the emergence of critical phenomena which is why it is also referred to as a critical phase transition. At a critical phase transition, the passing of the value $\alpha_{\text{crit}} = 0$ causes certain susceptibilities χ_i of a system to diverge and interesting observations can be made. For instance, the correlation length ξ diverges at a critical phase transition, rendering interactions on all length scales relevant [25, 53].

4.2. $\mathcal{O}(N)$ Scalar Model

In this section, we study the spontaneous symmetry breaking of a scalar field theory with $\mathcal{O}(N)$ symmetry as a case study for a specific phase transition [1, 25]. Not only is this a very good toy model from a pedagogical point of view, but it is also a useful one to describe the symmetry breaking of a mixed theory of bosons and fermions and a subsequent dynamical fermion mass generation.

Suppose, we have the following scalar field theory,

$$\mathcal{L} = (\partial^\mu \vec{\phi})(\partial_\mu \vec{\phi}) - U(\rho), \quad (4.12)$$

with N scalar fields that are collected in the label

$$\vec{\phi} = (\phi_1, \dots, \phi_N)^T. \quad (4.13)$$

Here, $U(\rho)$ represents the effective potential of our theory and

$$\rho = \frac{1}{2} \vec{\phi}^T \cdot \vec{\phi} = \frac{1}{2} (\phi_1^2 + \dots + \phi_N^2). \quad (4.14)$$

The quantity ρ and the kinetic term of our Lagrangian are invariant under a transformation of the $\mathcal{O}(N)$ symmetry group.

The curvature in this theory is spanned by a matrix that depends on the second derivatives of the potential,

$$\begin{aligned} K_{ab}(\phi) &= \frac{\partial^2 U(\rho)}{\partial \phi_a \partial \phi_b} \\ &= \frac{\partial}{\partial \phi_a} (\phi_b U'(\rho)) \\ &= \delta_{ab} U'(\rho) + \phi_a \phi_b U''(\rho). \end{aligned} \quad (4.15)$$

Introducing projection operators for the longitudinal and transversal modes,

$$P_{ab}^L = \frac{\phi_a \phi_b}{2\rho}, \quad P_{ab}^T = \delta_{ab} - P_{ab}^L, \quad (4.16)$$

with the appropriate properties of projectors,

$$(P^{T/L})^2 = P^{T/L}, \quad P^{T/L} \cdot P^{L/T} = 0, \quad P^T + P^L = \mathbf{1}, \quad (4.17)$$

we can rewrite the curvature matrix and obtain

$$K_{ab}(\rho) = [U'(\rho) + 2\rho U''(\rho)] P_{ab}^L + [U'(\rho)] P_{ab}^T. \quad (4.18)$$

Now we assume that the potential is bounded from below and that a stable global minimum $\vec{\phi}_0$ exists that is to be understood as the ground state of our system. Physical quantities therefore have to be evaluated in this given ground state. The curvature mass can be deduced from the curvature matrix K [1] and evaluated in the ground state yields

$$\begin{aligned} M_{ab}(\rho_0) &= K_{ab}(\rho)|_{\rho=\rho_0} \\ &= [U'(\rho_0) + 2\rho_0 U''(\rho_0)] P_{ab}^L + [U'(\rho_0)] P_{ab}^T \\ &= m_L^2(\rho_0) P_{ab}^L + m_T^2(\rho_0) P_{ab}^T. \end{aligned} \quad (4.19)$$

Here, $m_L^2(\rho_0)$ and $m_T^2(\rho_0)$ are the masses of the longitudinal and transversal modes in the ground state, with $\rho_0 = \frac{1}{2}\vec{\phi}_0^2$.

Taking the trace of those operators,

$$\text{Tr}(P^L) = \delta^{ab} P_{ab}^L = 1, \quad (4.20)$$

$$\text{Tr}(P^T) = \delta^{ab} P_{ab}^T = N - 1, \quad (4.21)$$

we observe that the longitudinal mode has 1 degree of freedom, while the transversal mode has $N - 1$ ones. Since these projectors form a complete basis, we can split our field into

those two components,

$$\vec{\phi} = \vec{\phi}_L + \vec{\phi}_T, \quad (4.22)$$

with each component being extracted with the help of the projection operators introduced above,

$$\vec{\phi}_{L/T} = P^{L/T} \vec{\phi}. \quad (4.23)$$

If we denote the operators without indices they are to be understood as matrices. These projected fields represent the eigenstates of the curvature mass operator \hat{M} that was introduced above in Eq. (4.19) ,

$$\hat{M}(\rho_0) \vec{\phi}_{L/T} = m_{L/T}^2(\rho_0) \vec{\phi}_{L/T}, \quad (4.24)$$

with the eigenvalues $m_{L/T}^2(\rho_0)$. For a better understanding of the dynamics, we introduce the fields σ and $\vec{\pi}$, that can be understood as the fields of physical particles, and associate them with the longitudinal and transversal modes,

$$\vec{\phi} = \begin{pmatrix} \vec{\pi} \\ \sigma \end{pmatrix}, \quad \vec{\phi}_L = \begin{pmatrix} 0 \\ \sigma \end{pmatrix}, \quad \vec{\phi}_T = \begin{pmatrix} \vec{\pi} \\ 0 \end{pmatrix}. \quad (4.25)$$

The first entry of the vector in field space introduced above is to be understood as containing $N - 1$ entries as it represents the $N - 1$ degrees of freedom of the transversal mode. The masses of those fields are given accordingly,

$$m_\sigma^2(\rho_0) = m_L^2(\rho_0) = U'(\rho_0) + 2\rho U''(\rho_0) \quad (4.26)$$

$$m_\pi^2(\rho_0) = m_T^2(\rho_0) = U'(\rho_0). \quad (4.27)$$

For a better understanding of how the symmetry emerges in the masses of those particles, we take a look at a very specific effective potential as an example given by

$$U(\rho) = m_0^2 \rho + \frac{\lambda}{2} \rho^2, \quad m_0, \lambda > 0, \quad (4.28)$$

that contains the $\mathcal{O}(N)$ symmetry. We take the derivative of said potential to compute the ground state,

$$\left. \frac{\partial U(\rho)}{\partial \phi_a} \right|_{\vec{\phi}=\vec{\phi}_0} \stackrel{!}{=} 0 \quad \Rightarrow \quad \vec{\phi}_0 U'(\rho_0) \stackrel{!}{=} 0, \quad (4.29)$$

and find out that the only real solution lies at the origin,

$$\vec{\phi}_0 = 0 \quad \Rightarrow \quad \rho_0 = 0. \quad (4.30)$$

The masses of those particles in the ground state read

$$m_\sigma^2(\rho_0) = m_0^2, \quad (4.31)$$

$$m_\pi^2(\rho_0) = m_0^2. \quad (4.32)$$

As we can see, the $\mathcal{O}(N)$ symmetry of our action is manifest in the masses of our model. Therefore, the system does not distinguish between longitudinal and transversal modes in this symmetric phase where the ground state of our effective potential lies at the origin.

Now we want to discuss the symmetry broken phase. Suppose a potential of the form

$$U(\rho) = -\mu^2\rho + \frac{\lambda}{2}\rho^2, \quad \mu, \lambda > 0. \quad (4.33)$$

Again, we compute its ground state,

$$\left. \frac{\partial U(\rho)}{\partial \phi_a} \right|_{\vec{\phi}=\vec{\phi}_0} \stackrel{!}{=} 0 \quad \Rightarrow \quad \vec{\phi}_0 U'(\rho_0) \stackrel{!}{=} 0, \quad (4.34)$$

and find the only stable state to be,

$$\rho_0 = \frac{\mu^2}{\lambda} \quad \Rightarrow \quad \phi_0 = \sqrt{\frac{2\mu^2}{\lambda}} \neq 0. \quad (4.35)$$

The ground state ϕ_0 is now located at a finite value of the field. The potential of Sec. 4.1 that contained a \mathbb{Z}_2 symmetry offered two new stable minima after spontaneous symmetry breaking. In the case of the a potential with an $\mathcal{O}(N)$ symmetry, the infinitely many possibilities for the new ground state form a subgroup, namely $\mathcal{O}(N - 1)$. This is observable if we take a look at the curvature masses in this new ground state,

$$m_\sigma^2(\rho_0) = 0 \quad (4.36)$$

$$m_\pi^2(\rho_0) = 2\mu^2. \quad (4.37)$$

We observe, that the breaking of the $\mathcal{O}(N)$ symmetry manifests itself in the masses of the particles. The $\vec{\pi}$ fields, which represent the transversal modes, are now massless, while the σ field, which represents the longitudinal mode, remains massive but changes its value. Since, there are $N - 1$ transversal modes and they all share the same value for their masses, they form a subgroup with the new symmetry group, the above mentioned $\mathcal{O}(N - 1)$. Therefore,

this particular phase transition changes the underlying symmetry group of our system,

$$\mathcal{O}(N) \rightarrow \mathcal{O}(N-1). \quad (4.38)$$

We define the direction of the σ field to be the one, in which the spontaneous symmetry breaking occurs, e.g.

$$\vec{\phi}_0 = \begin{pmatrix} 0 \\ \phi_0 \end{pmatrix} =: \begin{pmatrix} 0 \\ \sigma_0 \end{pmatrix}. \quad (4.39)$$

The new ground state of the potential is now located at ϕ_0 in the longitudinal direction.

The number of generators of the symmetry group [1] is given by

$$g[\mathcal{O}(N)] = \frac{N(N-1)}{2}. \quad (4.40)$$

This means that the number of generators that are broken during this phase transition is given by

$$g[\mathcal{O}(N)] - g[\mathcal{O}(N-1)] = N-1. \quad (4.41)$$

According to the Goldstone theorem, each broken generator of a continuous symmetry induces a massless bosonic mode [54, 55]. We associate these Goldstone modes with the $\vec{\pi}$ fields.

In nature, we can use a particular case of this model, namely the $\mathcal{O}(4)$ symmetry to study mesonic particles. The 4 fields described in this case are the three pions, π^0 , π^+ , π^- , and the σ particle which represents the order parameter of a chiral phase transition and therefore characterizes fermionic mass generation (see Sec. 4.3). Though the pions have a small mass in nature, they emerge as massless Goldstone bosons in this model. The reason for this is that the $\mathcal{O}(4)$ symmetry is just an approximate symmetry in the mesonic sector and in reality, that symmetry is slightly broken. This can be modeled by adding a small perturbation δU to the effective potential,

$$U \rightarrow U + \delta U, \quad \delta U = -c \cdot \sigma, \quad (4.42)$$

which is characterized by a small parameter c . This perturbation causes the pions to receive a small mass after spontaneous symmetry breaking making them so-called pseudo-Goldstone bosons [56].

An interesting feature of this model is that if the coupling of the linear operator in the potential (m_0^2 in the symmetric phase and $-\mu^2$ in the symmetry broken phase) continuously transitions from a positive to a negative value, a critical phase transition is occurring. This

is encoded in the chiral susceptibility,

$$\chi_\sigma = \frac{1}{m_\sigma^2}, \quad (4.43)$$

which diverges at the critical phase transition [57], as the mass of the longitudinal mode vanishes for $\mu = 0$.

4.3. Chiral Symmetry and Fermion Mass Generation

Dirac fermions contain a part with left-handed chirality and one with right-handed chirality [1]. We can define operators to project onto spinors that are right-handed and left-handed, respectively,

$$P_R = \frac{1}{2}(\mathbb{1} + \gamma_5), \quad P_L = \frac{1}{2}(\mathbb{1} - \gamma_5). \quad (4.44)$$

These operators obey the properties of projection operators,

$$P_{R/L}^2 = P_{R/L}, \quad P_{R/L} \cdot P_{L/R} = 0, \quad P_R + P_L = \mathbb{1}_{4 \times 4}. \quad (4.45)$$

Here, γ_5 is an additional gamma matrix with the properties

$$\{\gamma_5, \gamma_\mu\} = 0, \quad \gamma_5^\dagger = \gamma_5, \quad \gamma_5^2 = \mathbb{1}. \quad (4.46)$$

Especially in $D = 4$ spacetime dimensions and in the chiral basis, it reads

$$\gamma_5 = \begin{pmatrix} \mathbb{1}_{2 \times 2} & 0 \\ 0 & -\mathbb{1}_{2 \times 2} \end{pmatrix} \quad (4.47)$$

with $\mathbb{1}_{2 \times 2}$ being the 2×2 unit matrix. With these definitions, we can project a spinor ψ and its adjoint $\bar{\psi}$ onto their respective chiral parts,

$$\psi_{R/L} = P_{R/L}\psi, \quad \bar{\psi}_{R/L} = \bar{\psi}P_{L/R}. \quad (4.48)$$

The Dirac Lagrangian can now also be split into its chiral components,

$$\begin{aligned} \mathcal{L}_D &= \bar{\psi}(i\gamma^\mu\partial_\mu - m_\psi)\psi \\ &= \bar{\psi}_R(i\gamma^\mu\partial_\mu)\psi_R + \bar{\psi}_L(i\gamma^\mu\partial_\mu)\psi_L - m_\psi(\bar{\psi}_R\psi_L + \bar{\psi}_L\psi_R) \\ &= \mathcal{L}_{D,L} + \mathcal{L}_{D,R} - m_\psi(\bar{\psi}_R\psi_L + \bar{\psi}_L\psi_R). \end{aligned} \quad (4.49)$$

We observe that the kinetic part of the Dirac Lagrangian can be split into a purely right-handed and a purely left-handed part. An interaction between left-handed and right-handed fermions is only possible through their mass m_ψ . Therefore, for vanishing masses $m_\psi = 0$, the Dirac Lagrangian exhibits chiral symmetry [1], which is represented by the symmetry group

$$U(1)_R \otimes U(1)_L. \quad (4.50)$$

In return this means, that if the above introduced chiral symmetry were to be broken by the mechanism of spontaneous symmetry breaking, fermions would acquire a mass.

We now extend our analysis of chiral symmetry to a system with N_f fermions and $N = N_f^2$ bosons [58],

$$\mathcal{L} = \bar{\Psi}(i\gamma^\mu\partial_\mu)\Psi - y\bar{\Psi}(\sigma\mathbf{1}_{N_f \times N_f} + i\gamma_5\vec{\tau}\vec{\pi})\Psi - U(\rho). \quad (4.51)$$

Here, Ψ and its adjoint $\bar{\Psi}$ collect all N_f fermions into a tuple,

$$\Psi = \begin{pmatrix} \psi_1 \\ \vdots \\ \psi_{N_f} \end{pmatrix}, \quad \bar{\Psi} = (\bar{\Psi}_1, \dots, \bar{\Psi}_{N_f}). \quad (4.52)$$

$U(\rho)$ is the effective potential of our model and is expressed through the density ρ ,

$$\vec{\phi} = \begin{pmatrix} \vec{\pi} \\ \sigma \end{pmatrix}, \quad \rho = \frac{1}{2}\vec{\phi} \cdot \vec{\phi} = \frac{1}{2}(\sigma^2 + \vec{\pi}^2). \quad (4.53)$$

The field σ is a scalar-isoscalar and the $N - 1$ number of $\vec{\pi}$ are a pseudoscalar-isovector. The first part of the naming refers to the behavior under a Lorentz transformation (scalar for the σ field and pseudoscalar field for the $\vec{\pi}$) and the second part to the behaviour under a transformation in the internal flavor space (isoscalar for the σ field and isovector for the $\vec{\pi}$ field). The σ field enters the interaction with the fermions in the Lagrangian in Eq. (4.51) with a unit matrix, while each of the the $\vec{\pi}$ fields are contracted with the $N_f^2 - 1$ generators $\vec{\tau}$ of the $SU(N_f)$ symmetry group. The interaction type is a Yukawa interaction with y being the Yukawa coupling.

Chiral symmetry in this theory is expressed through the symmetry group [1]

$$U(N_f)_R \otimes U(N_f)_L, \quad (4.54)$$

which induces an $\mathcal{O}(N)$ symmetry in the scalar sector. This Lagrangian is an extension of the effective potential of a scalar field theory with $\mathcal{O}(N)$ symmetry discussed in Sec. 4.2, to a mixed systems consisting of bosons and chiral fermions. We know from the previous

section how the spontaneous breaking of the $\mathcal{O}(N)$ affects the bosonic sector. Now we want to study how it affects the chirality of the fermions in this mixed system.

We assume a potential that is in the phase of broken $\mathcal{O}(N)$ symmetry in accordance to the second part of Sec. 4.2,

$$U(\rho) = -\mu^2 \rho + \frac{\lambda}{2} \rho^2, \quad \mu, \lambda > 0. \quad (4.55)$$

The ground state of the potential in this broken phase can be computed and its absolute value reads,

$$\left. \frac{\partial U(\rho)}{\partial \phi_a} \right|_{\vec{\phi}=\vec{\phi}_0} \stackrel{!}{=} 0 \quad \Rightarrow \quad \phi_0 = \sqrt{2\rho_0} = \sqrt{\frac{2\mu^2}{\lambda}}. \quad (4.56)$$

Since it is a finite value, the ground state shifts from the origin along the direction of the σ field,

$$\vec{\phi}_0 = \begin{pmatrix} 0 \\ \sigma_0 \end{pmatrix}. \quad (4.57)$$

This non-zero value of the ground state can be interpreted as a condensate, that indicates that bosonic bound states are formed out of the fermions. It is referred to as a chiral condensate as it indicates chiral symmetry breaking. To better see, how chiral symmetry is broken, we now consider the fluctuations ξ around this ground state as a degree of freedom instead of the σ field itself,

$$\sigma = \sigma_0 + \xi. \quad (4.58)$$

For the interaction with the fermions, this yields

$$y\bar{\Psi}\sigma\Psi = y\bar{\Psi}\sigma_0\Psi + y\bar{\Psi}\xi\Psi, \quad (4.59)$$

and the fermions now have acquired a mass,

$$m_\Psi = y\sigma_0. \quad (4.60)$$

To better understand, how chiral symmetry is broken through the dynamical generation of a fermion mass, we first have to decompose the symmetry group of chiral symmetry into its subgroups [1],

$$U(N_f)_R \otimes U(N_f)_L \simeq SU(N_f)_V \otimes SU(N_f)_A \otimes U(1)_V \otimes U(1)_A. \quad (4.61)$$

Here $SU(N_f)_V$ and $SU(N_f)_A$ represent the vector and axial vector symmetries of the system.

Under a vector transformation [1], the spinor Ψ and its adjoint $\bar{\Psi}$ transform as

$$\Psi \longrightarrow (1 + i\vec{\theta}_V \vec{\tau})\Psi, \quad (4.62)$$

$$\bar{\Psi} \longrightarrow \bar{\Psi}(1 - i\vec{\theta}_V \vec{\tau}), \quad (4.63)$$

where $\vec{\theta}_V$ is the parameter for the vector transformation. The fermionic mass term transforms as

$$m_\Psi \bar{\Psi}\Psi \longrightarrow m_\Psi \bar{\Psi}\Psi, \quad (4.64)$$

and is therefore invariant under a vector transformation. Under an axial vector transformation [1], the spinor Ψ and its adjoint $\bar{\Psi}$ transform as

$$\Psi \longrightarrow (1 + i\gamma_5 \vec{\theta}_A \vec{\tau})\Psi, \quad (4.65)$$

$$\bar{\Psi} \longrightarrow \bar{\Psi}(1 + i\gamma_5 \vec{\theta}_A \vec{\tau}), \quad (4.66)$$

where $\vec{\theta}_A$ is the parameter for the axial vector transformation. The fermionic mass term transforms as

$$m_\Psi \bar{\Psi}\Psi \longrightarrow m_\Psi \bar{\Psi}\Psi - 2im_\Psi \gamma_5 \bar{\Psi} \vec{\theta}_A \vec{\tau} \Psi, \quad (4.67)$$

and is therefore not invariant under an axial vector transformation. This means that the spontaneous breaking of the $\mathcal{O}(N)$ symmetry in the bosonic sector breaks the $SU(N_f)_A$ symmetry in the fermionic sector and therefore also breaks chiral symmetry.

We demonstrated in this section, how the spontaneous symmetry breaking of an $\mathcal{O}(N)$ symmetric scalar field theory interacting with chiral fermions also spontaneously breaks chiral symmetry and dynamically induces a fermionic mass. This procedure is not only restricted to a scalar field theory with an $\mathcal{O}(N)$ symmetry, but generalizes to arbitrary systems of mixed bosons and fermions interacting with each other [50]. As long as the fermionic field interacts with the bosonic one in a Yukawa-type interaction and the breaking of the symmetry in the bosonic sector causes a condensate to appear – the ground state of this potential in the new phase – a fermionic mass will be generated.

In Chapter 5, we will use a similar mixed system consisting of fermions and bosons that interact with each other through a Yukawa interaction, and compute the effects of thermal fluctuations, characterized by the temperature T , quantum fluctuations, characterized by the RG scale k , and gravity, characterized by the curvature of hyperbolically curved space κ . The potential will have a polynomial shape like it did in this chapter,

$$U(\phi) = \frac{\alpha_2}{2} \phi^2 + \frac{\alpha_4}{4!} \phi^4, \quad (4.68)$$

with the couplings now depending on these explicit parameter,

$$\alpha_i \longrightarrow \alpha_{i,k}(T, \kappa). \quad (4.69)$$

The interplay between these parameters will determine how chiral symmetry behaves in the presence of thermal fluctuations and a gravitational background field and even if a critical phase transition might occur.

5. Gravitational Catalysis in Thermal Backgrounds

Chiral symmetry breaking and fermion mass generation is a central feature of interacting fermions relevant for both the Higgs sector of the standard model as well as QCD shaping many properties of matter in the universe. Whereas the long-range limit of gravity in the form of Einstein's general relativity is too weakly interacting to affect the status of chiral symmetry, gravity is expected to become more strongly interacting at or above the Planck scale. Whether or not gravity or its quantized form may exert a strong influence on the chiral features of fermions deserves to be studied. In fact, such an influence may even be used as an observational probe for scenarios of quantum gravity: as suggested in [59], viable scenarios of quantum gravity need to be compatible with the existence of light fermion as observed in Nature – a requirement that has the potential to impose constraints or even rule out certain scenarios of quantum gravity.

It is reassuring to see that quantum fluctuations of the metric do not support the same kind of chiral-symmetry breaking mechanism as is triggered by spin-one gauge fields or Yukawa interactions with scalars [59–67]. For both latter cases, the gauge or Yukawa couplings simply have to increase beyond a certain threshold which renders chiral-symmetry breaking in these scenarios a rather universal strong-coupling feature. This is not so in metric quantum gravity.

By contrast, gravity offers further mechanisms to trigger fermion mass generation which are generic to gravity in the sense that they proceed via the structure of spacetime itself. The most widely studied mechanism occurs on negatively curved spacetimes and can be summarized by *gravitational catalysis* [17]. It appears in a large variety of fermionic models [68–84], as it derives from a mechanism of dimensional reduction of the spectrum of the Dirac operator on hyperbolic spacetimes [85]; (on positively curved spacetimes, curvature effects can still exert an influence on the fermion mass formation in combination with magnetic catalysis [86, 87]). Another mechanism has recently been suggested and worked out in [88]: in quantum gravity scenarios allowing for topology fluctuations, gravitational instantons can contribute to anomalous chiral symmetry breaking and thereby generate fermion masses potentially in conflict with observation. In combination with abelian gauge interactions, gravity can trigger also conventional symmetry breaking mechanisms, as demonstrated in [89].

In this thesis, we further explore pure gravitational catalysis specifically by including the effects of finite temperature. Following an earlier zero-temperature analysis [18, 38], we study the phenomenon using a renormalization-group (RG) inspired scale-dependent approach. The advantage is that we can monitor the RG relevance of chiral interactions in this way. In fact, gravitational catalysis can be connected with four-fermion operators becoming RG relevant driving the symmetry-breaking interactions to criticality [90]. This makes the analysis of gravitational catalysis in the context of quantum gravity scenarios more subtle: It is not sufficient to check, whether the long-range curvature of spacetime is compatible with the existence of light fermions (which obviously is the case). Moreover, the influence of spacetime curvature on the symmetry-breaking operators has to be checked during the whole course of the RG flow, specifically in the Planckian regime and beyond. Provided a notion of curvature exists in that regime, gravitational catalysis could be active and drive the symmetry-breaking operators beyond criticality. This would result in correspondingly heavy fermions removing light fermions from the observable long-range spectrum. The precise connection between the curvature and the induced value of the fermion mass depends on the details of the induced fermion-self interactions, see, e.g., Ref. [90] for an explicit analysis. However, the scale for the induced masses is essentially set by the scale at which the symmetry-breaking operators become critical which in a quantum gravitational context would be clearly linked to the Planck scale.

This mechanism has been explored in [18] which lead to the notion of curvature bounds: in order to guarantee that a given quantum gravity scenario is not affected by the problem of gravitational catalysis, the averaged curvature of a local patch of spacetime should not exceed a certain bound. So far, these bounds have been derived for Riemannian hyperbolic spacetimes such as \mathbb{H}^D in general spacetime dimensions D , cf. [18].

In this thesis, we generalize the analysis to $\mathbb{R} \otimes \mathbb{H}^{D-1}$ or $S^1 \otimes \mathbb{H}^{D-1}$. The purpose is two-fold: first, this provides further information about the concrete dependence of the mechanism on the details of the averaged spacetime structure.

Second, this allows to monitor the influence of finite temperature on the mechanism. The latter is particularly relevant for studying the influence of gravitational catalysis in the course of the cosmological evolution. Indeed, our results provide evidence for a comparatively strong dependence of gravitational catalysis on the details of the background. At the same time, finite-temperature effects can significantly relax the curvature bounds – in line with the expectation that thermal fluctuations drive the system towards the disordered symmetric phase.

5.1. Chiral Channel and Effective Potential

In an RG picture, catalysis of chiral symmetry is triggered by four-fermion operators becoming RG relevant [90]. Considering N_f fermion flavors, we study the RG behavior of four-fermion operators with maximal chiral $U(N_f)_R \times U(N_f)_L$ symmetry as an example.

Operators with a lower degree of symmetry can be studied analogously. We focus on the so-called $(V) + (A)$ channel,

$$S_{\text{int}} \sim \int_x \left[(\bar{\psi}^a \gamma_\mu \psi^a)^2 + (\bar{\psi}^a \gamma_\mu i \gamma_5 \psi^a)^2 \right], \quad (5.1)$$

which is one out of the two Fierz-independent local interaction terms of maximal symmetry [91]. It is Fierz equivalent to the scalar-pseudoscalar channel of the Nambu–Jona-Lasinio (NJL) model which, using the projectors

$$P_L = \frac{\mathbb{1} - \gamma_5}{2}, \quad P_R = \frac{\mathbb{1} + \gamma_5}{2}, \quad \mathbb{1} = P_L + P_R \quad (5.2)$$

onto left and right chiral components, can be re-arranged as

$$S_{\text{int}}[\bar{\psi}, \psi] = -2 \int_x \bar{\lambda} (\bar{\psi}^a P_R \psi^b) (\bar{\psi}^b P_L \psi^a). \quad (5.3)$$

Here, we have introduced a (dimensionful) coupling constant $\bar{\lambda}$ parameterizing the strength of the chiral interaction. In the NJL model, this coupling is tuned beyond a critical value $\bar{\lambda} > \bar{\lambda}_{\text{cr}}$ triggering chiral symmetry breaking in terms of initial conditions. Incidentally, a thermal environment – breaking spacetime symmetries explicitly – allows for further sets of Fierz inequivalent interactions where spatial and temporal components of vector type channels are treated independently [92–94]. In the following, we ignore this potential splitting and concentrate on the NJL channel. Here, we always assume the initial condition to be subcritical such that this operator does not generate fermion masses on its own.

Introducing a non-dynamical Hubbard-Stratonovich field ϕ , the chiral channel can be rewritten in terms of a local Yukawa interaction,

$$\mathcal{L}_{\text{int}}[\phi, \bar{\psi}, \psi] = \bar{\psi}^a [P_L(\phi^\dagger)_{ab} + P_R \phi_{ab}] \psi^b + \frac{1}{2\lambda} \text{tr}(\phi^\dagger \phi). \quad (5.4)$$

The equivalence between Eq. (5.3) and Eq. (5.4) becomes obvious with the aid of the equation of motion for the chiral matrix field,

$$\begin{aligned} \phi_{ab} &= -2\bar{\lambda} \bar{\psi}^b P_L \psi^a, \\ (\phi^\dagger)_{ab} &= -2\bar{\lambda} \bar{\psi}^b P_R \psi^a. \end{aligned} \quad (5.5)$$

This scalar field, in fact, serves as an order parameter for the status of chiral symmetry. E.g.,

assuming a diagonalizable expectation value in flavor space, $\phi_{ab} = \phi_0 \delta_{ab}$ with $\phi_0 > 0$ being homogeneous in spacetime, the chiral group breaks to a residual vector symmetry similar to QCD-like theories, and all fermions acquire masses of order ϕ_0 . Including a fermion kinetic term, the action reads

$$S[\phi_0, \bar{\psi}, \psi] = \int_x \left\{ \bar{\psi} (\not{\nabla} + \phi_0) \psi + \frac{1}{2\lambda} N_f (\phi_0)^2 \right\}. \quad (5.6)$$

Our focus on a homogeneous condensate field ϕ_0 may preclude a study of inhomogeneous condensates for which examples are known that yield a deeper global minimum of the effective potential (or free energy). If such a case occurred for gravitational catalysis, the bounds derived below would even be strengthened. Furthermore, we confine ourselves to integrating out the fermion degrees of freedom and neglect order parameter fluctuations in the following. In this way, we obtain a mean-field expression for the effective potential of the order parameter

$$\begin{aligned} \tilde{U}(\phi_0) &= \frac{N_f}{2\lambda} (\phi_0)^2 - N_f \log \text{Det}_x (\not{\nabla} + \phi_0) \\ &= \frac{N_f}{2\lambda} (\phi_0)^2 - \frac{N_f}{2} \text{Tr}_x \log(-\not{\nabla}^2 + \phi_0^2), \end{aligned} \quad (5.7)$$

where we have used the γ_5 -hermiticity of the covariant Dirac operator in the last step. This mean-field approximation becomes exact in the limit of large fermion flavors $N_f \rightarrow \infty$. With an emphasis on the standard model and its extensions in the following, for which $N_f \geq 22.5$; we expect the mean-field level to be sufficiently accurate for our purposes. It is convenient to introduce the Fock-Schwinger proper-time representation,

$$\tilde{U}(\phi_0) = \frac{N_f}{2\lambda} (\phi_0)^2 + \frac{N_f}{2} \int_0^\infty \frac{ds}{s} e^{-\phi_0^2 s} \text{Tr}_x e^{\not{\nabla}^2 s}, \quad (5.8)$$

in order to arrive at the heat-kernel trace for the present differential operator of interest:

$$\text{Tr}_x e^{\not{\nabla}^2 s} = \text{Tr}_x K(x, x'; s) =: K_D(s). \quad (5.9)$$

The heat kernel $K(x, x'; s)$ satisfies a modified heat flow equation with the following boundary conditions

$$\frac{\partial}{\partial s} K = \not{\nabla}^2 K, \quad \lim_{s \rightarrow 0^+} K(x, x'; s) = \frac{\delta(x - x')}{\sqrt{g}}. \quad (5.10)$$

The proper-time representation is not only useful to evaluate the functional trace of the heat kernel on curved spacetimes, but also allows to regularize this fermionic fluctuation contribution in a scale-dependent and spin-base-invariant [42] fashion: contributions from

the infrared (IR) modes of the fermionic spectrum contribute predominantly to the large- s part of the proptime integral. Hence, these modes can be IR regularized by insertion of a regulator function f_k ,

$$f_k = e^{-(k^2 s)^p}, \quad (5.11)$$

into the proptime integral [95, 96]. The parameter $p > 0$ specifies the renormalization scheme and k corresponds to an IR regularization scale for the eigenvalues of the squared Dirac operator. For $p \rightarrow \infty$, all long range contributions are sharply cut off at the scale $s > 1/k^2$. The scale \sqrt{s} is a measure for the spatiotemporal range of the fluctuating modes. For finite values of p , the regularization scale is smeared out. In the limit $k \rightarrow 0$, the RG insertion factor becomes the identity, and the regularization is thus removed. Starting at an ultraviolet (UV) scale $k = \Lambda$ with the bare potential \tilde{U}_Λ , the potential in the IR at k_{IR} can be computed by

$$\tilde{U}_{k_{\text{IR}}} = \tilde{U}_\Lambda - \int_{k_{\text{IR}}}^\Lambda dk \partial_k \tilde{U}_k, \quad \tilde{U}_\Lambda = \frac{N_f}{2\bar{\lambda}_\Lambda} \phi_0^2, \quad \bar{\lambda}_\Lambda := \bar{\lambda}. \quad (5.12)$$

At intermediate scales k , the scale-dependent effective potential \tilde{U}_k satisfies the flow equation

$$\partial_k \tilde{U}_k = \frac{N_f}{2} \int_0^\infty \frac{ds}{s} e^{-\phi_0^2 s} (\partial_k f_k) K_D(s). \quad (5.13)$$

The advantage of performing the integral over the Schwinger proptime s first is that the cutoff Λ controls the UV divergences and thus assists to identify and fix counter terms for the corresponding relevant and marginal operators.

5.2. Heat Kernels at Finite Temperature

Aiming at an analysis of the scale-dependent effective potential of Eq. (5.13), the information about the spacetime structure enters via the heat-kernel trace $K_D(s)$. As we are interested in the mechanism of gravitational catalysis and the influence of finite temperature, we focus on spacetimes that feature a sufficient amount of negative curvature and allow for a simple use of thermal field theory in imaginary-time formalism. Therefore, a natural choice is $S^1 \otimes H^d$ with a compactified (Euclidean) time and the spatial part corresponding to a maximally symmetric hyperboloid with negative spatial curvature. The decompactified limit then corresponds to the zero-temperature case $\mathbb{R} \otimes H^d$ with a flat time direction.

It is important to emphasize that we do not at all consider these spacetimes as physical descriptions of the large-scale structure of the universe. By means of our scale-dependent

analysis, we focus on effective properties of quantum spacetime, say, in the trans-Planckian regime. Here, nothing specific is known about the microscopic spacetime structure. Hence, our choice of spacetime can be considered as a proxy for a possible structure of local patches of spacetime in that short-distance regime of quantum gravity. For the product manifolds considered here, the square of the Dirac operator can be decomposed as

$$\nabla_D^2 = (\partial_0)^2 + \nabla_d^2, \quad D = d + 1. \quad (5.14)$$

Correspondingly, the heat-kernel trace factorizes,

$$K_D(s) = \text{Tr}_t e^{(\partial_0)^2 s} \cdot \text{Tr}_x e^{\nabla_d^2 s} = K_t(s) \cdot K_d(s), \quad (5.15)$$

Let us first discuss the spatial part $K_d(s)$ for which an analytical result exists and has been worked out for general dimensions d [44]. Focusing in this work on $d = 3$ -dimensional space, the result is particularly simple:

$$K_{d=3}(s) = \frac{1}{(2\sqrt{\pi s})^3} \left(1 + \frac{1}{2} \kappa^2 s \right), \quad (5.16)$$

which holds for an arbitrary curvature parameter

$$\kappa^2 = -\frac{R}{d(d-1)} = -\frac{R}{6} > 0. \quad (5.17)$$

The temporal part depends on the circumference $\beta = \frac{1}{T}$ of the Euclidean time S^1 . Using anti-periodic boundary conditions for the fermionic fields, the trace if performed in momentum space runs over Matsubara frequencies $\omega_n = 2\pi T(n + 1/2)$, yielding

$$K_t(s) = T \sum_{n=-\infty}^{\infty} e^{-\omega_n^2 s} = T \vartheta_2 \left(0, e^{-(2\pi T)^2 s} \right). \quad (5.18)$$

Here we encounter the Jacobi theta function $\vartheta_2(z, q)$. For our purposes, a Poisson resummation connecting ϑ_2 to ϑ_3 is useful for later numerical evaluation. It also gives direct access to analytic studies of the low temperature-limit implying the decompactification $S^1 \rightarrow \mathbb{R}$ of the Euclidean time direction,

$$\begin{aligned} K_t(s) &= T \vartheta_2 \left(0, e^{-(2\pi T)^2 s} \right) \\ &= \frac{\sqrt{\pi}}{\sqrt{(2\pi)^2 s}} \vartheta_3 \left(\frac{\pi}{2}, e^{-\frac{\pi^2}{(2\pi T)^2 s}} \right) \\ &= \frac{1}{\sqrt{4\pi s}} \left[1 - 2 e^{-\frac{1}{4T^2 s}} + \mathcal{O} \left(\left(e^{-(4T^2 s)^{-1}} \right)^2 \right) \right]. \end{aligned}$$

Here, we obtain the standard zero-temperature results $K_t(s) = 1/\sqrt{4\pi s}$ for a fully decom-

pactified temporal direction.

5.3. Curvature Bounds

We are now in a position to derive bounds on the curvature parameter that characterize the parameter space free of gravitational catalysis. For this, we follow the reasoning of [18] and monitor the possible occurrence of nontrivial minima of the effective potential for the chiral order parameter ϕ_0 . In addition to the divergencies associated with matter operators to be renormalized, see next subsection, the effective potential $\tilde{U}(\phi_0)$ displayed, e.g., in Eq. (5.8), also contains a divergent zero-point energy, which we subtract by defining

$$U(\phi_0) = \tilde{U}(\phi_0) - \tilde{U}(0), \quad (5.19)$$

such that $U(0) = 0$ is fixed at the origin in field space [43]. A possible mixing of the subtraction terms with the cosmological-constant term is not considered in this work; we assume the – possibly scale-dependent – behavior of the cosmological constant to be provided by a given quantum gravity scenario (including matter backreactions).

To be more precise, our considerations can make direct contact with quantum gravity scenarios, provided that such a scenario allows for an effective description of spacetime in terms of (pseudo-)Riemannian manifolds with a potentially scale-dependent notion of effective curvature arising by suitably averaging over local patches of spacetime. In the course of the following considerations, we assume all gravity-related parameters to be provided by some quantum gravity scenario; in addition to an effective curvature, this includes potential further gravity-matter couplings, as well as the corresponding scale-dependence of these quantities. In our approach, we will ignore a possible direct contribution of gravity fluctuations to the matter couplings, e.g., to $\bar{\lambda}$; however, such contributions have been found to be less relevant for the status of chiral symmetry of the matter sector [59, 61].

5.3.1. Curvature Bounds at Zero Temperature

Let us first work out the renormalization of the effective potential, identifying all free parameters by accordingly fixing the required renormalization counter terms. Using the preceding results for the heat-kernel traces, the zero-temperature effective potential of Eq. (5.8) upon IR regularization (5.11) and zero-point subtraction (5.19) reads

$$U_k = \frac{N_f}{2\lambda} \phi_0^2 + \frac{N_f}{2(4\pi)^2} \int_0^\infty \frac{ds}{s^3} f_k \left(e^{-\phi_0^2 s} - 1 \right) \left(1 + \frac{1}{2} \kappa^2 s \right). \quad (5.20)$$

A power-counting analysis reveals the occurrence of a quadratic divergence for the ϕ_0^2 operator and two logarithmic divergences for the ϕ_0^4 and $\phi_0^2 R$ operators, respectively.

As a sufficient criterion for the occurrence of chiral symmetry breaking, we specifically monitor the sign of the ϕ_0^2 term in the Taylor expansion of the effective potential. If this sign turns negative, the ϕ_0^4 operator cannot inhibit chiral symmetry breaking. For the curvature bound derived below, the ϕ_0^4 operator is thus not relevant; from here on, we assume it to be properly renormalized such that the coupling has some finite value at the scale k at which we consider the theory. We add that the sign criterion of the ϕ_0^2 is not a necessary criterion for chiral symmetry breaking, as first-order-type transitions to a broken phase could go along with a positive ϕ_0^2 term. We ignore this option in the following; if it was realized our curvature bound would even get stronger.

The remaining divergences can conveniently be identified by using the flow equation (5.13), inserting the regulator (5.11) and expanding in ϕ_0 . To leading order, we obtain

$$\partial_k U_k = \frac{k N_f \phi_0^2}{2(4\pi)^2} \left[2 \Gamma \left(1 - \frac{1}{p} \right) + \frac{\kappa^2}{k^2} \right] + \mathcal{O}(\phi_0^4). \quad (5.21)$$

Here, we observe a divergence for the case of a regularization parameter $p = 1$.

This is expected, as this value would correspond to a mass-type Callan-Symanzik regularization scheme which is known to be insufficient for an adequate suppression of UV modes in 4 dimensions. In order not to be affected by this artificial divergence from the regulator, we suggest to use schemes with $p \geq 2$.

Next, we integrate the flow from an IR scale k_{IR} to a UV scale Λ , using for the UV boundary condition not only the flat space expression as in Eq. (5.12), but also including a possible scalar-curvature counter term,

$$U_\Lambda(\phi_0) = \frac{N_f}{2\lambda_\Lambda} \phi_0^2 + N_f \xi_\Lambda \phi_0^2 R, \quad (5.22)$$

with a UV coupling ξ_Λ . The resulting effective potential at $k = k_{\text{IR}}$ then reads up to order ϕ_0^2 and ignoring terms of order $\mathcal{O}(1/\Lambda)$:

$$U_{k_{\text{IR}}} = -\frac{N_f \phi_0^2}{2} \left(\frac{1}{\bar{\lambda}_{\text{cr}}} - \frac{1}{\bar{\lambda}_\Lambda} - \frac{k_{\text{IR}}^2}{16\pi^2} \Gamma \left(1 - \frac{1}{p} \right) \right) - 6N_f \xi_{k_{\text{IR}}} \phi_0^2 \kappa^2 + \mathcal{O}(\phi_0^4). \quad (5.23)$$

Here, we have introduced the (scheme-dependent) critical coupling of the chiral channel

$$\bar{\lambda}_{\text{cr}} = \frac{16\pi^2}{\Lambda^2 \Gamma \left(1 - \frac{1}{p} \right)}, \quad (5.24)$$

and defined the finite scalar-curvature coupling at the scale k_{IR} as

$$\xi_{k_{\text{IR}}} = \xi_{\Lambda} + \frac{1}{12(4\pi)^2} \log \left(\frac{\Lambda}{k_{\text{IR}}} \right). \quad (5.25)$$

In this work, we consider $\xi_{k_{\text{IR}}}$ to be a free parameter to be determined by the underlying quantum gravity theory. Equation (5.23) can be interpreted as follows: the first line contains the information about the symmetry status in flat spacetime. In a subcritical regime, e.g. $\bar{\lambda}_{\Lambda} < \bar{\lambda}_{\text{cr}}$, the mass-like term remains positive for zero curvature, indicating that the origin, $\phi_0 = 0$, is a local minimum of the potential (in fact, it is also a global one); hence the system is in the disordered phase and the fermion mass remains zero. In the supercritical regime however, e.g. $\bar{\lambda}_{\Lambda} > \bar{\lambda}_{\text{cr}}$, the mass-like term in the first line can become negative for decreasing k_{IR} resulting in a nontrivial minimum $\phi_0^2 > 0$ in the long-range limit. This implies chiral symmetry breaking and fermion mass generation in flat spacetime. Now, the second line of Eq. (5.23) contains the curvature contributions resulting from the hyperbolically curved space. Assuming $\xi_{k_{\text{IR}}}$ to be positive, the prefactor of this second term is negative and can therefore cause chiral symmetry breaking depending on the magnitude of the terms in the first line. Of course, we assume the fermionic self-interactions to be subcritical, otherwise the system would be in an NJL-like phase which does not conform with the low-mass scale of the standard-model fermions. While finite values of $\bar{\lambda}_{\Lambda}$ are expected to be generated by gauge and Yukawa interactions, we use the following simple estimate for the first line of Eq. (5.23):

$$-\frac{\phi_0^2}{2} \left(\frac{1}{\bar{\lambda}_{\text{cr}}} - \frac{1}{\bar{\lambda}_{\Lambda}} - \frac{k_{\text{IR}}^2}{16\pi^2} \Gamma \left(1 - \frac{1}{p} \right) \right) \geq \phi_0^2 \frac{k_{\text{IR}}^2}{32\pi^2} \Gamma \left(1 - \frac{1}{p} \right). \quad (5.26)$$

Comparing this to the curvature-dependent contribution $\sim \xi_{k_{\text{IR}}}$, we conclude that gravitational catalysis does not occur, if the ratio of the curvature of local patches of spacetime to the energy scale satisfies

$$\frac{\kappa^2}{k_{\text{IR}}^2} \leq \frac{\Gamma \left(1 - \frac{1}{p} \right)}{192\pi^2 \xi_{k_{\text{IR}}}}. \quad (5.27)$$

Any finite value of the fermionic self-interaction $\bar{\lambda}_{\Lambda}$ at the high scale would even strengthen the bound. We observe an apparent explicit scheme dependence of our bound through the regularization parameter p . For the region $2 \leq p < \infty$, this dependence is rather mild, since $1 < \Gamma(1 - \frac{1}{p}) \leq \sqrt{\pi}$. However, it should be noted that also the left-hand side carries an implicit scheme dependence, since the dimensionless ratio of curvature – which we consider as an effective curvature of spacetime patches – and the IR scale k_{IR} depends on the details of the spacetime averaging procedure. As the latter, if done explicitly, would go hand in hand with the average over the fermionic fluctuations on various length scales, we expect the

existence of such a bound as in Eq. (5.27) to have a universal meaning. We take the residual p dependence of (5.27) as a measure for our ignorance of the details of the averaging process. It is instructive to compare this result for the $\mathbb{R} \otimes H^3$ background with the corresponding bound for the maximally symmetric case H^4 . Here, the heat-kernel trace is a nonpolynomial function of the curvature leading to an integral representation of the curvature bound [18]. For the purpose of the present discussion, we use the simple analytic approximation also given in [18]:

$$H^4 : \frac{\kappa^3}{k_{\text{IR}}^3} + \frac{4}{3} \frac{\pi^{\frac{5}{2}}}{\Gamma\left(1 + \frac{1}{2p}\right)} \xi_{k_{\text{IR}}} \frac{\kappa^2}{k_{\text{IR}}^2} \leq \frac{\sqrt{\pi}}{2} \frac{\Gamma\left(1 - \frac{1}{p}\right)}{\Gamma\left(1 + \frac{1}{2p}\right)}. \quad (5.28)$$

Apart from numerical factors, the main difference arises from the first term $\sim \kappa^3$ in the H^4 case which is present independently of the marginal scalar-curvature coupling $\sim \xi$. Though the curvature bound itself does depend on the precise value of $\xi_{k_{\text{IR}}}$ also in H^4 , there is a meaningful bound for any value of, say, $\xi_{k_{\text{IR}}} \sim \mathcal{O}(1)$ with $\xi_{k_{\text{IR}}} = 0$ being a legitimate choice. This is not the case for our present result (5.27) for the bound which depends strongly on $\xi_{k_{\text{IR}}}$, yielding no meaningful result for $\xi_{k_{\text{IR}}} = 0$. The reason for this strong dependence lies in the fact that the heat-kernel trace on H^3 has the particularly simple polynomial form given in Eq. (5.16), the contribution of which to the effective potential can be fully absorbed in the renormalization of the marginal scalar-curvature coupling ξ .

We draw the following conclusions from this observation: first, this strong qualitative and quantitative difference between the curvature bounds of two example spacetimes with negative curvature demonstrates that the details of the average spacetime structure in the (trans-)Planckian regime of quantum gravity can take a strong influence on the presence or absence of gravitational catalysis. If a bound derived for one case is satisfied it may still be violated in another case. Since we have little access to general knowledge about the average spacetime structure in this short-distance regime where spacetime itself is expected to be strongly fluctuating, the exclusion of gravitational catalysis in order to reach compatibility with the existence of light fermions can thus be decisive criterion for the viability of a quantum gravity scenario.

Second, in addition to information about the averaged spacetime structure of local spacetime patches, a quantum gravity (plus matter) scenario has to provide also a prediction of the scalar curvature coupling ξ in order to test for gravitational catalysis. Since the scalar field in the present analysis arises from fermion interactions which may arise predominantly from classically scale-invariant gauge interactions, the use of a conformally coupled scalar field is a reasonable first guess.

5.3.2. Curvature Bounds at Finite Temperature

As in the zero-temperature case, we now derive curvature bounds from the effective potential for the chiral order parameter. For this, we write the regularized effective potential as

$$U_k^T = U_k + \Delta_T U_k, \quad (5.29)$$

where U_k denotes the zero-temperature part, cf. Eq. (5.20), and $\Delta_T U_k$ is the thermal correction satisfying $\Delta_{T=0} U_k = 0$. Based on the heat-kernel traces, this thermal part can be written as

$$\begin{aligned} \Delta_T U_k &= \frac{N_f}{2(4\pi)^2} \int_0^\infty \frac{ds}{s^3} f_k \left(e^{-\phi_0^2 s} - 1 \right) \left(1 + \frac{1}{2} \kappa^2 s \right) \\ &\quad \times \left[\vartheta_3 \left(\frac{\pi}{2}, e^{-\frac{\pi^2}{(2\pi T)^2 s}} \right) - 1 \right]. \end{aligned} \quad (5.30)$$

Since the presence of finite temperature does not modify the UV behavior of the theory, this expression is already finite. No further counterterms are required, and we consider all physical parameters to be fixed by the $T = 0$ renormalization conditions. After the substitution $\tilde{s} = k_{\text{IR}}^2 s$, the thermal correction to the effective potential up to quadratic order in ϕ_0 reads

$$\Delta_T U_k = \frac{N_f}{32\pi^2} \left[A^p(\zeta) \cdot k_{\text{IR}}^2 + C^p(\zeta) \cdot \kappa^2 \right] \phi_0^2, \quad \zeta = \frac{T}{k_{\text{IR}}}, \quad (5.31)$$

with the temperature-dependent coefficients functions

$$A^p(\zeta) = -\frac{1}{2} \int_0^\infty \frac{d\tilde{s}}{\tilde{s}^2} e^{-\tilde{s}^p} \left[\vartheta_3 \left(\frac{\pi}{2}, e^{-\frac{1}{4\zeta^2 \tilde{s}}} \right) - 1 \right], \quad (5.32)$$

$$C^p(\zeta) = -\frac{1}{4} \int_0^\infty \frac{d\tilde{s}}{\tilde{s}} e^{-\tilde{s}^p} \left[\vartheta_3 \left(\frac{\pi}{2}, e^{-\frac{1}{4\zeta^2 \tilde{s}}} \right) - 1 \right] \quad (5.33)$$

that depend on the regularization scheme parameter p and the rescaled temperature $\zeta = T/k_{\text{IR}}$. Both functions vanish in the zero-temperature limit, $A^p, C^p|_{\zeta \rightarrow 0} = 0$ for any legitimate scheme parameter p . The quadratic part of the effective potential at finite temperature can be expressed through these coefficients functions

$$\begin{aligned} U_{k_{\text{IR}}}^T &= -\frac{N_f \phi_0^2}{2} \left[\frac{1}{\lambda_{\text{cr}}} - \frac{1}{\lambda_\Lambda} - \frac{k_{\text{IR}}^2}{16\pi^2} \left(\Gamma \left(1 - \frac{1}{p} \right) + A^p(\zeta) \right) \right] \\ &\quad - N_f \kappa^2 \left(6\xi_{k_{\text{IR}}} - \frac{1}{32\pi^2} C^p(\zeta) \right) \phi_0^2 + \mathcal{O}(\phi_0^4), \end{aligned} \quad (5.34)$$

leading to the temperature-dependent curvature bound

$$\frac{\kappa^2}{k_{\text{IR}}^2} \leq B^p(\zeta) := \frac{\Gamma\left(1 - \frac{1}{p}\right) + A^p(\zeta)}{192\pi^2 \xi_{k_{\text{IR}}} - C^p(\zeta)}. \quad (5.35)$$

This bound represents a central result of our work. The integrals for the coefficients $A^p(\zeta)$ and $C^p(\zeta)$ can be evaluated numerically for arbitrary p rather straightforwardly. For analytic estimates, we expand the thermal part of the heat kernel, excluding the zero temperature contribution, in a Taylor expansion for the second argument of the Jacobi theta function

$$\left[\vartheta_3\left(\frac{\pi}{2}, e^{-\frac{\pi^2}{(2\pi T)^2 s}}\right) - 1 \right] = 2 \sum_{n=1}^{\infty} (-1)^n e^{-\frac{n^2}{4\zeta^2 s}}. \quad (5.36)$$

We observe that the contributions decrease exponentially for each additional order suggesting that expansions truncated at a certain order N can still represent a quantitatively accurate approximation up to a certain temperature. Expanding the thermal coefficients from Eq. (5.32) accordingly, we can express the result to all orders in the expansion by the two functions $a^p(z)$ and $c^p(z)$, respectively,

$$\begin{aligned} A^p(\zeta) &= - \sum_{n=1}^{\infty} (-1)^n \int_0^{\infty} \frac{d\tilde{s}}{\tilde{s}^2} e^{-\tilde{s}^p} e^{-\frac{n^2}{4\zeta^2 \tilde{s}}} \\ &=: \sum_{n=1}^{\infty} (-1)^n a^p(\zeta/n), \end{aligned} \quad (5.37)$$

$$\begin{aligned} C^p(\zeta) &= -\frac{1}{2} \sum_{n=1}^{\infty} (-1)^n \int_0^{\infty} \frac{d\tilde{s}}{\tilde{s}} e^{-\tilde{s}^p} e^{-\frac{n^2}{4\zeta^2 \tilde{s}}} \\ &=: \sum_{n=1}^{\infty} (-1)^n c^p(\zeta/n). \end{aligned} \quad (5.38)$$

These functions can be computed analytically for the scheme parameters $p = 1$ and $p = \infty$ and yield

$$a^{p=1}(z) = -8z K_1\left(\frac{1}{z}\right), \quad (5.39)$$

$$a^{p=\infty}(z) = -8z^2 e^{-\frac{1}{4z^2}}, \quad (5.40)$$

$$c^{p=1}(z) = -2K_0\left(\frac{1}{z}\right), \quad (5.41)$$

$$c^{p=\infty}(z) = \text{Ei}\left(-\frac{1}{4z^2}\right), \quad (5.42)$$

with $K_n(z)$ being the modified Bessel functions of the second kind, and $\text{Ei}(z)$ the exponential integral. Whereas the choice $p = 1$, corresponding to the Callan-Symanzik regulator, is

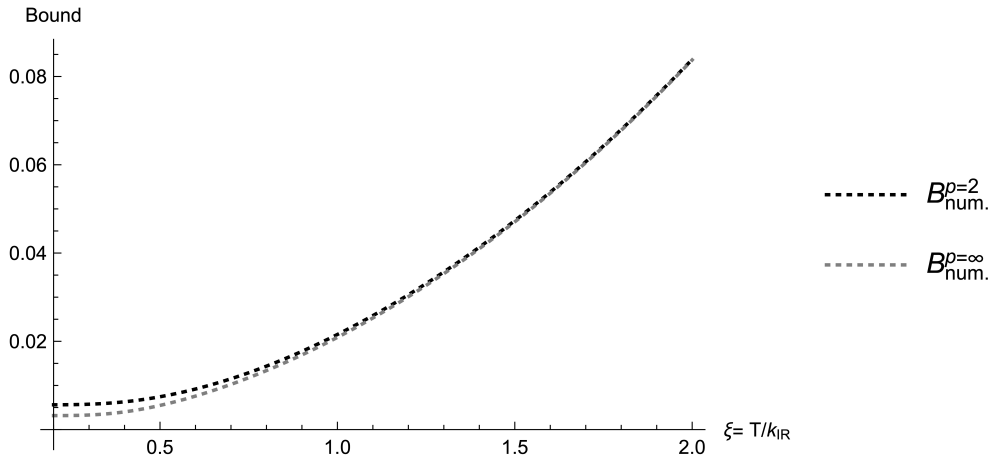


Fig. 5.1.: Numerical result for the curvature bound $B^p(\zeta)$ of Eq. (5.35) as a function of the rescaled temperature $\zeta = T/k_{\text{IR}}$ for regularization-scheme parameters $p = 2$ and $p = \infty$, respectively. The comparatively mild scheme dependence at zero temperature even weakens for increasing temperature.

insufficient for regularizing the quantum fluctuations as discussed above, there is no problem using it for the thermal part. While setting $p = 2$ for the quantum and $p = 1$ for the thermal fluctuations does not correspond to a fully consistent regularization scheme, the comparison between $p = \infty$ and the “ $p = 1, 2$ ” scheme can be used for analytical estimates of the scheme dependence. A full numerical comparison between the extreme choices $p = 2$ and $p = \infty$ is shown in Fig. 5.1. Here, the bound $B^p(\zeta)$ of Eq. (5.35) is shown as a function of rescaled temperature for the two schemes. While there is a quantitative difference for low temperatures which reflects the scheme dependences found in Eq. (5.27) for $T = 0$, this difference significantly weakens for increasing temperature. This enhances the predictivity of our quantitative estimates for the finite-temperature case. A fully analytical estimate is obtained by truncating the series in Eqs. (5.37) and (5.38) at a finite order in N using, say, the $p \rightarrow \infty$ scheme. In Fig. 5.2, we compare increasing orders for $N = 1, 3, 5$ with the corresponding full numerical result. We observe that already low-order estimates reflect the full behavior qualitatively rather well. For increasing order, also the quantitative precision increases. For instance, for $N = 15$ no difference between the analytical estimate and the numerical result would be visible in Fig. 5.2 in the shown regime of rescaled temperatures as large as $\zeta = 100$. The large- ζ behavior of the bound fits well to quadratic increase. A numerical fit yields $B^p(\zeta) \simeq 0.02\zeta^2$ for the leading high-temperature behavior. This matches also with the qualitative behavior of the large-temperature expansion of the heat-kernel. For the application of our curvature bound to a quantum gravity scenario below, we simply use the analytical estimate $B^{p \rightarrow \infty}(\zeta)$ for $N = 15$, as it is sufficiently accurate for all values of rescaled temperature ζ of interest.

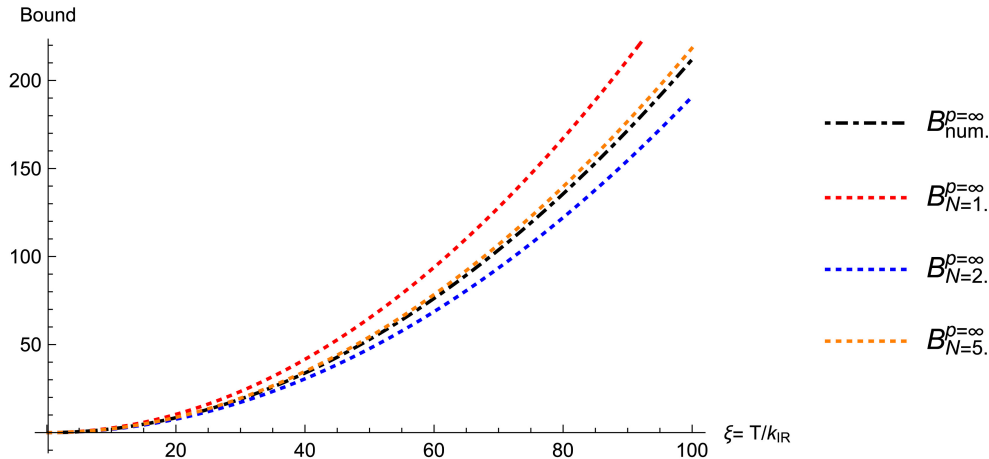


Fig. 5.2.: Numerical result for the curvature bound $B^{p \rightarrow \infty}(\zeta)$ of Eq. (5.35) as a function of the rescaled temperature $\zeta = T/k_{\text{IR}}$ in comparison with the analytical estimates of Eqs. (5.37) (5.38) for increasing truncations N . Even for large values of ζ , the analytical estimates approach the full result rather rapidly. For large temperatures, the curvature bound increases $\sim \zeta^2$.

5.4. Asymptotically Safe Gravity: from Curvature Bound to Matter Bound

The preceding results can be applied to generic quantum gravity scenarios as soon as they feature an effective metric based description below a certain high-energy scale. For this, we assume that such a scenario provides information about the effective spacetime structure at short-distance scales, e.g., in the form of a possibly scale-dependent effective metric, $\langle g_{\mu\nu} \rangle_k$. In addition, we assume that the quantum gravity scenario also accommodates a model of the cosmological evolution going along with a scale-dependent evolution of the temperature. In fact, the asymptotic-safety scenario for quantum gravity [6, 8, 97, 98] has witnessed rapid progress over the past two decades, as, e.g., reviewed in [13, 47, 99–106], and is thus able to provide us with required estimates also including matter degrees of freedom [63, 67, 89, 107–116]. The scenario therefore serves as an example in the following. Let us briefly summarize the corresponding line of argument developed in [18], generalizing it to the presence of finite temperature during a cosmological evolution. For simplicity, we work in the so-called Einstein-Hilbert truncation, assuming that higher-order curvature operators – though relevant for a more accurate picture of the UV behavior [9, 108, 117–128] – do not take a strong influence on the RG trajectory at the effective scales considered here. Incidentally, this approximation could straightforwardly be improved, e.g., by considering trajectories as in [129]. The effective scale-dependent metric obeys the quantum equation of motion which

– on the Einstein-Hilbert level – corresponds to Einstein’s equations,

$$R_{\mu\nu}(\langle g \rangle_k) - \frac{1}{2}R(\langle g \rangle_k)\langle g_{\mu\nu} \rangle_k + \bar{\Lambda}_k \langle g_{\mu\nu} \rangle_k = 0 \quad (5.43)$$

Within the asymptotic-safety scenario, the dimensionless version of the scale-dependent cosmological parameter $\bar{\Lambda}_k$ is governed by the Reuter fixed point, i.e., a non-Gaussian UV fixed point λ_* , in the trans-Planckian region of the RG flow. Even though typical RG trajectories appear to spiral around the fixed point towards the UV, i.e., quantitatively relevant values potentially oscillate about λ_* during the course of the RG evolution, we use this fixed-point value as an estimate for the effective curvature of local spacetime patches averaged over a length scale $\sim 1/k_{\text{IR}}$. Since the background $S^1 \otimes \mathbb{H}^3$ chosen for our finite temperature analysis is not a solution to the Einstein equation (5.43), i.e. it is not of Friedman-Lemaître-type, we cannot unambiguously link our background-curvature parameter κ to the fixed-point value λ_* of the asymptotic-safety scenario. In the following, we use the trace of the Einstein equation, which yields in the fixed point regime:

$$\frac{R}{k_{\text{IR}}^2} = 4\lambda_*. \quad (5.44)$$

Alternatively, we could use solely the spatial components of the Einstein equation for which \mathbb{H}^3 is a solution; in this case, a factor of 6 would replace the factor of 4 on the right-hand side of Eq. (5.44), mildly modifying our quantitative results below. In the following, we use the trace prescription leading to Eq. (5.44), as it implements isotropy on the level of the equation of motion. By means of this relation, the asymptotic-safety scenario relates the curvature of local spacetime patches in the trans-Planckian regime to the fixed-point value of the cosmological parameter. In those regimes where the latter is positive our curvature bounds are irrelevant, as they are automatically fulfilled. Hence, we concentrate on the case where $\lambda_* < 0$, for which we obtain an estimate for our curvature parameter:

$$\frac{\kappa^2}{k^2} = \frac{2|\lambda_*|}{3} > 0, \quad \text{for } \lambda_* < 0. \quad (5.45)$$

A crucial observation within the asymptotic-safety scenario is that the fixed-point properties depend on the matter content [107, 109, 130], i.e., on the nature of the fluctuating quantum degrees of freedom coupling to gravity. In the present setting, the dependence of λ_* on this matter content comes in through two parameter combinations:

$$d_g = N_S - 4N_V + 2N_f, \quad d_\lambda = N_S + 2N_V - 4N_f, \quad (5.46)$$

where N_S counts the number of scalar degrees of freedom, N_V denotes vector degrees of freedom, and N_f is the flavor number as before. (Here, we quote results for the so-called type IIa regulator [101] which accounts for the appropriate endomorphisms of the Laplacians

for particles with spin [109]). The precise dependence of λ_* on these matter parameters is not yet fully determined. Current results show some dependence on the details of the non-perturbative approximation, see e.g. [61, 101, 109, 131]. A quantitative comparison concerning gravitational catalysis in the zero-temperature limit can be found in [18]. Roughly speaking, λ_* in simple approximations is proportional to d_λ , such that a dominant number of fermion flavors N_f moves the system towards the region where gravitational catalysis could become relevant. For the following quantitative discussion, we use the fixed-point results of [131] and their dependence on d_g and d_λ as an example. We focus on the regularization scheme $p \rightarrow \infty$, and – unless stated otherwise – assume the scalar-curvature coupling at its conformally coupled point $\xi_{k_{\text{IR}}} = 1/6$ which is known to be a fixed-point of the universal part of the perturbative RG [116, 132–134]; the dependence of our quantitative results on $\xi_{k_{\text{IR}}}$ is also studied below. In order to complete the concrete scenario of our investigation, we need to connect the scale k_{IR} at which we consider the system with a value (or range of values) for the temperature T . In a specific cosmological model, the temperature would be connected with a relevant cosmological scale, say, a time parameter or an expansion scale. Within asymptotically-safe cosmologies, such scales are assumed to be linked to some suitable power of k by RG-improvement arguments [135–143]. In fact, several scale-setting procedures have been discussed in the literature [136, 143–145]. For the present study, we therefore use the rescaled temperature $\zeta = T/k_{\text{IR}}$ as a parameter, the value (or range of relevant values) will be fixed by a specific choice of the cosmological model. Simple RG-improvement arguments suggest to consider $\zeta \sim \mathcal{O}(1)$. Since or zero-temperature bound on $\mathbb{R} \otimes H^3$ is quantitatively stronger than the corresponding one on H^4 for $\xi_{k_{\text{IR}}} = 0$ as used in [18], we expect a correspondingly larger extent of the regime where gravitational catalysis could be active. Given our result that the curvature bound (5.35) weakens for increasing temperature, the region which is not affected by gravitational catalysis should increase with ζ . In fact, this is visible in Fig. 5.3: here the orange region in the upper part of the plot indicates the region where λ_* is positive in the asymptotic-safety scenario, hence this region is not affected by gravitational catalysis.

At finite rescaled temperature $\zeta = T/k_{\text{IR}}$, the solid lines separate the regions in this space of asymptotically safe theories with matter which are free of gravitational catalysis (regions above/left of lines) from those where our curvature bound is violated and gravitational catalysis could trigger fermion mass generation (darker shaded regions below/right of lines). In fact, the curvature bound for $\zeta = 0$ is rather close to the $R > 0$ curve with only a slim unaffected region extending along the negative d_g axis (hardly visible on the scale of this Fig. 5.3). This agrees with the comparatively strong curvature bound on $\mathbb{R} \otimes H^3$ for $\xi_{k_{\text{IR}}} = 1/6$ and should be taken as an indication that gravitational catalysis might be more relevant than previously anticipated for the H^4 background. In other words, the details of the spacetime structure of local spacetime patches do matter beyond the simple statement of positive or negative average curvature and thus need to be addressed by the quantum-gravity

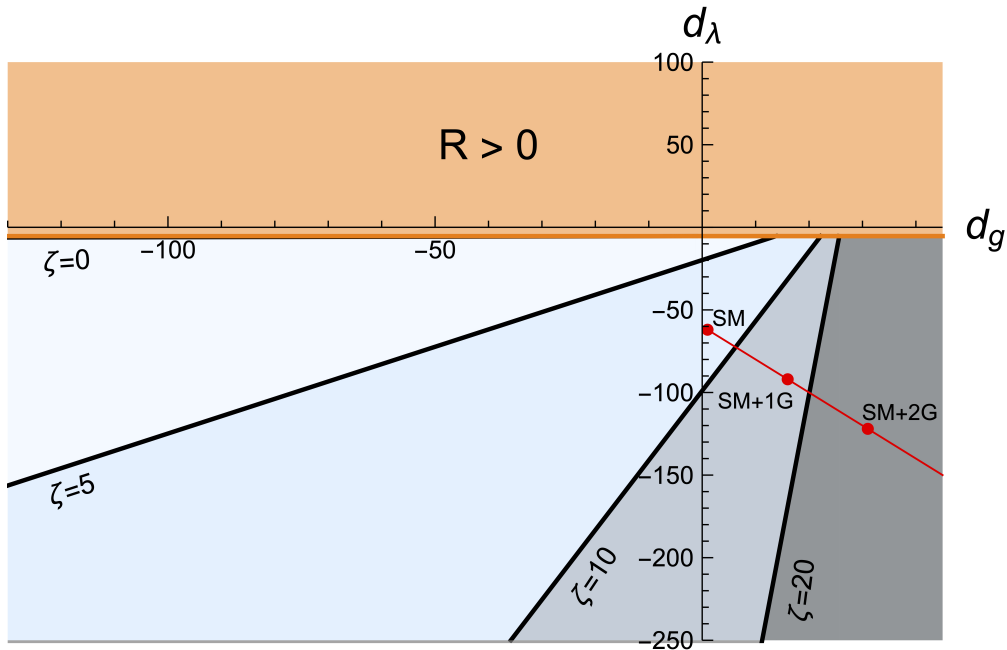


Fig. 5.3.: Space of asymptotically-safe quantum gravity theories with matter parametrized by d_g and d_λ according to Eq. (5.46). The orange area corresponds to regions with positive curvature. Each of the four solid lines distinguish regions free from gravitational catalysis (region above/left of each line) from regions that violate our curvature bound and could feature chiral symmetry breaking through gravitational catalysis (darker shaded region below/right of each line) – for the rescaled temperatures $\zeta = 0$ (barely visible in the upper left sector), 5, 10, and 20. The red dot marks the Standard Model (SM) matter content with the red line indicating the Standard Model with additional fermionic generations.

scenario under scrutiny.

For increasing rescaled temperature ζ the region satisfying the curvature bound increases; for $\zeta > \mathcal{O}(10)$, the boundary line approaches a vertical line that ultimately matches with a region where the computation of [131] does no longer find a viable UV fixed point.

It is interesting to observe that the standard model (SM) matter content with three generations and thus $N_S = 4$, $N_V = 12$ and $N_f = 45/2$ (excluding right-handed neutrino components) (red dot in Fig. 5.3) lies in the region violating the bound for small ζ but satisfying the bound for $\zeta > 8.3$ for the current assumptions. This illustrates directly that a given quantum gravity scenario does not automatically allow for an arbitrary matter content. Depending on the details of the local spacetime curvature, gravitational catalysis could be relevant and needs to be carefully scrutinized in this regime.

At the same time, our current study also reveals, how gravitational catalysis endangering the existence of light fermions could be tamed in the course of the cosmological evolution: even a critical spacetime curvature violating the zero-temperature bound may not give rise to gravitational catalysis and fermion mass generation provided the temperature remains sufficiently high compared to the averaging scale k_{IR} . From an RG perspective, this can be understood in terms of the thermal masses of the fermions, which effectively suppress the

fermionic fluctuations. This inhibits the symmetry breaking channels to become RG relevant as predicted by zero-temperature catalysis. A similar mechanism has been investigated in scenarios of Higgs inflation in order not to be affected by further minima in the Higgs potential [146].

This argument can also be inverted: in order to evading gravitational catalysis for a given matter content in asymptotically safe gravity, the cosmological evolution in the early universe has to go along with a sufficiently high (rescaled) temperature. In this way, gravitational catalysis can put bounds on the cosmological model.

As we parametrize such models using the rescaled temperature, a given value of ζ – which should be understood as a lowest value in a given model in the early universe – can accommodate a certain matter content. In order to illustrate this dependence, we concentrate on standard-model-like theories possibly with extra generations of fermions. In Fig. 5.3, these theories move along the red line towards the region increasingly endangered by gravitational catalysis with the cases of additional complete generations (“+1G”, “+2G”) marked by red dots.

By virtue of the fixed-point structure, an arbitrarily large number of fermions is not supported. This is visible in Fig. 5.4, where the allowed number of fermions N_f compatible with our bound is plotted as a function of ζ . The observed threshold set by the standard-model fermion content is marked by a horizontal dashed line; it is surpassed for $\zeta > 8.3$. Even at asymptotic temperatures, a maximum fermion number of $N_{f\text{max}} = 35.5$ is approached. In this figure, we also illustrate the scheme dependence of our finite temperature results by showing the extremal parameter choices $p \rightarrow \infty$ and the mixed approximate scheme $p = 1, 2$. On the scale of this figure, hardly any variation is recognizable, which illustrates that the scheme-dependencies are under control here.

By contrast, there is a stronger dependence on the scalar-curvature coupling $\xi_{k_{\text{IR}}}$. Nevertheless, while the zero-temperature bound is inversely proportional to and thus rather strongly varying with $\xi_{k_{\text{IR}}}$, the finite-temperature results are somewhat less sensitive. This is visible in Fig. 5.5, where the number of fermions N_f that can be accommodated is shown for $\xi_{k_{\text{IR}}} = 0.05$ and $\xi_{k_{\text{IR}}} = 1$. Both curves eventually surpass the standard-model threshold, however for different values of the rescaled temperature.

In summary, the asymptotic-safety scenario for quantum gravity together with standard-model matter content can evade the curvature bound imposed by gravitational catalysis provided the temperature is sufficiently high in the course of the cosmological evolution. By contrast, theories with a more dominant fermionic matter content either require much higher temperatures to comply with the bounds or fail to support a UV-completing fixed point.

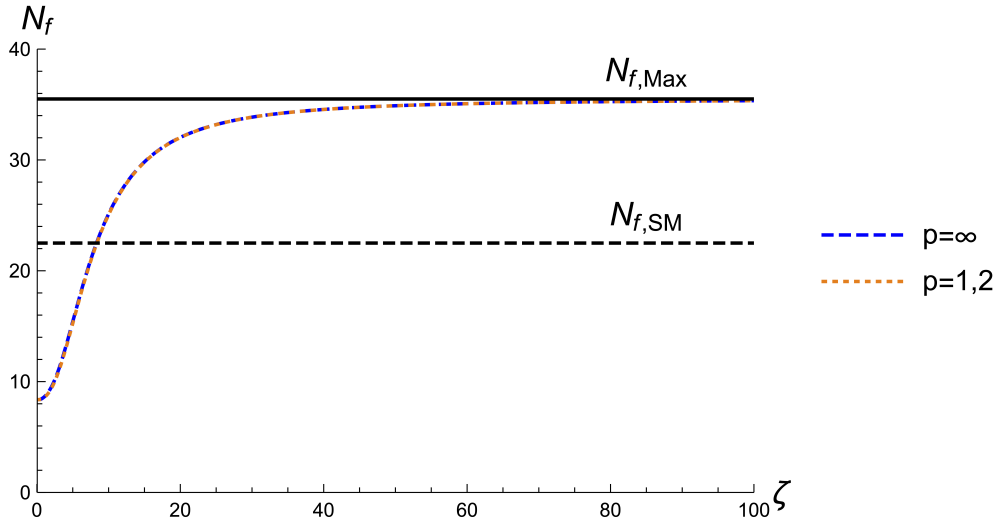


Fig. 5.4.: Number of fermion species for a standard-model-like particle content ($N_S = 4, N_V = 12$) compatible with the curvature bound from gravitational catalysis as a function of the rescaled temperature ζ for different regularization schemes p and the scalar-curvature coupling $\xi_{k_{\text{IR}}} = 1/6$. The solid black line represents the upper bound $N_{f, \text{Max}} = 35.5$ which is approached in the limit $\zeta \rightarrow \infty$; the dashed line marks the number of fermions in the standard model $N_{f, \text{SM}} = 22.5$.

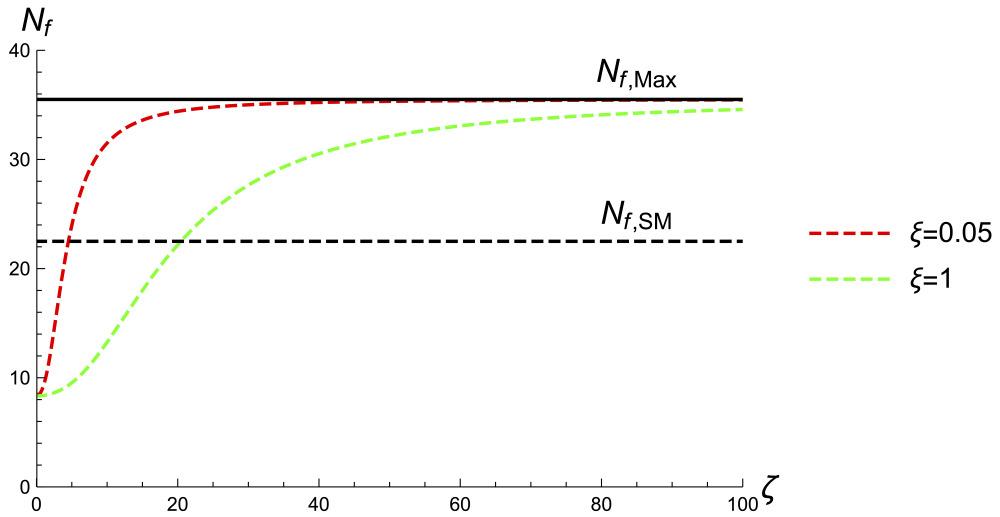


Fig. 5.5.: Number of fermion species for a standard-model-like particle content ($N_S = 4, N_V = 12$) compatible with the curvature bound from gravitational catalysis as a function of the rescaled temperature ζ for different scalar-curvature coupling parameters $\xi_{k_{\text{IR}}}$ using the regularization scheme $p = \infty$. The horizontal lines are as in Fig. 5.4.

6. Asymptotically Safe Hilbert-Palatini Gravity

For the approach to quantizing gravity both the degrees of freedom to be quantized as well as the correct quantization method are a matter of intense debate. A priori different choices could lead to different potentially consistent theories of quantum gravity ultimately requiring experimental data to single out the theory realized in nature.

It is well known that – already on the classical level – very different choices for the degrees of freedom can lead to the same classical equation of motion, namely Einstein’s equation [147–150]. This includes of course the maybe simplest choice being the metric, but also the vierbein, possibly in combinations with various forms of connections. Of course, classical equivalence does not entail quantum equivalence, therefore different choices might rather be expected to lead to different quantum theories.

In turn, different choices of degrees of freedom or even the quantization procedure could finally describe the same quantum theory if they lead to the same universality class as for instance identified by a renormalization group analysis. In discrete approaches this can be indicated by the presence of a second order phase transition or even quantified in terms of critical exponents of a corresponding quantum critical point; in the context of gravity, cf. [151–154].

Research in recent years has accumulated evidence that such a quantum critical point exists for gravity when using the metric as the fundamental degree of freedom together with a (standard) quantization procedure that is able to capture non-perturbative information. The latter is necessary, since the quantum critical point corresponds to a fixed point of the renormalization group at a finite coupling, realizing Weinberg’s asymptotic safety scenario for Einstein gravity [6, 97]. This Reuter fixed point has been discovered by applying functional renormalization group (RG) methods to gravity [8], and confirmed in many refined studies, see [13, 46, 102, 103, 105, 106] for recent reviews.

Functional RG methods and a classification of universality classes [155] are not limited to the metric as the quantum degree of freedom. In fact, pioneering studies have been performed for Einstein-Cartan theory with the Hilbert-Palatini action being generalized to the Holst action [156–158] or constrained to self-dual connections [159], or for “tetrad only” formulations [160]. All these works find indications for the existence of UV fixed points supporting asymptotic safety of such quantum gravity theories, with the fixed points likely

representing universality classes different from that of quantum Einstein gravity. In fact rather complex phase diagrams are partly found being paralleled by the complexity of the computations involving such a large number of gauge degrees of freedom. On the other hand, it is interesting to observe that also reduced versions such as unimodular gravity [114, 161–164] or conformally reduced gravity [165–168] exhibit UV complete renormalization group trajectories (see however [169] for a critical view on conformally reduced gravity.)

A major motivation to study formulations of gravity based on the metric and the connection is the greater similarity to gauge theories of particle physics. In addition to this structural resemblance, also a larger technical toolkit developed for gauge theories may become available for concrete calculations; specifically lattice formulations for gravity become accessible [170, 171].

In this thesis, we suggest to reduce the amount of complexity introduced by the large number of gauge degrees of freedom of a metric-affine formulation by an on-shell reduction scheme: at a given expansion order, we only quantize those degrees of freedom which remain after using the equations of motion of the preceding order. For instance at lowest order in the curvature (Einstein-Hilbert level), different choices of degrees of freedom boil down to the Einstein equation for the metric; hence the on-shell reduction suggests to quantize only the metric at this level. At higher order in the curvature, connection degrees of freedom typically develop their independent dynamics. In the present work, we will focus on the second-order curvature level where a co-vector field remains as an independent degree of freedom in the connection after on-shell reduction. The corresponding additional action to be quantized is of Maxwell type.

In the asymptotic safety scenario, this on-shell reduction scheme helps to monitor the quantitative modifications of the RG flow and of the universality class associated with RG fixed points in a controlled and systematic way. We observe a UV-attractive fixed point of Reuter type with more stabilized critical exponents at a smaller value of the Newton coupling G .

6.1. Classical Hilbert-Palatini Gravity

In the Einstein formulation of gravity, the connection is linked to the metric in the form of the Levi-Civita connection. By contrast, the Hilbert-Palatini formulation of gravity treats the metric and the connection as independent degrees of freedom. Therefore, the connection can a priori carry additional degrees of freedom that may or may not be fully linked to the metric via the equations of motion. In the following, we start with a general connection and study the on-shell constraints at increasing orders of curvature.

6.1.1. General Connection on Smooth Manifolds

Suppose we have a vector field V on a smooth manifold with metric g and connection $\tilde{\Gamma}$. The covariant derivative $\tilde{\nabla}$ of this vector field reads

$$\tilde{\nabla}_\mu V^\alpha = \partial_\mu V^\alpha + \tilde{\Gamma}_{\mu\nu}^\alpha V^\nu. \quad (6.1)$$

In the most general case, the connection $\tilde{\Gamma}$ can be decomposed into the expressions for the Levi-Civita connection Γ (Christoffel symbols), contorsion K and displacement L (though the latter does not have a collectively agreed upon name [19]),

$$\tilde{\Gamma}_{\mu\nu}^\alpha = \Gamma_{\mu\nu}^\alpha + K_{\mu\nu}^\alpha + L_{\mu\nu}^\alpha. \quad (6.2)$$

The Levi-Civita connection is constructed from the metric, $\Gamma = \Gamma[g]$ and can be used to define the standard covariant derivative ∇ of Einstein gravity

$$\nabla_\mu V^\alpha = \partial_\mu V^\alpha + \Gamma_{\mu\nu}^\alpha V^\nu. \quad (6.3)$$

The Levi-Civita part of the connection Γ accounts for curvature through the Riemann tensor defined below. The contorsion tensor K is related to Cartan torsion T which corresponds to the anti-symmetric part of the connection with respect to the lower indices,

$$T_{\mu\nu}^\alpha := \tilde{\Gamma}_{\mu\nu}^\alpha - \tilde{\Gamma}_{\nu\mu}^\alpha = K_{\mu\nu}^\alpha - K_{\nu\mu}^\alpha. \quad (6.4)$$

The displacement tensor L induces non-metricity Q which is symmetric in the last two indices,

$$Q_{\mu\alpha\beta} := -\tilde{\nabla}_\mu g_{\alpha\beta} = L_{\mu\alpha\beta} + L_{\mu\beta\alpha} \quad (6.5)$$

One can also reverse these terms to express the contorsion K and displacement L in terms of torsion T and non-metricity Q , respectively,

$$K_{\alpha\beta\gamma} = \frac{1}{2} (T_{\alpha\beta\gamma} + T_{\beta\alpha\gamma} - T_{\alpha\gamma\beta}) \quad (6.6)$$

$$L_{\alpha\beta\gamma} = \frac{1}{2} (Q_{\alpha\beta\gamma} + Q_{\gamma\beta\alpha} - Q_{\beta\alpha\gamma}). \quad (6.7)$$

For more information on the linear relation between contorsion K and torsion T , and analogously on the displacement L and the non-metricity Q , see Refs. [19, 172, 173].

The general connection (6.2) can be used to define a generalized Riemann tensor analogously to the pure metric formulation,

$$[\tilde{\nabla}_\mu, \tilde{\nabla}_\nu] V_\sigma = \tilde{R}^\rho{}_{\sigma\mu\nu} V_\rho, \quad (6.8)$$

taking the familiar form

$$\tilde{R}^\rho{}_{\sigma\mu\nu} = \partial_\mu \tilde{\Gamma}^\rho_{\nu\sigma} - \partial_\nu \tilde{\Gamma}^\rho_{\mu\sigma} + \tilde{\Gamma}^\rho_{\mu\lambda} \tilde{\Gamma}^\lambda_{\nu\sigma} - \tilde{\Gamma}^\rho_{\nu\lambda} \tilde{\Gamma}^\lambda_{\mu\sigma}. \quad (6.9)$$

In contrast to the standard case, where the Riemann tensor is composed out of the metric, we can view \tilde{R} as dependent on the metric, the contorsion and the displacement, $\tilde{R} = \tilde{R}[g, K, L]$. Since the general connection $\tilde{\Gamma}$ is not symmetric in the lower two indices anymore, the generalized Riemann tensor $\tilde{R} \dots$ is not anti-symmetric in the first two indices, as will be important below.

Analogously, we can construct a generalized Ricci tensor by contracting the first and the third index

$$\tilde{R}_{\sigma\nu} = \tilde{R}^\rho{}_{\sigma\mu\nu} g^\mu{}_\rho, \quad (6.10)$$

which - contrary to Einstein gravity - is not purely symmetric anymore. Contracting this tensor further leads to a generalized Ricci scalar,

$$\tilde{R} = \tilde{R}_{\sigma\nu} g^{\sigma\nu}. \quad (6.11)$$

As in Einstein gravity, we can use these generalized curvature forms to construct curvature invariants and formulate an action S governing the dynamics of a theory, with the metric, the contorsion/torsion and the displacement/non-metricity as fundamental degrees of freedom, $S = S[g, K, L]$. In a quantized version, all these degrees of freedom have to be integrated out, requiring appropriate gauge fixing also for the connection degrees of freedom, cf. for instance [156].

6.1.2. Einstein-Hilbert-Palatini Action

Let us focus on a Palatini formulation of gravity starting with the lowest nontrivial order in the curvature. This corresponds to the Einstein-Hilbert action (also referred to as Einstein-Hilbert-Palatini action in order to emphasize the dependence on the general connection),

$$S[g, \tilde{\Gamma}] = \int d^4x \sqrt{g} \frac{1}{16\pi G} (\Lambda - 2\tilde{R}). \quad (6.12)$$

Classically, the corresponding fields (the metric g and the connection $\tilde{\Gamma}$) are constrained by their equations of motions, namely

$$\frac{\delta S}{\delta g_{\mu\nu}} \stackrel{!}{=} 0 \quad \Rightarrow \quad \frac{1}{2}(\tilde{R}_{\mu\nu} - \tilde{R}_{\nu\mu}) - \frac{1}{2}\tilde{R}g_{\mu\nu} = 0, \quad (6.13)$$

which is a partial differential equation for the metric, and additionally in the Palatini formulation,

$$\frac{\delta S}{\delta \tilde{\Gamma}_{\mu\nu}^{\lambda}} \stackrel{!}{=} 0 \quad \Rightarrow \quad \tilde{\nabla}_{\lambda} g_{\mu\nu} - T_{\nu\lambda}^{\sigma} g_{\sigma\mu} - \frac{1}{3} T_{\sigma\lambda}^{\sigma} g_{\mu\nu} - \frac{1}{3} T_{\sigma\nu}^{\sigma} g_{\mu\lambda} = 0. \quad (6.14)$$

This new equation can be interpreted as an equation of motion for the contorsion K and displacement L . As the derivative terms turn out to be total derivatives, Eq. (6.14) is a purely algebraic equation for K and L and can be directly solved to find an expression for the general connection $\tilde{\Gamma}$. For this, we define the left-hand side of Eq. (6.14) as a tensor in which the covariant derivative is written in terms of a partial derivative and the general connection [22],

$$\Xi_{\lambda\mu\nu} := \partial_{\lambda} g_{\mu\nu} - \tilde{\Gamma}_{\lambda\mu}^{\sigma} g_{\sigma\nu} - \tilde{\Gamma}_{\nu\lambda}^{\sigma} g_{\mu\sigma} - \frac{1}{3} T_{\sigma\lambda}^{\sigma} g_{\mu\nu} - \frac{1}{3} T_{\sigma\nu}^{\sigma} g_{\mu\lambda} = 0. \quad (6.15)$$

This tensor Ξ and its permutations are constrained by Eq. (6.14),

$$\Xi_{\lambda\mu\nu} = 0, \quad \Xi_{\mu\nu\lambda} = 0, \quad \Xi_{\nu\lambda\mu} = 0. \quad (6.16)$$

We add the last two permutations of Ξ and subtract the first one to directly solve the resulting equation for the general connection $\tilde{\Gamma}$,

$$\Xi_{\nu\lambda\mu} + \Xi_{\mu\nu\lambda} - \Xi_{\lambda\mu\nu} = 0 \quad \Rightarrow \quad \tilde{\Gamma}_{\mu\nu}^{\lambda} = \Gamma_{\mu\nu}^{\lambda} - \frac{1}{3} T_{\sigma\mu}^{\sigma} \delta_{\nu}^{\lambda}. \quad (6.17)$$

The trace of the torsion tensor can be fully expressed in terms of a co-vector [174, 175],

$$T_{\mu\alpha}^{\alpha} = -3A_{\mu}, \quad (6.18)$$

leading to the final solution for the general connection,

$$\tilde{\Gamma}_{\mu\nu}^{\alpha} = \Gamma_{\mu\nu}^{\alpha} + A_{\mu} \delta_{\nu}^{\alpha}, \quad (6.19)$$

with the above introduced general co-vector field A as the independent degree of freedom from the Levi-Cevita connection Γ [20]. For the discussion of a relation to the affine Weyl connection, see [176, 177].

The generalized curvature tensors in the Palatini formulation can now be expressed in terms of curvature quantities familiar from ordinary Einstein gravity which derive from the

Levi-Cevita connection and additional terms that depend on the new vector field A ,

$$\tilde{R}_{\rho\sigma\mu\nu} = R_{\rho\sigma\mu\nu} + g_{\rho\sigma}F_{\mu\nu} \quad (6.20)$$

$$\tilde{R}_{\sigma\nu} = R_{\sigma\nu} + F_{\sigma\nu} \quad (6.21)$$

$$\tilde{R} = R, \quad (6.22)$$

with the tensor F acquiring the form of a Maxwellian field strength,

$$F_{\mu\nu} = \partial_\mu A_\nu - \partial_\nu A_\mu. \quad (6.23)$$

In Eq. (6.22) we observe that the generalized Ricci scalar reduces to the standard Ricci scalar on shell. Therefore, the classical action (6.12) is on-shell equivalent to the Einstein-Hilbert action of classical GR, see [20, 21, 178] for recent detailed discussions. Since each component $A_\mu \in \mathbb{R}$, the Einstein-Hilbert-Palatini action has an \mathbb{R}^4 gauge invariance.

Interestingly, the A field appears in the form of a Maxwell-type field strength tensor F as the anti-symmetric part of the generalized Ricci tensor. At higher orders in the curvature, we can thus expect that more general gravity theories of higher order in the curvature will exhibit Maxwellian gauge invariance. This implies that the \mathbb{R}^4 invariance for this part of the general connection reduces to a $U(1)$ invariance at higher orders.

Let us therefore consider terms to second order in the curvature. More specifically, we concentrate on terms that can be constructed from a Ricci-like tensor. Since the generalized Riemann tensor $\tilde{R} \dots$ is not anti-symmetric in the first two indices, we can construct a second Ricci-like tensor of rank two \tilde{L} by instead contracting the second and the fourth index

$$\tilde{L}_{\sigma\nu} = g^{\rho\mu} \tilde{R}_{\sigma\rho\nu\mu} = R_{\sigma\nu} - F_{\sigma\nu}. \quad (6.24)$$

The tensors \tilde{L} and \tilde{R} obviously coincide in the limit $A \rightarrow 0$, reducing to the ordinary Ricci tensor R . In the general case, we can use both curvature tensors for the construction of invariants, yielding

$$\tilde{R}_{\sigma\nu} \tilde{R}^{\sigma\nu} = \tilde{L}_{\sigma\nu} \tilde{L}^{\sigma\nu} = R_{\sigma\nu} R^{\sigma\nu} + F_{\sigma\nu} F^{\sigma\nu}, \quad (6.25)$$

$$\tilde{R}_{\sigma\nu} \tilde{L}^{\sigma\nu} = R_{\sigma\nu} R^{\sigma\nu} - F_{\sigma\nu} F^{\sigma\nu}. \quad (6.26)$$

We observe that only two combinations are independent. A general contribution to the action can thus be spanned by the linear combination of the two independent invariants. On shell, we have the equivalence for general couplings σ^1, σ^2 :

$$\begin{aligned} & \sigma^1 \tilde{R}_{\mu\nu} \tilde{R}^{\mu\nu} + \sigma^2 \tilde{R}_{\mu\nu} \tilde{L}^{\mu\nu} \\ &= \sigma^R R_{\mu\nu} R^{\mu\nu} + \sigma^F F_{\mu\nu} F^{\mu\nu}. \end{aligned} \quad (6.27)$$

The corresponding couplings in front of the standard Ricci-squared and Maxwell terms satisfy

$$\sigma^R = \sigma^1 + \sigma^2 \quad (6.28)$$

$$\sigma^F = \sigma^1 - \sigma^2. \quad (6.29)$$

Equation (6.27) illustrates that a second order curvature theory built from the generalized Ricci-like tensors is on-shell equivalent to a second-order metric theory plus an abelian gauge field. Of course, a further independent second-order invariant can be formed by suitably squaring the generalized Riemann tensor. As is obvious from Eq. (6.20), this boils down to a square of the Riemann tensor and a Maxwell term as well,

$$\begin{aligned} \tilde{R}^{\alpha\beta\mu\nu} \tilde{R}_{\alpha\beta\mu\nu} &= (R^{\alpha\beta\mu\nu} + g^{\alpha\beta} F^{\mu\nu}) (R_{\alpha\beta\mu\nu} + g_{\alpha\beta} F_{\mu\nu}) \\ &= R^{\alpha\beta\mu\nu} R_{\alpha\beta\mu\nu} + 4F^{\mu\nu} F_{\mu\nu}. \end{aligned} \quad (6.30)$$

In the following, we ignore such terms to quadratic order in the Riemann tensor for simplicity.

6.1.3. Geodesic Trajectory in Hilbert-Palatini Gravity

If we insert our solution for the most general connection for the Einstein-Hilbert-Palatini action of Eq. (6.19) into the modified Einstein field equations of this formalism from Eq. (6.13), we obtain the ordinary Einstein field equations derived from the Einstein-Hilbert action of Sec. 3.4. Therefore, the field equations of the Hilbert-Palatini formulation do not vary from those of ordinary Einstein gravity on the level of the Einstein-Hilbert truncation.

To observe deviations of Hilbert-Palatini gravity from Einstein gravity, we consider the geodesic equation in this formalism,

$$u^\mu \tilde{\nabla}_\mu u^\alpha = 0 \quad \Rightarrow \quad \frac{du^\alpha}{d\tau} + \Gamma_{\mu\nu}^\alpha u^\mu u^\nu = -A_\mu u^\mu u^\alpha, \quad (6.31)$$

with the vector field

$$u^\alpha = \frac{dx^\alpha(\tau)}{d\tau}. \quad (6.32)$$

As we can see, Eq. (6.31) contains additional terms on its right-hand side compared to the ordinary geodesic equation that originates from the general connection $\tilde{\Gamma}$ instead of the Levi-Civita connection Γ . Nonetheless, the geodesic trajectory that one obtains as a solution to this equation is the same as in ordinary Einstein gravity [22]. To illustrate this, we define

the quantity

$$G(\tau) = \int_0^\tau d\tau' A_\mu \frac{dx^\mu(\tau')}{d\tau'}, \quad (6.33)$$

and introduce a new parameter,

$$\lambda = \int_0^\tau d\tau' e^{-G(\tau')}, \quad (6.34)$$

which acts as a modified eigentime. We now express our geodesic trajectories in terms of this new parameter,

$$x^\mu(\tau) \rightarrow x^\mu(\lambda), \quad (6.35)$$

and define the velocity along this new parameterization of the trajectory accordingly,

$$v^\mu := \frac{dx^\mu(\lambda)}{d\lambda}. \quad (6.36)$$

Now, we express all terms appearing in the geodesic equation in Hilbert-Palatini gravity in terms of this new parameter λ , starting with the velocity,

$$\begin{aligned} u^\mu &= \frac{dx^\mu(\tau)}{d\tau} \\ &= \frac{d\lambda}{d\tau} \frac{dx^\mu(\tau)}{d\lambda} \\ &= e^{-G} v^\mu. \end{aligned} \quad (6.37)$$

As we can see, the velocity $u^\mu(\tau)$ can be interpreted as a rescaled velocity $v^\mu(\lambda)$ with the scaling prefactor e^{-G} . The derivative of the velocity u^μ reads

$$\begin{aligned} \frac{du^\mu}{d\tau} &= \frac{d}{d\tau} (e^{-G} v^\mu) \\ &= -G'(\tau) e^{-G} v^\mu + e^{-G} \frac{dv^\mu}{d\tau}. \end{aligned} \quad (6.38)$$

Expressing the derivative of the scaling prefactor,

$$\begin{aligned} G'(\tau) &= A_\nu u^\nu \\ &= A_\nu e^{-G} v^\nu, \end{aligned} \quad (6.39)$$

and the derivative of the velocity v^μ in terms of the new parameter λ ,

$$\begin{aligned}\frac{dv^\mu}{d\tau} &= \frac{d\lambda}{d\tau} \frac{dv^\mu}{d\lambda} \\ &= e^{-G} \frac{dv^\mu}{d\lambda},\end{aligned}\tag{6.40}$$

we obtain our final result for the derivative of u^μ expressed in terms of λ ,

$$\begin{aligned}\frac{du^\mu}{d\tau} &= -G'(\tau) e^{-G} v^\mu + e^{-G} \frac{dv^\mu}{d\tau} \\ &= -A_\nu e^{-2G} v^\nu v^\mu + e^{-2G} \frac{dv^\mu}{d\lambda} \\ &= e^{-2G} \left(-A_\nu v^\nu v^\mu + \frac{dv^\mu}{d\lambda} \right).\end{aligned}\tag{6.41}$$

The first part of Eq-(6.41) precisely cancels the right-hand side of Eq. (6.31) and the scaling prefactor becomes a global prefactor of the equation that can be omitted. This leads to the final result of the geodesic equation of Hilbert-Palatini gravity expressed in terms of the parameter λ ,

$$\frac{dv^\alpha}{d\lambda} + \Gamma_{\mu\nu}^\alpha v^\mu v^\nu = 0.\tag{6.42}$$

As we can see, this matches the geodesic equation in ordinary Einstein gravity. This means that the geodesic trajectory one can measure in nature for Hilbert-Palatini gravity does not differ from the one in ordinary Einstein gravity. The velocity along the curve however is changed by the scaling prefactor e^{-G} . This means that the time it takes for a test particle to move from point A to point B along a geodesic trajectory differs in Hilbert-Palatini gravity from Einstein gravity and that difference is determined by the structure of the additional contribution to the connection A_μ .

6.2. Quantum Hilbert-Palatini Gravity

The preceding observations on the classical level suggest to study the quantized version of Hilbert-Palatini gravity in the on-shell reduction scheme: we use the degrees of freedom of the on-shell form found for the general connection to first order in the curvature, i.e., Eq. (6.19), to quantize the theory to second order in the curvature. In practice, this corresponds to extending results for quantum Einstein gravity to this order by including a Maxwell-type gauge field.

6.2.1. Renormalization Flow of Hilbert-Palatini Gravity

We now investigate the renormalization flow of the gravitational effective action $\Gamma_k[g, \tilde{\Gamma}]$ in the theory space spanned by the Hilbert-Palatini action including the terms to quadratic order in Ricci-like curvature tensors as discussed above,

$$\Gamma_{\text{gr},k}[g, \tilde{\Gamma}] = \int d^4x \sqrt{g} \frac{1}{16\pi\bar{G}_k} \left[\bar{\Lambda}_k - 2\tilde{R} + \bar{\sigma}_k^1 \tilde{R}^{\mu\nu} \tilde{R}_{\mu\nu} + \bar{\sigma}_k^2 \tilde{L}^{\mu\nu} \tilde{R}_{\mu\nu} \right]. \quad (6.43)$$

Here, k denotes a renormalization scale at which the theory is considered, and all coupling constants are considered to be k dependent. Now, instead of considering all degrees of freedom of the general connection $\tilde{\Gamma}$, we perform the on-shell reduction of Eq. (6.19) which allows us to understand the action as a functional of the metric and the abelian gauge field,

$$\Gamma_{\text{gr},k}[g, A] = \int d^4x \sqrt{g} \frac{1}{16\pi\bar{G}_k} \left[\bar{\Lambda}_k - 2R + \bar{\sigma}_k^R R^{\mu\nu} R_{\mu\nu} + \bar{\sigma}_k^F F^{\mu\nu} F_{\mu\nu} \right]. \quad (6.44)$$

We are interested in the scale dependence of the running Newton coupling \bar{G}_k , the cosmological parameter $\bar{\Lambda}_k$, the higher curvature coupling $\bar{\sigma}_k^R$, and the wave function renormalization Z_k^A of the abelian field strength defined by

$$Z_k^A = \frac{\bar{\sigma}_k^F}{4\pi\bar{G}_k}. \quad (6.45)$$

For a treatment of the gauge degrees of freedom, we use the background field formalism and perform a linear split of the metric g and the gauge field A into fluctuations around their respective background fields which are denoted by a bar

$$g_{\mu\nu} = \bar{g}_{\mu\nu} + \bar{\kappa} h_{\mu\nu}, \quad (6.46)$$

$$A_\mu = \bar{A}_\mu + a_\mu, \quad (6.47)$$

with the abbreviation

$$\bar{\kappa}^2 = 32\pi\bar{G}. \quad (6.48)$$

The rescaling of the metric fluctuation h by the quantity $\bar{\kappa}$ ensures a standard canonical mass dimension of the field. For the Faddeev-Popov quantization, we include gauge-fixing terms

$$\Gamma_{\text{gf},k} = \frac{1}{2} \int d^4x \sqrt{\bar{g}} \left(\frac{1}{\alpha_{\text{gr}}} \mathcal{F}^\mu \mathcal{F}_\mu + \frac{1}{\alpha_A} \mathcal{G}\mathcal{G} \right) \quad (6.49)$$

with gauge parameters α_{gr} and α_A . As gauge-fixing conditions for the metric sector \mathcal{F} and the abelian gauge sector \mathcal{G} , we use

$$\mathcal{F}^\mu = \sqrt{2\bar{\kappa}} \left(\bar{g}^{\mu\kappa} \bar{\nabla}^\lambda - \frac{1+\beta}{4} \bar{g}^{\kappa\lambda} \bar{\nabla}^\mu \right) h_{\kappa\lambda} \quad (6.50)$$

$$\mathcal{G} = \sqrt{Z_k^A} (\bar{\nabla}_\mu a^\mu), \quad (6.51)$$

where β denotes another gauge parameter of the metric sector. Also including the corresponding ghost terms $\Gamma_{\text{gh},k}$ for both sectors, the total effective (average) action reads

$$\Gamma_k[\bar{\Phi}, \Phi] = \Gamma_{\text{gr},k} + \Gamma_{\text{gf},k} + \Gamma_{\text{gh},k}. \quad (6.52)$$

Here, $\bar{\Phi}$ and Φ denote collective field variables, representing the background and fluctuations fields, respectively,

$$(\Phi) = (h, a, \bar{c}, c, \bar{b}, b) \quad (6.53)$$

$$(\bar{\Phi}) = (\bar{g}, \bar{A}) \quad (6.54)$$

with \bar{c} and c being the (anti-)ghost fields for the gravitational sector and \bar{b} and b being the (anti-)ghost fields for the abelian gauge sector.

We quantize the system, using the Wetterich equation [7, 33, 179, 180],

$$\partial_t \Gamma_k[\bar{\Phi}, \Phi] = \frac{1}{2} \text{STr} \left[\left(\Gamma_k^{(2)}[\bar{\Phi}, \Phi] + \mathcal{R}_k \right)^{-1} \partial_t \mathcal{R}_k \right], \quad (6.55)$$

to compute the renormalization flows of the renormalized, dimensionless couplings denoted without a bar

$$G_k = k^2 \bar{G}_k, \quad \Lambda_k = \frac{1}{k^2} \bar{\Lambda}_k, \quad \sigma_k^R = k^2 \bar{\sigma}_k^R, \quad (6.56)$$

For simplicity, we focus on the Landau gauge, choosing

$$\alpha_A \rightarrow 0, \quad (6.57)$$

$$\alpha_{\text{gr}} \rightarrow 0, \quad (6.58)$$

$$\beta = 0, \quad (6.59)$$

see [49, 181–183] for studies of gauge or parametrization dependencies in the metric context. For the computation of the traces and the identification of the corresponding operators on both sides, we use a spherical background \bar{g} , and a covariantly constant background field \bar{A} . For the details of the regularization around the scale k controlled by the regulator \mathcal{R}_k in Eq. (6.55), we choose a Type I regularization scheme, following the computation of

[9]. Computations that include further invariants and higher order curvature terms are, in principle, possible, e.g., along the lines of [9–11, 117, 120, 123, 128, 184–186]

Using the flows for the dimensionless, renormalized couplings, the wave function renormalization Z_k^A occurs only through the corresponding anomalous dimension

$$\eta_A = -\frac{k\partial_k Z_k^A}{Z_k^A}, \quad (6.60)$$

which is determined by an algebraic equation. The flows of the couplings as driven by the metric fluctuations has been computed in [9]. These are amended by contributions from the abelian vector field which we evaluate analogously to [15], but to second order in the curvature. The anomalous dimension of the abelian gauge field subject to metric fluctuations has been computed in [114]; see the Appendix.

We collect all running couplings into \vec{u} which is a vector in the truncated theory space

$$\vec{u}_k = \begin{pmatrix} G_k \\ \Lambda_k \\ \sigma_k \end{pmatrix}, \quad (6.61)$$

allowing for a compact notation for the flow equations

$$\vec{\beta}(\vec{u}) = \begin{pmatrix} \beta_G \\ \beta_\Lambda \\ \beta_\sigma \end{pmatrix} = \begin{pmatrix} k\partial_k G_k \\ k\partial_k \Lambda_k \\ k\partial_k \sigma_k \end{pmatrix}. \quad (6.62)$$

The explicit flows are summarized in the Appendix. We are specifically interested in fixed points \vec{u}_* of the RG flow which satisfy

$$\vec{\beta}(\vec{u}_*) \stackrel{!}{=} 0. \quad (6.63)$$

In order to characterize the fixed points, we linearize the flow equations around the fixed point and determine the critical exponents related to the eigenvalues of the Jacobian (stability matrix) of the expansion,

$$\{\theta_1, \theta_2, \theta_3\} = -\text{eig} \left(\vec{\nabla}_{\vec{u}} \otimes \vec{\beta} \right) \Big|_{\vec{u}=\vec{u}_*}. \quad (6.64)$$

Positive critical exponents characterize RG relevant directions which are attracted by the fixed point towards the UV. These directions determine the long-range properties of the theory towards the IR and correspond to physical parameters.

	Palatini gravity (this work)	Metric gravity [9]
G_*	1.132	1.467
Λ_*	0.214	0.171
σ_*	0.326	0.339
$\theta_{1,2}$	$2.057 \pm 3.195 \cdot i$	$1.627 \pm 2.570 \cdot i$
θ_3	12.780	21.232
$\eta_{A,*}$	-0.0924	-

Tab. 6.1.: Fixed-point solutions and critical exponents in second order truncation for Hilbert-Palatini gravity (this work) and metric gravity for the present truncation [9].

6.2.2. Results

The fixed point equations (6.63) turn out to be rational equations in the couplings, see the Appendix, and can be solved analytically. In addition to the Gaussian fixed point, we find five non-Gaussian fixed points. Discarding those with a negative Newton coupling for physical reasons, those with $\Lambda_* > \frac{1}{2}$ which is beyond a singularity in the graviton propagator, and those with very large values for G_* which we consider as artifacts of the approximations involved, we end up with one viable fixed point the quantitative results of which are listed in Tab. 6.1.

For comparison, we also list the results for the Reuter fixed point in pure metric gravity obtained in the analogous approximation as obtained in [9]. In general, we observe that the results are rather similar to one another which we interpret as evidence that a direct analogue of the Reuter fixed point in metric gravity also exists in on-shell reduced Hilbert-Palatini gravity with additional dynamical degrees of freedom in the general connection. For comparison, we plot the fixed point positions projected onto the G, Λ plane in Fig. 6.1. The fixed point labeled as “EH” marks the Reuter fixed point in metric gravity in the lowest-order Einstein-Hilbert truncation. Upon inclusion of terms quadratic in the Ricci tensor, this fixed point moves a bit to larger values of the coupling parameters (labeled by “Ric²” in the figure and listed in the second column of Tab. 6.1). The position of the corresponding fixed point in Hilbert-Palatini found in this work is labeled by “HP” in Fig. 6.1.

Inspecting the results of Tab. 6.1 more closely, we observe that specifically the fixed-point value of the Newton coupling is somewhat smaller. This can serve as an indication that a quantum gravity theory with independent connection variables may more easily be compatible with weak-gravity bounds [62, 89, 113, 116, 187–193] which arise from the demand for gravity-matter systems to be compatible with particle-physics observations.

While the leading critical exponents become somewhat larger in Hilbert-Palatini gravity, the most decisive change occurs for the third critical exponent θ_3 which becomes much smaller by almost a factor of 2. The story of this critical exponent is somewhat involved: already in the first analysis of the asymptotic safety scenario at the quadratic curvature order [117], this exponents was found to be rather large which seemed to contradict the expected

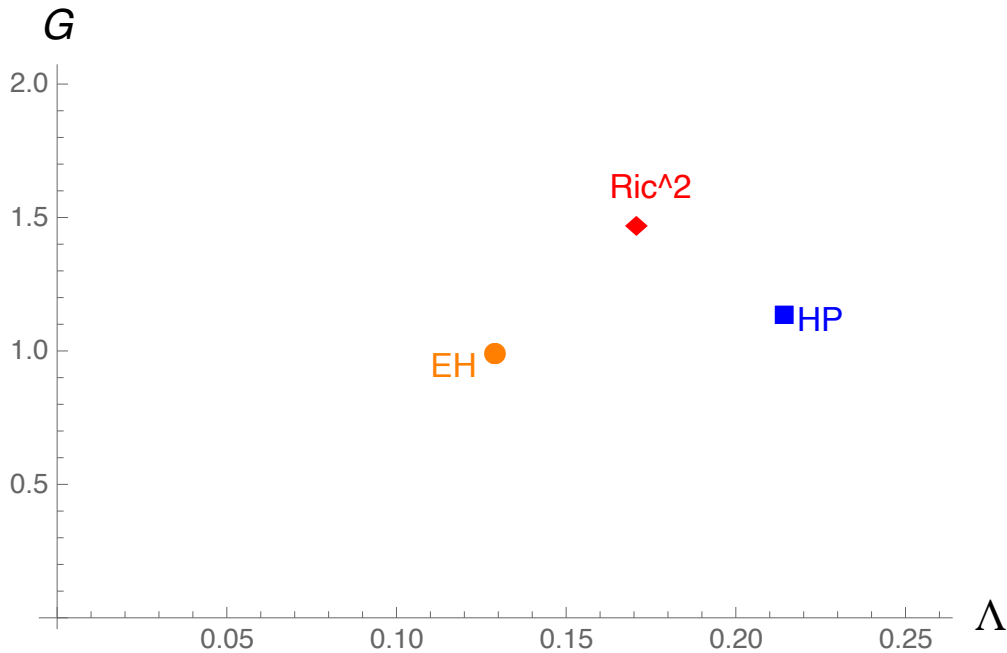


Fig. 6.1.: Fixed-point positions projected onto the G, Λ plane. The orange circle and red diamond represent metric gravity in the Einstein-Hilbert truncation (EH) and its extension to quadratic order in the Ricci tensor (Ric^2) [9], while the blue square represents Hilbert-Palatini gravity (HP) to the second order in the Ricci-tensor found in this work using on-shell reduction.

hierarchy of decreasing critical exponents for higher order operators. In fact, subsequent higher-order truncations revealed that this large value $\theta \gtrsim 20$ is a truncation artifact [108, 119, 194], stabilizing at $\mathcal{O}(1)$ if computed at higher order. In the light of these findings, we interpret the reduction of θ_3 by a factor of 2 as a hint that Hilbert-Palatini gravity may not be so severely affected by the truncation artifact.

It is interesting to observe that the anomalous dimension of the U(1) vector field at the fixed point $\eta_{A,*}$ is negative. This is in agreement with studies of the influence of gravitational fluctuations on (non-)abelian gauge fields, where (depending on the matter sector) $\eta_{A,*} < 0$ can go along with either (i) an asymptotically free gauge sector even for abelian gauge theories or (ii) an asymptotically safe gauge sector with a higher degree of predictivity [16, 195, 196]. Both scenarios indicate that the fluctuations of the additional degrees of freedom in the connection do not induce new UV problems such as Landau pole singularities despite their similarity to abelian gauge theories in the on-shell reduction scheme.

For the physical validity of the fixed point, a crucial question is as to whether an RG trajectory exists that connects the high-energy fixed-point regime with the regime of classical gravity where the dimensionful renormalized Newton coupling and cosmological constant are indeed constant over a wide range of scales (higher order curvature couplings are not tightly constraint by observations). For this, an RG trajectory must exist that emanates from the UV fixed point and passes by sufficiently near the Gaussian fixed point for G and Λ such that they satisfy canonical scaling. The fact that such trajectories exist is illustrated

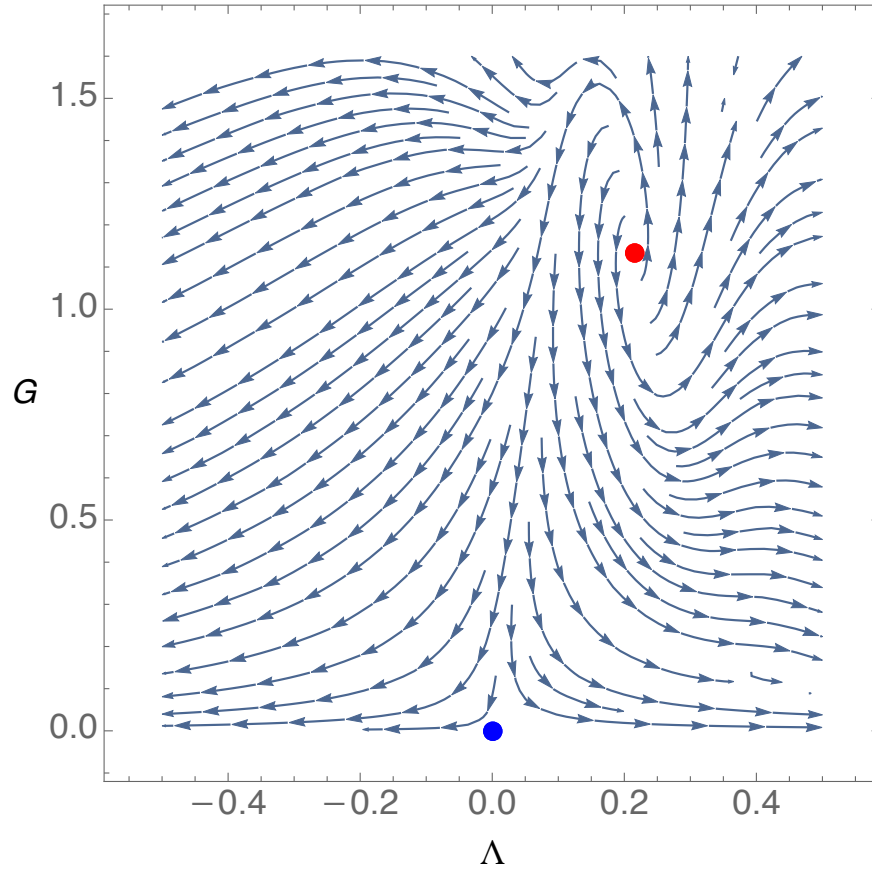


Fig. 6.2.: Flow diagram in the theory space spanned by the couplings Λ and G with the third coupling set to its UV fixed-point value σ_* . The red dot represents the non-Gaussian UV fixed-point and the blue dot the Gaussian IR fixed-point. The arrows flow towards the IR.

by the stream plot in the G, Λ plane (evaluated at $\sigma = \sigma_*$) in Fig. 6.2 where the arrows indicate the RG flow towards the IR. We conclude that our findings support the existence of a UV-complete RG trajectory in quantum Hilbert-Palatini gravity that features a long-range regime where classical GR holds as an effective low-energy theory.

7. Conclusions

The results of the first part of this thesis generalize the concept of curvature bounds from gravitational catalysis [18] to finite temperatures as well as to the case of a spatially curved space. In addition to the role played by the thermal effects, we observe that the details of the averaged curvature of local patches of spacetime matters significantly: First, gravitational catalysis is more strongly triggered for the spacetime $\mathbb{R} \otimes H^3$ than for the maximally symmetric case H^4 . Second, also the dependence on the scalar-curvature coupling $\sim \xi \phi^2 R$ is much more prominent for the former case than for the latter. Both observations have a strong influence on the curvature bound that indicates how the details of the curvature background matter for the phenomenon of gravitational catalysis.

It is important to emphasize that the curvature bound derived in this thesis is an estimate for the extent of the region that is not affected by gravitational catalysis according to our assumptions. If a system (e.g., subject to a specific quantum gravity scenario) violates the curvature bound, this does not necessarily imply that fermion mass generation kicks in as a manifestation of gravitational catalysis. Further dynamical mechanisms could still avoid the occurrence of gravitational catalysis. For instance, fluctuations of the scalar order parameter tend to weaken the symmetry-breaking channel. On the other hand, a finite initial fermionic self-interaction could enhance the tendency towards fermionic gap formation. Also, the curvature bound does not account for the possibility of further local minima which could become the global one at a first-order transition; our method is only sensitive to second-order transitions. Of course, first-order transitions could straightforwardly be detected by a global study of the effective potential. If they occur, they would strengthen our bounds.

As a first example, we have applied the curvature bound to the asymptotic-safety scenario for quantum gravity. A rather robust prediction of this scenario that relies on the existence of an interacting UV-fixed point is that the cosmological constant can have a negative sign in the short-distance regime (with a dynamical transition to positive values for the long-range physics) depending on the matter content. In particular, a dominance of fermionic matter degrees of freedom pushes the fixed point of the cosmological term to negative values. RG-improvement arguments then suggest that the properties of the quantum spacetime in the short-distance regime can effectively be described by a scale-dependent version of Einstein's equations (or higher-derivative versions thereof). For our purposes this suggests that local patches of spacetime appear as effectively negatively curved. If so, this effective negative curvature also enhances the symmetry-breaking channels of fermionic fluctuations by (the

scale-dependent version of) gravitational catalysis. If symmetry breaking was triggered in the high-energy regime of gravity, fermions would acquire a mass proportional to the scale of symmetry breaking. Gravitational catalysis would therefore inhibit the existence of light fermions in Nature.

This line of argument thus connects the observational fact of light fermions with properties of quantum spacetime in the high-energy regime. By extending the RG-improvement argument to a cosmological setting, our reasoning connects the curvature bound of gravitational catalysis to a combination of matter degrees of freedom such as the fermion flavor number together with the thermal evolution of the universe, parameterized in this work by the rescaled temperature ζ .

Whereas our results for the general curvature bound have a clear quantitative meaning within the given assumptions, the application to the asymptotic safety scenario should be considered as more qualitative because of the approximations involved and the genuine qualitative nature of RG improvement. Therefore, we interpret these results as an indication that the asymptotic-safety scenario for quantum gravity can indeed be compatible with the existence of light fermions; there is definitely room for evading the bounds imposed by gravitational catalysis for particle models with a matter content similar to that of the standard model. While our line of argument based on gravitational catalysis can put an upper bound on the number of fermionic degrees of freedom, it is interesting to see that a combination of gravity and abelian gauge interactions of fermions can also produce a lower bound [89].

We believe that it will be highly worthwhile to check for the role of gravity, specifically gravitational catalysis, and the consistency with light fermions in other scenarios of quantum gravity as well. While our bounds can be applied in other settings, the inclusion of matter degrees of freedom is a common effort in many research directions of quantum gravity [65, 197–201].

In the second part of this thesis, we have analyzed the renormalization flow of Hilbert-Palatini gravity using the functional renormalization group. Our study provides evidence for the existence of a non-Gaussian UV fixed point similar to the Reuter-fixed point of metric gravity. This result is based on an analysis of an expansion of the action in terms of curvature invariants including squares of generalized Ricci-like tensors and uses an on-shell reduction scheme that allows to gradually include the additional degrees of freedom introduced by a general connection in comparison to a pure metric formulation.

The discovered fixed point supports the existence of UV-complete RG trajectories in Hilbert-Palatini gravity within an asymptotic safety scenario. Quantitatively, the fixed point occurs at coupling values similar to those of metric gravity. A similar comment applies to the critical exponents – although we even find indications for a larger degree of stability under the increase of the expansion order. Importantly, there exist RG trajectories emanating from this fixed point which can be connected to a low-energy regime with the long-range limit corresponding to Einstein’s classical GR.

Within our on-shell reduction scheme, the additional degrees of freedom in the general connection reduce to a vector field that is related to the trace of the Cartan torsion. In our present truncation, the vector field features a local $U(1)$ invariance and thus contributes similarly to an abelian gauge field. This observation holds true for any truncation built from local curvature invariants of the generalized Riemann tensor.

To higher-orders in the on-shell reduction scheme and the curvature expansion, we expect that further additional degrees of freedom acquire their own dynamics and start to contribute to the flow. At the present order, they drop out, because their equation of motion is algebraic and their action corresponds to that of simple quadratic mass terms. Therefore, we expect that their dynamics at higher orders corresponds to that of massive modes. This does not only suggest that they decouple towards the IR, but are also likely to contribute to the UV only at the prize of corresponding mass suppression factors. This observation justifies to consider the on-shell reduction scheme as a quantitatively controlled expansion scheme, provided the underlying curvature expansion scheme has satisfactory convergence properties for observables.

While the differences to metric gravity as found in this work are comparatively small, the question remains as to whether the additional connection degrees of freedom exert a stronger influence on other sectors. In particular, since the additional field after on-shell reduction is a vector field resembling an abelian gauge field, a possible impact on the matter sector in the fixed-point regime or beyond is conceivable. Towards low-energies, this degree of freedom has been discussed as a candidate for dark matter (dark photon) [202]. A particularly relevant question for the high-energy regime where gravity is non-perturbative refers to possible consequences of this degree of freedom for the realization of symmetries such as chiral symmetry of fermionic matter particles [18, 23, 59, 61, 63, 64]. The latter is closely related to the existence of light fermions in nature which are an observational fact that needs to be supported also by the quantum gravitational sector.

Finally, we believe that our on-shell reduction scheme can also be useful in further formulations of quantum gravity with different and/or additional degrees of freedom. An example would be given by “tetrad-only” formulations [160] or generalizations of Hilbert-Palatini gravity using the spin-base invariant formalism [42]. In the latter case, it has been shown that on-shell reduction of a generalized spin connection would entail two vector fields [203], presumably with analogous consequences for the construction of an asymptotic safety scenario as found in the present work.

Beyond quantum gravity, on-shell reduction is a rather obvious scheme in functional RG approaches to supersymmetric theories [204]. In this case, on-shell reduction eliminates the auxiliary field(s) that are introduced for a superfield formulation in superspace. While the functional RG can be employed both in the on-shell as well as the off-shell case, the off-shell formulation is advantageous for the description of phase transitions in connection with order parameters related to the off-shell sector [205–208]. As a word of caution, it may therefore

be advisable not to use the on-shell reduction scheme for systems in which the off-shell sector is relevant for critical phenomena.

Appendix A.

Flow Equations for Hilbert-Palatini Gravity

The anomalous dimension for an abelian gauge field η^A has been computed in Appendix D of Ref. [114] and expressed in our notation reads

$$\eta^A = -\frac{G(10 - 40\Lambda + 7\sigma)}{18\pi(1 - 2\Lambda + \sigma)^2}. \quad (\text{A.1})$$

The flow equations for the three remaining couplings Λ , G and σ have been computed along the lines of [9]. The right-hand side of the Wetterich equation – labeled as I in [9] – is extended by the contributions from the abelian gauge field to quadratic order in the curvature according to [46]. The final results for the flow equations are

$$\beta_\Lambda = -\frac{A_\Lambda}{B_\Lambda}, \quad \beta_G = \frac{A_G}{B_G}, \quad \beta_\sigma = 2\frac{A_\sigma}{B_\sigma}, \quad (\text{A.2})$$

with

$$\begin{aligned} A_\Lambda = & -432\pi^2 G^2 (-2\Lambda + \sigma + 1)^2 \cdot A_\Lambda^{(2)} \\ & -67184640\pi^4 \Lambda (4\Lambda + 6\sigma - 3)^3 (-2\Lambda + \sigma + 1)^5 \\ & + G^4 \cdot A_\Lambda^{(4)} + 31104\pi^3 G (-2\Lambda + \sigma + 1)^2 \cdot A_\Lambda^{(1)} + 3\pi G^3 \cdot A_\Lambda^{(3)} \end{aligned} \quad (\text{A.3})$$

$$\begin{aligned}
 A_{\Lambda}^{(1)} = & -27\Lambda (16200\sigma^6 + 90996\sigma^5 - 92998\sigma^4 - 145681\sigma^3 \\
 & + 120465\sigma^2 - 8599\sigma - 5701) \\
 & + 622080\Lambda^7 + 128\Lambda^6(9000\sigma - 15743) - 32\Lambda^5 (71460\sigma^2 + 48998\sigma - 87891) \\
 & + 18\Lambda^2 (79200\sigma^5 - 188908\sigma^4 - 502556\sigma^3 + 553149\sigma^2 - 80446\sigma - 25643) \\
 & + 12\Lambda^3 (101880\sigma^4 + 825560\sigma^3 - 1166136\sigma^2 + 173151\sigma + 96557) \\
 & - 8\Lambda^4 (483840\sigma^3 - 1212552\sigma^2 + 53236\sigma + 279421) \\
 & + 7290 (2\sigma^2 + \sigma - 1)^2 (20\sigma^2 + \sigma - 4)
 \end{aligned} \tag{A.4}$$

$$\begin{aligned}
 A_{\Lambda}^{(2)} = & 5633536\Lambda^6 + 64\Lambda^5(463464\sigma - 478897) \\
 & + 32\Lambda^4 (865786\sigma^2 - 3584586\sigma + 1918663) \\
 & + 27\Lambda (79720\sigma^5 + 712632\sigma^4 - 2374666\sigma^3 \\
 & - 1147514\sigma^2 + 1342848\sigma - 200281) \\
 & + 36\Lambda^2 (160900\sigma^4 + 1825044\sigma^3 + 1414833\sigma^2 - 3232750\sigma + 848251) \\
 & - 243 (41500\sigma^5 - 43496\sigma^4 + 14055\sigma^3 - 31589\sigma^2 + 5968\sigma + 1608) \\
 & - 12\Lambda^3 (2566696\sigma^3 + 5505748\sigma^2 - 13621200\sigma + 5113385)
 \end{aligned} \tag{A.5}$$

$$\begin{aligned}
 A_{\Lambda}^{(3)} = & -54\Lambda (242816\sigma^6 - 43621136\sigma^5 - 105741110\sigma^4 \\
 & - 33856598\sigma^3 + 65125975\sigma^2 - 58567640\sigma + 19071545) \\
 & - 81 (3694416\sigma^6 + 14436454\sigma^5 + 16191029\sigma^4 - 889985\sigma^3 \\
 & - 4324109\sigma^2 + 5270879\sigma - 1603988) \\
 & + 36\Lambda^2 (3194560\sigma^5 - 152974904\sigma^4 - 131239628\sigma^3 + 194163574\sigma^2 \\
 & - 197711957\sigma + 83407825) \\
 & 106823680\Lambda^7 + 512\Lambda^6(387008\sigma - 938935) \\
 & - 64\Lambda^5 (661408\sigma^2 + 23286680\sigma - 1885541) \\
 & - 24\Lambda^3 (12370624\sigma^4 - 146478720\sigma^3 + 172896708\sigma^2 \\
 & - 225254630\sigma + 165900405) \\
 & + 16\Lambda^4 (24289856\sigma^3 + 27106560\sigma^2 + 18900738\sigma + 133505315)
 \end{aligned} \tag{A.6}$$

$$\begin{aligned}
A_\Lambda^{(4)} = & 67230720\Lambda^5 + 128\Lambda^4(578163\sigma - 1781875) \\
& -16\Lambda^3(2661552\sigma^2 + 8298109\sigma - 18340280) \\
& +27(1232336\sigma^5 + 5064046\sigma^4 + 5332307\sigma^3 \\
& +620285\sigma^2 - 500522\sigma - 193960) \\
& -18\Lambda(15761360\sigma^4 + 36304598\sigma^3 + 6154946\sigma^2 - 3194187\sigma - 2801570) \\
& +12\Lambda^2(44960536\sigma^3 + 7553626\sigma^2 + 425125\sigma - 14839910)
\end{aligned} \tag{A.7}$$

$$\begin{aligned}
B_\Lambda = & 216\pi^2(-2\Lambda + \sigma + 1)^2 \cdot \left[155520\pi^2(8\Lambda^2 + 8\Lambda\sigma - 10\Lambda - 6\sigma^2 - 3\sigma + 3)^3 \right. \\
& \left. + G^2 \cdot B_\Lambda^{(2)} + 144\pi G \cdot B_\Lambda^{(1)} \right]
\end{aligned} \tag{A.8}$$

$$\begin{aligned}
B_\Lambda^{(1)} = & 101248\Lambda^5 + 64\Lambda^4(4693\sigma - 7716) + 8\Lambda^3(27216\sigma^2 - 180968\sigma + 119287) \\
& +27(3012\sigma^5 + 9284\sigma^4 + 11483\sigma^3 - 26775\sigma^2 + 15752\sigma - 2887) \\
& -18\Lambda(14444\sigma^4 + 17728\sigma^3 - 99747\sigma^2 + 94133\sigma - 23561) \\
& +12\Lambda^2(12640\sigma^3 - 106428\sigma^2 + 201663\sigma - 75629)
\end{aligned} \tag{A.9}$$

$$\begin{aligned}
B_\Lambda^{(2)} = & 334208\Lambda^4 + 32\Lambda^3(8839\sigma - 14089) + 48\Lambda^2(487\sigma^2 + 49392\sigma - 11720) \\
& -27(51700\sigma^4 + 197344\sigma^3 + 129897\sigma^2 - 108638\sigma + 13984) \\
& +18\Lambda(230868\sigma^3 + 155580\sigma^2 - 325499\sigma + 57664)
\end{aligned} \tag{A.10}$$

$$A_G = 2G(4\Lambda + 6\sigma - 3)^3 \left[-3 \cdot A_G^{(1)} \cdot A_G^{(2)} + G^2 \cdot A_G^{(3)} \cdot A_G^{(4)} \right] \tag{A.11}$$

$$\begin{aligned}
A_G^{(1)} = & 30\pi G(4\Lambda + 6\sigma - 3)^2(-6\Lambda(5\sigma + 3) + 9\sigma^2 + 44\sigma + 25) \\
& -54\pi G(4\Lambda(4\sigma - 3) + 72\sigma^2 - 46\sigma + 9)(-2\Lambda + \sigma + 1)^2 \\
& +243\pi G(4\Lambda + 6\sigma - 3)^2(-2\Lambda + \sigma + 1)^2 \\
& -432\pi^2(4\Lambda + 6\sigma - 3)^2(-2\Lambda + \sigma + 1)^2 \\
& G^2(4\Lambda + 6\sigma - 3)^2(40\Lambda - 7\sigma - 10)
\end{aligned} \tag{A.12}$$

$$\begin{aligned}
 A_G^{(2)} &= -6G(496\Lambda^2 + 24\Lambda(22\sigma - 31) - 9(276\sigma^2 + 44\sigma - 31))(-2\Lambda + \sigma + 1)^3 \\
 &\quad + 5G(4\Lambda + 6\sigma - 3)^3(116\Lambda^2 - 4\Lambda(19\sigma + 129) + 24\sigma^2 + 118\sigma + 469) \\
 &\quad + 1080\pi(-4\Lambda - 6\sigma + 3)^3(-2\Lambda + \sigma + 1)^3
 \end{aligned} \tag{A.13}$$

$$A_G^{(3)} = 24(4\Lambda + 15\sigma - 3)(-2\Lambda + \sigma + 1)^2 + 5(4\Lambda + 6\sigma - 3)^2(20\Lambda - 7\sigma - 22) \tag{A.14}$$

$$\begin{aligned}
 A_G^{(4)} &= 54\pi(16\Lambda^2(62\sigma + 29) + 24\Lambda(4\sigma^2 + 86\sigma - 29) \\
 &\quad + 9(-1192\sigma^3 + 788\sigma^2 - 234\sigma + 29))(-2\Lambda + \sigma + 1)^3 \\
 &\quad + 90\pi(-4\Lambda - 6\sigma + 3)^3(4\Lambda^2(29\sigma - 1) - 2\Lambda(43\sigma^2 + 351\sigma + 178) \\
 &\quad + 44\sigma^3 + 117\sigma^2 + 822\sigma + 499) \\
 &\quad - G(-4\Lambda - 6\sigma + 3)^3(-40\Lambda + 7\sigma + 10)(-2\Lambda + \sigma + 1) \\
 &\quad + 7038\pi(-4\Lambda - 6\sigma + 3)^3(-2\Lambda + \sigma + 1)^3
 \end{aligned} \tag{A.15}$$

$$\begin{aligned}
 B_G &= 9\pi(-4\Lambda - 6\sigma + 3)^5(-2\Lambda + \sigma + 1)^2 \left[-155520\pi^2(8\Lambda^2 + 8\Lambda\sigma \right. \\
 &\quad \left. - 10\Lambda - 6\sigma^2 - 3\sigma + 3)^3 + G^2 \cdot B_G^{(2)} + 144\pi G \cdot B_G^{(1)} \right]
 \end{aligned} \tag{A.16}$$

$$\begin{aligned}
 B_G^{(1)} &= 101248\Lambda^5 + 64\Lambda^4(4693\sigma - 7716) + 8\Lambda^3(27216\sigma^2 - 180968\sigma + 119287) \\
 &\quad + 27(3012\sigma^5 + 9284\sigma^4 + 11483\sigma^3 - 26775\sigma^2 + 15752\sigma - 2887) \\
 &\quad - 18\Lambda(14444\sigma^4 + 17728\sigma^3 - 99747\sigma^2 + 94133\sigma - 23561) \\
 &\quad + 12\Lambda^2(12640\sigma^3 - 106428\sigma^2 + 201663\sigma - 75629)
 \end{aligned} \tag{A.17}$$

$$\begin{aligned}
 B_G^{(2)} &= -334208\Lambda^4 - 32\Lambda^3(8839\sigma - 14089) - 48\Lambda^2(487\sigma^2 + 49392\sigma - 11720) \\
 &\quad + 27(51700\sigma^4 + 197344\sigma^3 + 129897\sigma^2 - 108638\sigma + 13984) \\
 &\quad - 18\Lambda(230868\sigma^3 + 155580\sigma^2 - 325499\sigma + 57664)
 \end{aligned} \tag{A.18}$$

$$\begin{aligned}
 A_\sigma &= -1399680\pi^3\sigma(-2\Lambda + \sigma + 1)^5(4\Lambda + 6\sigma - 3)^3 + 9\pi G^2(-2\Lambda + \sigma + 1)^2 \cdot A_\sigma^{(2)} \\
 &\quad - 648\pi^2 G(-2\Lambda + \sigma + 1)^2 \cdot A_\sigma^{(1)} + G^3 \cdot A_\sigma^{(3)}
 \end{aligned} \tag{A.19}$$

$$\begin{aligned}
A_\sigma^{(1)} = & -27 (16200\sigma^7 + 32644\sigma^6 - 41054\sigma^5 - 133133\sigma^4 \\
& + 105227\sigma^3 + 29329\sigma^2 - 41471\sigma + 8812) \\
& + 18\Lambda (79200\sigma^6 - 182460\sigma^5 - 431284\sigma^4 + 633841\sigma^3 \\
& + 11688\sigma^2 - 255583\sigma + 74494) \\
& + 12\Lambda^2 (101880\sigma^5 + 826616\sigma^4 - 1214152\sigma^3 \\
& + 27963\sigma^2 + 743483\sigma - 278368) \\
& - 8\Lambda^3 (483840\sigma^4 - 1152328\sigma^3 - 432924\sigma^2 + 1510489\sigma - 629598) \\
& 512\Lambda^6 (1215\sigma - 1564) + 128\Lambda^5 (9000\sigma^2 - 37931\sigma + 23614) \\
& - 32\Lambda^4 (71460\sigma^3 + 126606\sigma^2 - 340887\sigma + 156880)
\end{aligned} \tag{A.20}$$

$$\begin{aligned}
A_\sigma^{(2)} = & 27 (79720\sigma^6 + 174652\sigma^5 - 1081722\sigma^4 + 689497\sigma^3 \\
& + 249706\sigma^2 - 327888\sigma + 72432) \\
& + 18\Lambda (321800\sigma^5 + 1596732\sigma^4 - 2697526\sigma^3 \\
& + 781767\sigma^2 + 915448\sigma - 386209) \\
& - 24\Lambda^2 (1283348\sigma^4 + 242426\sigma^3 + 987572\sigma^2 - 319735\sigma - 233846) \\
& 128\Lambda^5 (44012\sigma + 27247) + 128\Lambda^4 (231732\sigma^2 + 1394\sigma - 75545) \\
& + 8\Lambda^3 (3463144\sigma^3 - 3908896\sigma^2 - 2731276\sigma + 691313)
\end{aligned} \tag{A.21}$$

$$\begin{aligned}
A_\sigma^{(3)} = & 27 (30352\sigma^7 + 131896\sigma^6 + 424260\sigma^5 + 105248\sigma^4 - 509251\sigma^3 \\
& + 49896\sigma^2 + 147724\sigma - 42080) \\
& - 18\Lambda (399320\sigma^6 + 1353488\sigma^5 + 1610334\sigma^4 - 4440304\sigma^3 \\
& + 753902\sigma^2 + 1625577\sigma - 561570) \\
& + 24\Lambda^2 (773164\sigma^5 + 1232404\sigma^4 - 6465153\sigma^3 \\
& + 3676846\sigma^2 + 2410429\sigma - 1353600) \\
& - 8\Lambda^3 (3036232\sigma^4 - 10230572\sigma^3 + 19821964\sigma^2 + 2913489\sigma - 6181090) \\
& - 5120\Lambda^6 (1304\sigma + 189) - 128\Lambda^5 (96752\sigma^2 - 253283\sigma - 94070) \\
& + 64\Lambda^4 (41338\sigma^3 + 1428338\sigma^2 - 555863\sigma - 578655)
\end{aligned} \tag{A.22}$$

$$\begin{aligned}
 B_\sigma &= 9\pi(-2\Lambda + \sigma + 1)^2 \left[155520\pi^2 (8\Lambda^2 + 8\Lambda\sigma - 10\Lambda - 6\sigma^2 - 3\sigma + 3)^3 \right. \\
 &\quad \left. + G^2 \cdot B_\sigma^{(2)} + 144\pi G \cdot B_\sigma^{(1)} \right]
 \end{aligned} \tag{A.23}$$

$$\begin{aligned}
 B_\sigma^{(1)} &= 101248\Lambda^5 + 64\Lambda^4(4693\sigma - 7716) + 8\Lambda^3 (27216\sigma^2 - 180968\sigma + 119287) \\
 &\quad + 27 (3012\sigma^5 + 9284\sigma^4 + 11483\sigma^3 - 26775\sigma^2 + 15752\sigma - 2887) \\
 &\quad - 18\Lambda (14444\sigma^4 + 17728\sigma^3 - 99747\sigma^2 + 94133\sigma - 23561) \\
 &\quad + 12\Lambda^2 (12640\sigma^3 - 106428\sigma^2 + 201663\sigma - 75629)
 \end{aligned} \tag{A.24}$$

$$\begin{aligned}
 B_\sigma^{(2)} &= 334208\Lambda^4 + 32\Lambda^3(8839\sigma - 14089) + 48\Lambda^2 (487\sigma^2 + 49392\sigma - 11720) \\
 &\quad - 27 (51700\sigma^4 + 197344\sigma^3 + 129897\sigma^2 - 108638\sigma + 13984) \\
 &\quad + 18\Lambda (230868\sigma^3 + 155580\sigma^2 - 325499\sigma + 57664)
 \end{aligned} \tag{A.25}$$

Bibliography

- [1] M. E. Peskin and D. V. Schroeder. *An Introduction to quantum field theory*. 1995.
- [2] K. G. Wilson and J. B. Kogut. “The Renormalization group and the epsilon expansion.” In: *Phys. Rept.* 12 (1974), pp. 75–200. DOI: [10.1016/0370-1573\(74\)90023-4](https://doi.org/10.1016/0370-1573(74)90023-4).
- [3] A. Shomer. “A Pedagogical explanation for the non-renormalizability of gravity.” In: (Sept. 2007). arXiv: [0709.3555](https://arxiv.org/abs/0709.3555) [[hep-th](#)].
- [4] K. Becker, M. Becker, and J. H. Schwarz. *String theory and M-theory: A modern introduction*. Cambridge University Press, Dec. 2006. DOI: [10.1017/CB09780511816086](https://doi.org/10.1017/CB09780511816086).
- [5] C. Rovelli. “Loop quantum gravity.” In: *Living Rev. Rel.* 11 (2008), p. 5.
- [6] S. Weinberg. “Ultraviolet Divergences in Quantum Theories of Gravitation.” In: *General Relativity: An Einstein Centenary Survey*. 1980, pp. 790–831.
- [7] C. Wetterich. “Exact evolution equation for the effective potential.” In: *Phys. Lett. B* 301 (1993), pp. 90–94. DOI: [10.1016/0370-2693\(93\)90726-X](https://doi.org/10.1016/0370-2693(93)90726-X).
- [8] M. Reuter. “Nonperturbative evolution equation for quantum gravity.” In: *Phys. Rev. D* 57 (1998), pp. 971–985. DOI: [10.1103/PhysRevD.57.971](https://doi.org/10.1103/PhysRevD.57.971). arXiv: [hep-th/9605030](https://arxiv.org/abs/hep-th/9605030) [[hep-th](#)].
- [9] K. G. Falls et al. “Asymptotic safety of quantum gravity beyond Ricci scalars.” In: (2017). arXiv: [1801.00162](https://arxiv.org/abs/1801.00162) [[hep-th](#)].
- [10] Y. Kluth and D. F. Litim. “Fixed Points of Quantum Gravity and the Dimensionality of the UV Critical Surface.” In: (Aug. 2020). arXiv: [2008.09181](https://arxiv.org/abs/2008.09181) [[hep-th](#)].
- [11] Y. Kluth and D. F. Litim. “Functional Renormalisation for $f(R_{\mu\nu\rho\sigma})$ Quantum Gravity.” In: (Feb. 2022). arXiv: [2202.10436](https://arxiv.org/abs/2202.10436) [[hep-th](#)].
- [12] J. F. Donoghue. “A Critique of the Asymptotic Safety Program.” In: *Front. in Phys.* 8 (2020), p. 56. DOI: [10.3389/fphy.2020.00056](https://doi.org/10.3389/fphy.2020.00056). arXiv: [1911.02967](https://arxiv.org/abs/1911.02967) [[hep-th](#)].
- [13] A. Bonanno et al. “Critical reflections on asymptotically safe gravity.” In: *Front. in Phys.* 8 (2020), p. 269. DOI: [10.3389/fphy.2020.00269](https://doi.org/10.3389/fphy.2020.00269). arXiv: [2004.06810](https://arxiv.org/abs/2004.06810) [[gr-qc](#)].
- [14] A. Platania and C. Wetterich. “Non-perturbative unitarity and fictitious ghosts in quantum gravity.” In: *Phys. Lett. B* 811 (2020), p. 135911. DOI: [10.1016/j.physletb.2020.135911](https://doi.org/10.1016/j.physletb.2020.135911). arXiv: [2009.06637](https://arxiv.org/abs/2009.06637) [[hep-th](#)].
- [15] P. Donà, A. Eichhorn, and R. Percacci. “Matter matters in asymptotically safe quantum gravity.” In: *Phys. Rev. D* 89.8 (2014), p. 084035. DOI: [10.1103/PhysRevD.89.084035](https://doi.org/10.1103/PhysRevD.89.084035). arXiv: [1311.2898](https://arxiv.org/abs/1311.2898) [[hep-th](#)].
- [16] U. Harst and M. Reuter. “QED coupled to QEG.” In: *JHEP* 05 (2011), p. 119. DOI: [10.1007/JHEP05\(2011\)119](https://doi.org/10.1007/JHEP05(2011)119). arXiv: [1101.6007](https://arxiv.org/abs/1101.6007) [[hep-th](#)].
- [17] D. Ebert, A. V. Tyukov, and V. C. Zhukovsky. “Gravitational catalysis of chiral and color symmetry breaking of quark matter in hyperbolic space.” In: *Phys. Rev. D* 80 (2009), p. 085019. DOI: [10.1103/PhysRevD.80.085019](https://doi.org/10.1103/PhysRevD.80.085019). arXiv: [0808.2961](https://arxiv.org/abs/0808.2961) [[hep-th](#)].

- [18] H. Gies and R. Martini. “Curvature bound from gravitational catalysis.” In: *Phys. Rev. D* 97.8 (2018), p. 085017. DOI: [10.1103/PhysRevD.97.085017](https://doi.org/10.1103/PhysRevD.97.085017). arXiv: [1802.02865 \[hep-th\]](https://arxiv.org/abs/1802.02865).
- [19] A. Baldazzi, O. Melichev, and R. Percacci. “Metric-Affine Gravity as an effective field theory.” In: *Annals Phys.* 438 (2022), p. 168757. DOI: [10.1016/j.aop.2022.168757](https://doi.org/10.1016/j.aop.2022.168757). arXiv: [2112.10193 \[gr-qc\]](https://arxiv.org/abs/2112.10193).
- [20] N. Dadhich and J. M. Pons. “On the equivalence of the Einstein-Hilbert and the Einstein-Palatini formulations of general relativity for an arbitrary connection.” In: *Gen. Rel. Grav.* 44 (). DOI: [10.1007/s10714-012-1393-9](https://doi.org/10.1007/s10714-012-1393-9). arXiv: [1010.0869 \[gr-qc\]](https://arxiv.org/abs/1010.0869).
- [21] B. Janssen et al. “(Non-)Uniqueness of Einstein–Palatini Gravity.” In: 2021, pp. 49–59. DOI: [10.1007/978-3-030-52923-9_5](https://doi.org/10.1007/978-3-030-52923-9_5). arXiv: [1901.02326 \[gr-qc\]](https://arxiv.org/abs/1901.02326).
- [22] A. N. Bernal et al. “On the (non-)uniqueness of the Levi-Civita solution in the Einstein–Hilbert–Palatini formalism.” In: *Phys. Lett. B* 768 (2017), pp. 280–287. DOI: [10.1016/j.physletb.2017.03.001](https://doi.org/10.1016/j.physletb.2017.03.001). arXiv: [1606.08756 \[gr-qc\]](https://arxiv.org/abs/1606.08756).
- [23] H. Gies and A. S. Salek. “Curvature bound from gravitational catalysis in thermal backgrounds.” In: *Phys. Rev. D* 103.12 (2021), p. 125027. DOI: [10.1103/PhysRevD.103.125027](https://doi.org/10.1103/PhysRevD.103.125027). arXiv: [2103.05542 \[hep-th\]](https://arxiv.org/abs/2103.05542).
- [24] H. Gies and A. S. Salek. “Asymptotically safe Hilbert–Palatini gravity in an on-shell reduction scheme.” In: *Eur. Phys. J. C* 83.2 (2023), p. 173. DOI: [10.1140/epjc/s10052-023-11324-1](https://doi.org/10.1140/epjc/s10052-023-11324-1). arXiv: [2209.10435 \[hep-th\]](https://arxiv.org/abs/2209.10435).
- [25] P. Kopietz, L. Bartosch, and F. Schütz. *Introduction to the functional renormalization group*. Vol. 798. 2010. DOI: [10.1007/978-3-642-05094-7](https://doi.org/10.1007/978-3-642-05094-7).
- [26] A. S. Salek. “Master thesis.” Frankfurt 2019.
- [27] R. P. Feynman. “An Operator calculus having applications in quantum electrodynamics.” In: *Phys. Rev.* 84 (1951). Ed. by L. M. Brown, pp. 108–128. DOI: [10.1103/PhysRev.84.108](https://doi.org/10.1103/PhysRev.84.108).
- [28] T. Matsubara. “A New approach to quantum statistical mechanics.” In: *Prog. Theor. Phys.* 14 (1955), pp. 351–378. DOI: [10.1143/PTP.14.351](https://doi.org/10.1143/PTP.14.351).
- [29] L. D. Faddeev and V. N. Popov. “Feynman Diagrams for the Yang-Mills Field.” In: *Phys. Lett.* B25 (1967), pp. 29–30. DOI: [10.1016/0370-2693\(67\)90067-6](https://doi.org/10.1016/0370-2693(67)90067-6).
- [30] D. Zwanziger. “Fundamental modular region, Boltzmann factor and area law in lattice gauge theory.” In: *Nucl. Phys. B* 412 (1994), pp. 657–730. DOI: [10.1016/0550-3213\(94\)90396-4](https://doi.org/10.1016/0550-3213(94)90396-4).
- [31] A. Maas. “Constructing non-perturbative gauges using correlation functions.” In: *Phys. Lett. B* 689 (2010), pp. 107–111. DOI: [10.1016/j.physletb.2010.04.052](https://doi.org/10.1016/j.physletb.2010.04.052). arXiv: [0907.5185 \[hep-lat\]](https://arxiv.org/abs/0907.5185).
- [32] H. Gies. “Introduction to the functional RG and applications to gauge theories.” In: *Lect. Notes Phys.* 852 (2012), pp. 287–348. DOI: [10.1007/978-3-642-27320-9_6](https://doi.org/10.1007/978-3-642-27320-9_6). arXiv: [hep-ph/0611146 \[hep-ph\]](https://arxiv.org/abs/hep-ph/0611146).
- [33] T. R. Morris. “The Exact renormalization group and approximate solutions.” In: *Int. J. Mod. Phys. A* 9 (1994), pp. 2411–2450. DOI: [10.1142/S0217751X94000972](https://doi.org/10.1142/S0217751X94000972). arXiv: [hep-ph/9308265 \[hep-ph\]](https://arxiv.org/abs/hep-ph/9308265).

- [34] L. P. Kadanoff. “Scaling laws for Ising models near $T(c)$.” In: *Physics* 2 (1966), pp. 263–272.
- [35] A. Ugolotti. “Asymptotically free Gauged-Yukawa systems.” PhD thesis. Jena U., 2020. DOI: [10.22032/dbt.47022](https://doi.org/10.22032/dbt.47022).
- [36] D. F. Litim. “Optimized renormalization group flows.” In: *Phys. Rev. D* 64 (2001), p. 105007. DOI: [10.1103/PhysRevD.64.105007](https://doi.org/10.1103/PhysRevD.64.105007). arXiv: [hep-th/0103195](https://arxiv.org/abs/hep-th/0103195) [[hep-th](#)].
- [37] J. Eser et al. “Low-energy limit of the $O(4)$ quark-meson model from the functional renormalization group approach.” In: *Phys. Rev. D* 98.1 (2018), p. 014024. DOI: [10.1103/PhysRevD.98.014024](https://doi.org/10.1103/PhysRevD.98.014024). arXiv: [1804.01787](https://arxiv.org/abs/1804.01787) [[hep-ph](#)].
- [38] R. Martini. “Aspects of critical phenomena in curved space.” PhD thesis. Friedrich-Schiller-Universität Jena, Physikalisch-Astronomische Fakultät, Deutschland, 2019. DOI: [10.22032/dbt.39405](https://doi.org/10.22032/dbt.39405).
- [39] S. M. Carroll. *Spacetime and Geometry*. Cambridge University Press, July 2019.
- [40] R. Penrose and W. Rindler. *Spinors and Space-Time*. Cambridge Monographs on Mathematical Physics. Cambridge, UK: Cambridge Univ. Press, Apr. 2011. DOI: [10.1017/CB09780511564048](https://doi.org/10.1017/CB09780511564048).
- [41] H. A. Weldon. “Fermions without vierbeins in curved space-time.” In: *Phys. Rev. D* 63 (2001), p. 104010. DOI: [10.1103/PhysRevD.63.104010](https://doi.org/10.1103/PhysRevD.63.104010). arXiv: [gr-qc/0009086](https://arxiv.org/abs/gr-qc/0009086).
- [42] H. Gies and S. Lippoldt. “Fermions in gravity with local spin-base invariance.” In: *Phys. Rev. D* 89.6 (2014), p. 064040. DOI: [10.1103/PhysRevD.89.064040](https://doi.org/10.1103/PhysRevD.89.064040). arXiv: [1310.2509](https://arxiv.org/abs/1310.2509) [[hep-th](#)].
- [43] D. Vassilevich. “Heat kernel expansion: User’s manual.” In: *Phys. Rept.* 388 (2003), pp. 279–360. DOI: [10.1016/j.physrep.2003.09.002](https://doi.org/10.1016/j.physrep.2003.09.002). arXiv: [hep-th/0306138](https://arxiv.org/abs/hep-th/0306138).
- [44] R. Camporesi. “The Spinor heat kernel in maximally symmetric spaces.” In: *Commun. Math. Phys.* 148 (1992), pp. 283–308. DOI: [10.1007/BF02100862](https://doi.org/10.1007/BF02100862).
- [45] Y. Kluth and D. F. Litim. “Heat kernel coefficients on the sphere in any dimension.” In: *Eur. Phys. J. C* 80.3 (2020), p. 269. DOI: [10.1140/epjc/s10052-020-7784-2](https://doi.org/10.1140/epjc/s10052-020-7784-2). arXiv: [1910.00543](https://arxiv.org/abs/1910.00543) [[hep-th](#)].
- [46] R. Percacci. *An Introduction to Covariant Quantum Gravity and Asymptotic Safety*. Vol. 3. 100 Years of General Relativity. World Scientific, 2017. DOI: [10.1142/10369](https://doi.org/10.1142/10369).
- [47] M. Reuter and F. Saueressig. “Quantum Einstein Gravity.” In: *New J. Phys.* 14 (2012), p. 055022. DOI: [10.1088/1367-2630/14/5/055022](https://doi.org/10.1088/1367-2630/14/5/055022). arXiv: [1202.2274](https://arxiv.org/abs/1202.2274) [[hep-th](#)].
- [48] O. Lauscher and M. Reuter. “Ultraviolet fixed point and generalized flow equation of quantum gravity.” In: *Phys. Rev. D* 65 (2002), p. 025013. DOI: [10.1103/PhysRevD.65.025013](https://doi.org/10.1103/PhysRevD.65.025013). arXiv: [hep-th/0108040](https://arxiv.org/abs/hep-th/0108040) [[hep-th](#)].
- [49] H. Gies, B. Knorr, and S. Lippoldt. “Generalized Parametrization Dependence in Quantum Gravity.” In: (2015). arXiv: [1507.08859](https://arxiv.org/abs/1507.08859) [[hep-th](#)].
- [50] Y. Nambu and G. Jona-Lasinio. “Dynamical Model of Elementary Particles Based on an Analogy with Superconductivity. 1.” In: *Phys. Rev.* 122 (1961). Ed. by T. Eguchi, pp. 345–358. DOI: [10.1103/PhysRev.122.345](https://doi.org/10.1103/PhysRev.122.345).
- [51] J. Bardeen, L. N. Cooper, and J. R. Schrieffer. “Theory of Superconductivity.” In: *Phys. Rev.* 108 (5 1957), pp. 1175–1204. DOI: [10.1103/PhysRev.108.1175](https://doi.org/10.1103/PhysRev.108.1175).

- [52] P. W. Anderson. “Plasmons, Gauge Invariance, and Mass.” In: *Phys. Rev.* 130 (1963), pp. 439–442. DOI: [10.1103/PhysRev.130.439](https://doi.org/10.1103/PhysRev.130.439).
- [53] J. Zinn-Justin. “Quantum field theory and critical phenomena.” In: *Int. Ser. Monogr. Phys.* 92 (1996), pp. 1–1008.
- [54] Y. Nambu. “Quasiparticles and Gauge Invariance in the Theory of Superconductivity.” In: *Phys. Rev.* 117 (1960), pp. 648–663. DOI: [10.1103/PhysRev.117.648](https://doi.org/10.1103/PhysRev.117.648).
- [55] J. Goldstone. “Field Theories with Superconductor Solutions.” In: *Nuovo Cim.* 19 (1961), pp. 154–164. DOI: [10.1007/BF02812722](https://doi.org/10.1007/BF02812722).
- [56] C. P. Burgess. “Goldstone and pseudoGoldstone bosons in nuclear, particle and condensed matter physics.” In: *Phys. Rept.* 330 (2000), pp. 193–261. DOI: [10.1016/S0370-1573\(99\)00111-8](https://doi.org/10.1016/S0370-1573(99)00111-8). arXiv: [hep-th/9808176](https://arxiv.org/abs/hep-th/9808176).
- [57] J. Braun, B. Klein, and P. Piasecki. “On the scaling behavior of the chiral phase transition in QCD in finite and infinite volume.” In: *Eur. Phys. J. C* 71 (2011), p. 1576. DOI: [10.1140/epjc/s10052-011-1576-7](https://doi.org/10.1140/epjc/s10052-011-1576-7). arXiv: [1008.2155](https://arxiv.org/abs/1008.2155) [[hep-ph](#)].
- [58] J. S. Schwinger. “A Theory of the Fundamental Interactions.” In: *Annals Phys.* 2 (1957), pp. 407–434. DOI: [10.1016/0003-4916\(57\)90015-5](https://doi.org/10.1016/0003-4916(57)90015-5).
- [59] A. Eichhorn and H. Gies. “Light fermions in quantum gravity.” In: *New J. Phys.* 13 (2011), p. 125012. DOI: [10.1088/1367-2630/13/12/125012](https://doi.org/10.1088/1367-2630/13/12/125012). arXiv: [1104.5366](https://arxiv.org/abs/1104.5366) [[hep-th](#)].
- [60] O. Zanusso et al. “Gravitational corrections to Yukawa systems.” In: *Phys. Lett.* B689 (2010), pp. 90–94. DOI: [10.1016/j.physletb.2010.04.043](https://doi.org/10.1016/j.physletb.2010.04.043). arXiv: [0904.0938](https://arxiv.org/abs/0904.0938) [[hep-th](#)].
- [61] J. Meibohm and J. M. Pawłowski. “Chiral fermions in asymptotically safe quantum gravity.” In: *Eur. Phys. J. C* 76.5 (2016), p. 285. DOI: [10.1140/epjc/s10052-016-4132-7](https://doi.org/10.1140/epjc/s10052-016-4132-7). arXiv: [1601.04597](https://arxiv.org/abs/1601.04597) [[hep-th](#)].
- [62] A. Eichhorn, A. Held, and J. M. Pawłowski. “Quantum-gravity effects on a Higgs-Yukawa model.” In: *Phys. Rev.* D94.10 (2016), p. 104027. DOI: [10.1103/PhysRevD.94.104027](https://doi.org/10.1103/PhysRevD.94.104027). arXiv: [1604.02041](https://arxiv.org/abs/1604.02041) [[hep-th](#)].
- [63] A. Eichhorn and S. Lippoldt. “Quantum gravity and Standard-Model-like fermions.” In: *Phys. Lett.* B767 (2017), pp. 142–146. DOI: [10.1016/j.physletb.2017.01.064](https://doi.org/10.1016/j.physletb.2017.01.064). arXiv: [1611.05878](https://arxiv.org/abs/1611.05878) [[gr-qc](#)].
- [64] A. Eichhorn, S. Lippoldt, and M. Schiffer. “Zooming in on fermions and quantum gravity.” In: *Phys. Rev. D* 99.8 (2019), p. 086002. DOI: [10.1103/PhysRevD.99.086002](https://doi.org/10.1103/PhysRevD.99.086002). arXiv: [1812.08782](https://arxiv.org/abs/1812.08782) [[hep-th](#)].
- [65] S. Catterall, J. Laiho, and J. Unmuth-Yockey. “Kähler-Dirac fermions on Euclidean dynamical triangulations.” In: *Phys. Rev. D* 98.11 (2018), p. 114503. DOI: [10.1103/PhysRevD.98.114503](https://doi.org/10.1103/PhysRevD.98.114503). arXiv: [1810.10626](https://arxiv.org/abs/1810.10626) [[hep-lat](#)].
- [66] G. P. De Brito et al. “On the impact of Majorana masses in gravity-matter systems.” In: *JHEP* 08 (2019), p. 142. DOI: [10.1007/JHEP08\(2019\)142](https://doi.org/10.1007/JHEP08(2019)142). arXiv: [1905.11114](https://arxiv.org/abs/1905.11114) [[hep-th](#)].
- [67] J. Daas et al. “Asymptotically safe gravity with fermions.” In: *Phys. Lett. B* 809 (2020), p. 135775. DOI: [10.1016/j.physletb.2020.135775](https://doi.org/10.1016/j.physletb.2020.135775). arXiv: [2005.12356](https://arxiv.org/abs/2005.12356) [[hep-th](#)].

- [68] I. L. Buchbinder and E. N. Kirillova. “Phase transitions induced by curvature in the Gross-Neveu model.” In: *Sov. Phys. J.* 32 (1989), pp. 446–450. DOI: [10.1007/BF00898628](https://doi.org/10.1007/BF00898628).
- [69] I. L. Buchbinder and E. N. Kirillova. “Gross-Neveu Model in Curved Space-time: The Effective Potential and Curvature Induced Phase Transition.” In: *Int. J. Mod. Phys.* A4 (1989), pp. 143–149. DOI: [10.1142/S0217751X89000054](https://doi.org/10.1142/S0217751X89000054).
- [70] T. Inagaki, T. Muta, and S. D. Odintsov. “Nambu-Jona-Lasinio model in curved space-time.” In: *Mod. Phys. Lett.* A8 (1993), pp. 2117–2124. DOI: [10.1142/S0217732393001835](https://doi.org/10.1142/S0217732393001835). arXiv: [hep-th/9306023](https://arxiv.org/abs/hep-th/9306023) [hep-th].
- [71] I. Sachs and A. Wipf. “Temperature and curvature dependence of the chiral symmetry breaking in 2-D gauge theories.” In: *Phys. Lett.* B326 (1994), pp. 105–110. DOI: [10.1016/0370-2693\(94\)91200-9](https://doi.org/10.1016/0370-2693(94)91200-9). arXiv: [hep-th/9310085](https://arxiv.org/abs/hep-th/9310085) [hep-th].
- [72] E. Elizalde, S. Leseduarte, and S. D. Odintsov. “Chiral symmetry breaking in the Nambu-Jona-Lasinio model in curved space-time with nontrivial topology.” In: *Phys. Rev.* D49 (1994), pp. 5551–5558. DOI: [10.1103/PhysRevD.49.5551](https://doi.org/10.1103/PhysRevD.49.5551). arXiv: [hep-th/9312164](https://arxiv.org/abs/hep-th/9312164) [hep-th].
- [73] E. Elizalde et al. “Phase structure of renormalizable four fermion models in space-times of constant curvature.” In: *Phys. Rev.* D53 (1996), pp. 1917–1926. DOI: [10.1103/PhysRevD.53.1917](https://doi.org/10.1103/PhysRevD.53.1917). arXiv: [hep-th/9505065](https://arxiv.org/abs/hep-th/9505065) [hep-th].
- [74] S. Kanemura and H.-T. Sato. “Approach to D-dimensional Gross-Neveu model at finite temperature and curvature.” In: *Mod. Phys. Lett.* A11 (1996), pp. 785–794. DOI: [10.1142/S0217732396000795](https://doi.org/10.1142/S0217732396000795). arXiv: [hep-th/9511059](https://arxiv.org/abs/hep-th/9511059) [hep-th].
- [75] T. Inagaki. “Curvature induced phase transition in a four fermion theory using the weak curvature expansion.” In: *Int. J. Mod. Phys.* A11 (1996), pp. 4561–4576. DOI: [10.1142/S0217751X9600211X](https://doi.org/10.1142/S0217751X9600211X). arXiv: [hep-th/9512200](https://arxiv.org/abs/hep-th/9512200) [hep-th].
- [76] T. Inagaki and K.-i. Ishikawa. “Thermal and curvature effects to the dynamical symmetry breaking.” In: *Phys. Rev.* D56 (1997), pp. 5097–5107. DOI: [10.1103/PhysRevD.56.5097](https://doi.org/10.1103/PhysRevD.56.5097).
- [77] G. Miele and P. Vitale. “Three-dimensional Gross-Neveu model on curved spaces.” In: *Nucl. Phys.* B494 (1997), pp. 365–387. DOI: [10.1016/S0550-3213\(97\)00155-7](https://doi.org/10.1016/S0550-3213(97)00155-7). arXiv: [hep-th/9612168](https://arxiv.org/abs/hep-th/9612168) [hep-th].
- [78] P. Vitale. “Temperature induced phase transitions in four fermion models in curved space-time.” In: *Nucl. Phys.* B551 (1999), pp. 490–510. DOI: [10.1016/S0550-3213\(99\)00212-6](https://doi.org/10.1016/S0550-3213(99)00212-6). arXiv: [hep-th/9812076](https://arxiv.org/abs/hep-th/9812076) [hep-th].
- [79] T. Inagaki, T. Muta, and S. D. Odintsov. “Dynamical symmetry breaking in curved space-time: Four fermion interactions.” In: *Prog. Theor. Phys. Suppl.* 127 (1997), p. 93. DOI: [10.1143/PTPS.127.93](https://doi.org/10.1143/PTPS.127.93). arXiv: [hep-th/9711084](https://arxiv.org/abs/hep-th/9711084) [hep-th].
- [80] J. Hashida et al. “Curvature induced phase transitions in the inflationary universe: Supersymmetric Nambu-Jona-Lasinio model in de Sitter space-time.” In: *Phys. Rev.* D61 (2000), p. 044015. DOI: [10.1103/PhysRevD.61.044015](https://doi.org/10.1103/PhysRevD.61.044015). arXiv: [gr-qc/9907014](https://arxiv.org/abs/gr-qc/9907014) [gr-qc].
- [81] E. V. Gorbar and V. P. Gusynin. “Gap generation for Dirac fermions on Lobachevsky plane in a magnetic field.” In: *Annals Phys.* 323 (2008), pp. 2132–2146. DOI: [10.1016/j.aop.2007.11.005](https://doi.org/10.1016/j.aop.2007.11.005). arXiv: [0710.2292](https://arxiv.org/abs/0710.2292) [hep-ph].

- [82] M. Hayashi, T. Inagaki, and H. Takata. “Multi-fermion interaction models in curved spacetime.” In: (2008). arXiv: [0812.0900 \[hep-ph\]](#).
- [83] T. Inagaki and M. Hayashi. “Topological and Curvature Effects in a Multi-fermion Interaction Model.” In: *Strong coupling gauge theories in LHC era. Proceedings, International Workshop, SCGT 09, Nagoya, Japan, December 8-11, 2009*. 2011, pp. 184–190. DOI: [10.1142/9789814329521_0021](#). arXiv: [1003.1173 \[hep-ph\]](#).
- [84] E. V. Gorbar. “Dynamical symmetry breaking in spaces with constant negative curvature.” In: *Phys. Rev. D* 61 (2000), p. 024013. DOI: [10.1103/PhysRevD.61.024013](#). arXiv: [hep-th/9904180 \[hep-th\]](#).
- [85] E. V. Gorbar. “On Effective Dimensional Reduction in Hyperbolic Spaces.” In: *Ukr. J. Phys.* 54 (2009), pp. 541–546. arXiv: [0809.2558 \[hep-th\]](#).
- [86] A. Flachi and K. Fukushima. “Chiral Mass-Gap in Curved Space.” In: *Phys. Rev. Lett.* 113.9 (2014), p. 091102. DOI: [10.1103/PhysRevLett.113.091102](#). arXiv: [1406.6548 \[hep-th\]](#).
- [87] A. Flachi, K. Fukushima, and V. Vitagliano. “Geometrically induced magnetic catalysis and critical dimensions.” In: *Phys. Rev. Lett.* 114.18 (2015), p. 181601. DOI: [10.1103/PhysRevLett.114.181601](#). arXiv: [1502.06090 \[hep-th\]](#).
- [88] Y. Hamada, J. M. Pawłowski, and M. Yamada. “Gravitational instantons and anomalous chiral symmetry breaking.” In: (Sept. 2020). arXiv: [2009.08728 \[hep-th\]](#).
- [89] G. P. de Brito, A. Eichhorn, and M. Schiffer. “Light charged fermions in quantum gravity.” In: *Phys. Lett. B* 815 (2021), p. 136128. DOI: [10.1016/j.physletb.2021.136128](#). arXiv: [2010.00605 \[hep-th\]](#).
- [90] H. Gies and S. Lippoldt. “Renormalization flow towards gravitational catalysis in the 3d Gross-Neveu model.” In: *Phys. Rev. D* 87 (2013), p. 104026. DOI: [10.1103/PhysRevD.87.104026](#). arXiv: [1303.4253 \[hep-th\]](#).
- [91] H. Gies, J. Jaeckel, and C. Wetterich. “Towards a renormalizable standard model without fundamental Higgs scalar.” In: *Phys. Rev. D* 69 (2004), p. 105008. DOI: [10.1103/PhysRevD.69.105008](#). arXiv: [hep-ph/0312034 \[hep-ph\]](#).
- [92] J. Braun, M. Leonhardt, and M. Pospiech. “Fierz-complete NJL model study: Fixed points and phase structure at finite temperature and density.” In: *Phys. Rev. D* 96.7 (2017), p. 076003. DOI: [10.1103/PhysRevD.96.076003](#). arXiv: [1705.00074 \[hep-ph\]](#).
- [93] J. Braun, M. Leonhardt, and M. Pospiech. “Fierz-complete NJL model study. II. Toward the fixed-point and phase structure of hot and dense two-flavor QCD.” In: *Phys. Rev. D* 97.7 (2018), p. 076010. DOI: [10.1103/PhysRevD.97.076010](#). arXiv: [1801.08338 \[hep-ph\]](#).
- [94] J. Braun, M. Leonhardt, and M. Pospiech. “Fierz-complete NJL model study III: Emergence from quark-gluon dynamics.” In: *Phys. Rev. D* 101.3 (2020), p. 036004. DOI: [10.1103/PhysRevD.101.036004](#). arXiv: [1909.06298 \[hep-ph\]](#).
- [95] S.-B. Liao. “On connection between momentum cutoff and the proper time regularizations.” In: *Phys. Rev. D* 53 (1996), pp. 2020–2036. DOI: [10.1103/PhysRevD.53.2020](#). arXiv: [hep-th/9501124 \[hep-th\]](#).

- [96] S.-B. Liao. “Operator cutoff regularization and renormalization group in Yang-Mills theory.” In: *Phys. Rev. D* 56 (1997), pp. 5008–5033. DOI: [10.1103/PhysRevD.56.5008](https://doi.org/10.1103/PhysRevD.56.5008). arXiv: [hep-th/9511046](https://arxiv.org/abs/hep-th/9511046) [hep-th].
- [97] S. Weinberg. “Critical Phenomena for Field Theorists.” In: *Erice Subnucl. Phys. 1976:1*. 1976, p. 1.
- [98] D. Dou and R. Percacci. “The running gravitational couplings.” In: *Class. Quant. Grav.* 15 (1998), pp. 3449–3468. DOI: [10.1088/0264-9381/15/11/011](https://doi.org/10.1088/0264-9381/15/11/011). arXiv: [hep-th/9707239](https://arxiv.org/abs/hep-th/9707239) [hep-th].
- [99] M. Niedermaier and M. Reuter. “The Asymptotic Safety Scenario in Quantum Gravity.” In: *Living Rev. Rel.* 9 (2006), pp. 5–173. DOI: [10.12942/lrr-2006-5](https://doi.org/10.12942/lrr-2006-5).
- [100] D. F. Litim. “Renormalisation group and the Planck scale.” In: *Phil. Trans. Roy. Soc. Lond. A* 369 (2011), pp. 2759–2778. DOI: [10.1098/rsta.2011.0103](https://doi.org/10.1098/rsta.2011.0103). arXiv: [1102.4624](https://arxiv.org/abs/1102.4624) [hep-th].
- [101] R. Percacci. World Scientific, 2017. DOI: [10.1142/9789813207189](https://doi.org/10.1142/9789813207189). eprint: <http://www.worldscientific.com/doi/pdf/10.1142/9789813207189>.
- [102] A. D. Pereira. “Quantum spacetime and the renormalization group: Progress and visions.” In: *Progress and Visions in Quantum Theory in View of Gravity: Bridging foundations of physics and mathematics*. Apr. 2019. arXiv: [1904.07042](https://arxiv.org/abs/1904.07042) [gr-qc].
- [103] M. Reuter and F. Saueressig. *Quantum Gravity and the Functional Renormalization Group: The Road towards Asymptotic Safety*. Cambridge University Press, Jan. 2019.
- [104] N. Dupuis et al. “The nonperturbative functional renormalization group and its applications.” In: *Phys. Rept.* (2021). DOI: [10.1016/j.physrep.2021.01.001](https://doi.org/10.1016/j.physrep.2021.01.001). arXiv: [2006.04853](https://arxiv.org/abs/2006.04853) [cond-mat.stat-mech].
- [105] M. Reichert. “Lecture notes: Functional Renormalisation Group and Asymptotically Safe Quantum Gravity.” In: *PoS* 384 (2020), p. 005. DOI: [10.22323/1.384.0005](https://doi.org/10.22323/1.384.0005).
- [106] J. M. Pawłowski and M. Reichert. “Quantum gravity: a fluctuating point of view.” In: (July 2020). arXiv: [2007.10353](https://arxiv.org/abs/2007.10353) [hep-th].
- [107] R. Percacci and D. Perini. “Constraints on matter from asymptotic safety.” In: *Phys. Rev. D* 67 (2003), p. 081503. DOI: [10.1103/PhysRevD.67.081503](https://doi.org/10.1103/PhysRevD.67.081503). arXiv: [hep-th/0207033](https://arxiv.org/abs/hep-th/0207033) [hep-th].
- [108] A. Codello, R. Percacci, and C. Rahmede. “Investigating the Ultraviolet Properties of Gravity with a Wilsonian Renormalization Group Equation.” In: *Annals Phys.* 324 (2009), pp. 414–469. DOI: [10.1016/j.aop.2008.08.008](https://doi.org/10.1016/j.aop.2008.08.008). arXiv: [0805.2909](https://arxiv.org/abs/0805.2909) [hep-th].
- [109] P. Donà and R. Percacci. “Functional renormalization with fermions and tetrads.” In: *Phys. Rev. D* 87.4 (2013), p. 045002. DOI: [10.1103/PhysRevD.87.045002](https://doi.org/10.1103/PhysRevD.87.045002). arXiv: [1209.3649](https://arxiv.org/abs/1209.3649) [hep-th].
- [110] J. Meibohm, J. M. Pawłowski, and M. Reichert. “Asymptotic safety of gravity-matter systems.” In: *Phys. Rev. D* 93.8 (2016), p. 084035. DOI: [10.1103/PhysRevD.93.084035](https://doi.org/10.1103/PhysRevD.93.084035). arXiv: [1510.07018](https://arxiv.org/abs/1510.07018) [hep-th].
- [111] N. Christiansen et al. “One force to rule them all: asymptotic safety of gravity with matter.” In: (2017). arXiv: [1710.04669](https://arxiv.org/abs/1710.04669) [hep-th].

- [112] Y. Hamada and M. Yamada. “Asymptotic safety of higher derivative quantum gravity non-minimally coupled with a matter system.” In: *JHEP* 08 (2017), p. 070. DOI: [10.1007/JHEP08\(2017\)070](https://doi.org/10.1007/JHEP08(2017)070). arXiv: [1703.09033](https://arxiv.org/abs/1703.09033) [[hep-th](#)].
- [113] A. Eichhorn and A. Held. “Viability of quantum-gravity induced ultraviolet completions for matter.” In: *Phys. Rev. D* 96.8 (2017), p. 086025. DOI: [10.1103/PhysRevD.96.086025](https://doi.org/10.1103/PhysRevD.96.086025). arXiv: [1705.02342](https://arxiv.org/abs/1705.02342) [[gr-qc](#)].
- [114] G. P. De Brito, A. Eichhorn, and A. D. Pereira. “A link that matters: Towards phenomenological tests of unimodular asymptotic safety.” In: *JHEP* 09 (2019), p. 100. DOI: [10.1007/JHEP09\(2019\)100](https://doi.org/10.1007/JHEP09(2019)100). arXiv: [1907.11173](https://arxiv.org/abs/1907.11173) [[hep-th](#)].
- [115] B. Bürger et al. “Curvature dependence of quantum gravity with scalars.” In: (Dec. 2019). arXiv: [1912.01624](https://arxiv.org/abs/1912.01624) [[hep-th](#)].
- [116] A. Eichhorn and M. Pauly. “Constraining power of asymptotic safety for scalar fields.” In: *Phys. Rev. D* 103.2 (2021), p. 026006. DOI: [10.1103/PhysRevD.103.026006](https://doi.org/10.1103/PhysRevD.103.026006). arXiv: [2009.13543](https://arxiv.org/abs/2009.13543) [[hep-th](#)].
- [117] O. Lauscher and M. Reuter. “Flow equation of quantum Einstein gravity in a higher derivative truncation.” In: *Phys. Rev. D* 66 (2002), p. 025026. DOI: [10.1103/PhysRevD.66.025026](https://doi.org/10.1103/PhysRevD.66.025026). arXiv: [hep-th/0205062](https://arxiv.org/abs/hep-th/0205062) [[hep-th](#)].
- [118] A. Codello and R. Percacci. “Fixed points of higher derivative gravity.” In: *Phys. Rev. Lett.* 97 (2006), p. 221301. DOI: [10.1103/PhysRevLett.97.221301](https://doi.org/10.1103/PhysRevLett.97.221301). arXiv: [hep-th/0607128](https://arxiv.org/abs/hep-th/0607128) [[hep-th](#)].
- [119] A. Codello, R. Percacci, and C. Rahmede. “Ultraviolet properties of f(R)-gravity.” In: *Int. J. Mod. Phys. A* 23 (2008), pp. 143–150. DOI: [10.1142/S0217751X08038135](https://doi.org/10.1142/S0217751X08038135). arXiv: [0705.1769](https://arxiv.org/abs/0705.1769) [[hep-th](#)].
- [120] D. Benedetti, P. F. Machado, and F. Saueressig. “Asymptotic safety in higher-derivative gravity.” In: *Mod. Phys. Lett. A* 24 (2009), pp. 2233–2241. DOI: [10.1142/S0217732309031521](https://doi.org/10.1142/S0217732309031521). arXiv: [0901.2984](https://arxiv.org/abs/0901.2984) [[hep-th](#)].
- [121] K. Falls et al. “A bootstrap towards asymptotic safety.” In: (2013). arXiv: [1301.4191](https://arxiv.org/abs/1301.4191) [[hep-th](#)].
- [122] K. Falls et al. “Further evidence for asymptotic safety of quantum gravity.” In: *Phys. Rev. D* 93.10 (2016), p. 104022. DOI: [10.1103/PhysRevD.93.104022](https://doi.org/10.1103/PhysRevD.93.104022). arXiv: [1410.4815](https://arxiv.org/abs/1410.4815) [[hep-th](#)].
- [123] H. Gies et al. “Gravitational Two-Loop Counterterm Is Asymptotically Safe.” In: *Phys. Rev. Lett.* 116.21 (2016), p. 211302. DOI: [10.1103/PhysRevLett.116.211302](https://doi.org/10.1103/PhysRevLett.116.211302). arXiv: [1601.01800](https://arxiv.org/abs/1601.01800) [[hep-th](#)].
- [124] T. Denz, J. M. Pawłowski, and M. Reichert. “Towards apparent convergence in asymptotically safe quantum gravity.” In: (2016). arXiv: [1612.07315](https://arxiv.org/abs/1612.07315) [[hep-th](#)].
- [125] N. Christiansen. “Four-Derivative Quantum Gravity Beyond Perturbation Theory.” In: (2016). arXiv: [1612.06223](https://arxiv.org/abs/1612.06223) [[hep-th](#)].
- [126] A. Eichhorn et al. “Effective universality in quantum gravity.” In: *SciPost Phys.* 5.4 (2018), p. 031. DOI: [10.21468/SciPostPhys.5.4.031](https://doi.org/10.21468/SciPostPhys.5.4.031). arXiv: [1804.00012](https://arxiv.org/abs/1804.00012) [[hep-th](#)].
- [127] K. G. Falls, D. F. Litim, and J. Schröder. “Aspects of asymptotic safety for quantum gravity.” In: *Phys. Rev. D* 99.12 (2019), p. 126015. DOI: [10.1103/PhysRevD.99.126015](https://doi.org/10.1103/PhysRevD.99.126015). arXiv: [1810.08550](https://arxiv.org/abs/1810.08550) [[gr-qc](#)].

- [128] K. Falls, N. Ohta, and R. Percacci. “Towards the determination of the dimension of the critical surface in asymptotically safe gravity.” In: *Phys. Lett. B* 810 (2020), p. 135773. DOI: [10.1016/j.physletb.2020.135773](https://doi.org/10.1016/j.physletb.2020.135773). arXiv: [2004.04126](https://arxiv.org/abs/2004.04126) [hep-th].
- [129] G. Gubitosi et al. “Consistent early and late time cosmology from the RG flow of gravity.” In: *JCAP* 12 (2018), p. 004. DOI: [10.1088/1475-7516/2018/12/004](https://doi.org/10.1088/1475-7516/2018/12/004). arXiv: [1806.10147](https://arxiv.org/abs/1806.10147) [hep-th].
- [130] A. Eichhorn. “An asymptotically safe guide to quantum gravity and matter.” In: *Front. Astron. Space Sci.* 5 (2019), p. 47. DOI: [10.3389/fspas.2018.00047](https://doi.org/10.3389/fspas.2018.00047). arXiv: [1810.07615](https://arxiv.org/abs/1810.07615) [hep-th].
- [131] J. Biemans, A. Platania, and F. Saueressig. “Renormalization group fixed points of foliated gravity-matter systems.” In: *JHEP* 05 (2017), p. 093. DOI: [10.1007/JHEP05\(2017\)093](https://doi.org/10.1007/JHEP05(2017)093). arXiv: [1702.06539](https://arxiv.org/abs/1702.06539) [hep-th].
- [132] I. L. Buchbinder, S. D. Odintsov, and I. L. Shapiro. *Effective action in quantum gravity*. 1992.
- [133] I. L. Shapiro, P. Morais Teixeira, and A. Wipf. “On the functional renormalization group for the scalar field on curved background with non-minimal interaction.” In: *Eur. Phys. J. C* 75 (2015), p. 262. DOI: [10.1140/epjc/s10052-015-3488-4](https://doi.org/10.1140/epjc/s10052-015-3488-4). arXiv: [1503.00874](https://arxiv.org/abs/1503.00874) [hep-th].
- [134] B. S. Merzlikin et al. “Renormalization group flows and fixed points for a scalar field in curved space with nonminimal $F(\phi)R$ coupling.” In: *Phys. Rev. D* 96.12 (2017), p. 125007. DOI: [10.1103/PhysRevD.96.125007](https://doi.org/10.1103/PhysRevD.96.125007). arXiv: [1711.02224](https://arxiv.org/abs/1711.02224) [hep-th].
- [135] A. Bonanno and M. Reuter. “Cosmology with selfadjusting vacuum energy density from a renormalization group fixed point.” In: *Phys. Lett. B* 527 (2002), pp. 9–17. DOI: [10.1016/S0370-2693\(01\)01522-2](https://doi.org/10.1016/S0370-2693(01)01522-2). arXiv: [astro-ph/0106468](https://arxiv.org/abs/astro-ph/0106468).
- [136] A. Bonanno and M. Reuter. “Cosmology of the Planck era from a renormalization group for quantum gravity.” In: *Phys. Rev. D* 65 (2002), p. 043508. DOI: [10.1103/PhysRevD.65.043508](https://doi.org/10.1103/PhysRevD.65.043508). arXiv: [hep-th/0106133](https://arxiv.org/abs/hep-th/0106133).
- [137] B. Guberina, R. Horvat, and H. Stefancic. “Renormalization group running of the cosmological constant and the fate of the universe.” In: *Phys. Rev. D* 67 (2003), p. 083001. DOI: [10.1103/PhysRevD.67.083001](https://doi.org/10.1103/PhysRevD.67.083001). arXiv: [hep-ph/0211184](https://arxiv.org/abs/hep-ph/0211184).
- [138] M. Reuter and F. Saueressig. “From big bang to asymptotic de Sitter: Complete cosmologies in a quantum gravity framework.” In: *JCAP* 09 (2005), p. 012. DOI: [10.1088/1475-7516/2005/09/012](https://doi.org/10.1088/1475-7516/2005/09/012). arXiv: [hep-th/0507167](https://arxiv.org/abs/hep-th/0507167).
- [139] A. Bonanno and A. Platania. “Asymptotically safe inflation from quadratic gravity.” In: *Phys. Lett. B* 750 (2015), pp. 638–642. DOI: [10.1016/j.physletb.2015.10.005](https://doi.org/10.1016/j.physletb.2015.10.005). arXiv: [1507.03375](https://arxiv.org/abs/1507.03375) [gr-qc].
- [140] A. Bonanno and F. Saueressig. “Asymptotically safe cosmology – A status report.” In: *Comptes Rendus Physique* 18 (2017), pp. 254–264. DOI: [10.1016/j.crhy.2017.02.002](https://doi.org/10.1016/j.crhy.2017.02.002). arXiv: [1702.04137](https://arxiv.org/abs/1702.04137) [hep-th].
- [141] A. Bonanno, A. Platania, and F. Saueressig. “Cosmological bounds on the field content of asymptotically safe gravity-matter models.” In: *Phys. Lett. B* 784 (2018), pp. 229–236. DOI: [10.1016/j.physletb.2018.06.047](https://doi.org/10.1016/j.physletb.2018.06.047). arXiv: [1803.02355](https://arxiv.org/abs/1803.02355) [gr-qc].

- [142] A. Platania. “The inflationary mechanism in Asymptotically Safe Gravity.” In: *Universe* 5.8 (2019). Ed. by A. Eichhorn, R. Percacci, and F. Saueressig, p. 189. DOI: [10.3390/universe5080189](https://doi.org/10.3390/universe5080189). arXiv: [1908.03897](https://arxiv.org/abs/1908.03897) [gr-qc].
- [143] A. Platania. “From renormalization group flows to cosmology.” In: *Front. in Phys.* 8 (2020), p. 188. DOI: [10.3389/fphy.2020.00188](https://doi.org/10.3389/fphy.2020.00188). arXiv: [2003.13656](https://arxiv.org/abs/2003.13656) [gr-qc].
- [144] A. Babic et al. “Renormalization-group running cosmologies. A Scale-setting procedure.” In: *Phys. Rev. D* 71 (2005), p. 124041. DOI: [10.1103/PhysRevD.71.124041](https://doi.org/10.1103/PhysRevD.71.124041). arXiv: [astro-ph/0407572](https://arxiv.org/abs/astro-ph/0407572).
- [145] B. Koch, P. Rioseco, and C. Contreras. “Scale Setting for Self-consistent Backgrounds.” In: *Phys. Rev. D* 91.2 (2015), p. 025009. DOI: [10.1103/PhysRevD.91.025009](https://doi.org/10.1103/PhysRevD.91.025009). arXiv: [1409.4443](https://arxiv.org/abs/1409.4443) [hep-th].
- [146] F. Bezrukov, J. Rubio, and M. Shaposhnikov. “Living beyond the edge: Higgs inflation and vacuum metastability.” In: *Phys. Rev. D* 92.8 (2015), p. 083512. DOI: [10.1103/PhysRevD.92.083512](https://doi.org/10.1103/PhysRevD.92.083512). arXiv: [1412.3811](https://arxiv.org/abs/1412.3811) [hep-ph].
- [147] T. W. B. Kibble. “Lorentz invariance and the gravitational field.” In: *J. Math. Phys.* 2 (1961). Ed. by J.-P. Hsu and D. Fine, pp. 212–221. DOI: [10.1063/1.1703702](https://doi.org/10.1063/1.1703702).
- [148] D. W. Sciama. “The Physical structure of general relativity.” In: *Rev. Mod. Phys.* 36 (1964). [Erratum: *Rev. Mod. Phys.* 36, 1103–1103 (1964)], pp. 463–469. DOI: [10.1103/RevModPhys.36.1103](https://doi.org/10.1103/RevModPhys.36.1103).
- [149] K. Krasnov and R. Percacci. “Gravity and Unification: A review.” In: *Class. Quant. Grav.* 35.14 (2018), p. 143001. DOI: [10.1088/1361-6382/aac58d](https://doi.org/10.1088/1361-6382/aac58d). arXiv: [1712.03061](https://arxiv.org/abs/1712.03061) [hep-th].
- [150] K. Krasnov. *Formulations of General Relativity*. Cambridge Monographs on Mathematical Physics. Cambridge University Press, Nov. 2020. DOI: [10.1017/9781108674652](https://doi.org/10.1017/9781108674652).
- [151] J. Ambjorn et al. “Nonperturbative Quantum Gravity.” In: *Phys. Rept.* 519 (2012), pp. 127–210. DOI: [10.1016/j.physrep.2012.03.007](https://doi.org/10.1016/j.physrep.2012.03.007). arXiv: [1203.3591](https://arxiv.org/abs/1203.3591) [hep-th].
- [152] D. Coumbe and J. Laiho. “Exploring Euclidean Dynamical Triangulations with a Non-trivial Measure Term.” In: *JHEP* 04 (2015), p. 028. DOI: [10.1007/JHEP04\(2015\)028](https://doi.org/10.1007/JHEP04(2015)028). arXiv: [1401.3299](https://arxiv.org/abs/1401.3299) [hep-th].
- [153] B. Bahr and S. Steinhaus. “Numerical evidence for a phase transition in 4d spin foam quantum gravity.” In: *Phys. Rev. Lett.* 117.14 (2016), p. 141302. DOI: [10.1103/PhysRevLett.117.141302](https://doi.org/10.1103/PhysRevLett.117.141302). arXiv: [1605.07649](https://arxiv.org/abs/1605.07649) [gr-qc].
- [154] M. Asaduzzaman and S. Catterall. “Euclidean Dynamical Triangulations Revisited.” In: (July 2022). arXiv: [2207.12642](https://arxiv.org/abs/2207.12642) [hep-lat].
- [155] R. Martini, A. Ugelotti, and O. Zanusso. “The Search for the Universality Class of Metric Quantum Gravity.” In: *Universe* 7.6 (2021), p. 162. DOI: [10.3390/universe7060162](https://doi.org/10.3390/universe7060162). arXiv: [2105.11870](https://arxiv.org/abs/2105.11870) [hep-th].
- [156] J. E. Daum and M. Reuter. “Renormalization Group Flow of the Holst Action.” In: *Phys. Lett. B* 710 (2012), pp. 215–218. DOI: [10.1016/j.physletb.2012.01.046](https://doi.org/10.1016/j.physletb.2012.01.046). arXiv: [1012.4280](https://arxiv.org/abs/1012.4280) [hep-th].
- [157] J. E. Daum and M. Reuter. “Einstein-Cartan gravity, Asymptotic Safety, and the running Immirzi parameter.” In: *Annals Phys.* 334 (2013), pp. 351–419. DOI: [10.1016/j.aop.2013.04.002](https://doi.org/10.1016/j.aop.2013.04.002). arXiv: [1301.5135](https://arxiv.org/abs/1301.5135) [hep-th].

- [158] U. Harst and M. Reuter. “A new functional flow equation for Einstein–Cartan quantum gravity.” In: *Annals Phys.* 354 (2015), pp. 637–704. DOI: [10.1016/j.aop.2015.01.006](https://doi.org/10.1016/j.aop.2015.01.006). arXiv: [1410.7003](https://arxiv.org/abs/1410.7003) [hep-th].
- [159] U. Harst and M. Reuter. “On selfdual spin-connections and Asymptotic Safety.” In: *Phys. Lett. B* 753 (2016), pp. 395–400. DOI: [10.1016/j.physletb.2015.12.016](https://doi.org/10.1016/j.physletb.2015.12.016). arXiv: [1509.09122](https://arxiv.org/abs/1509.09122) [hep-th].
- [160] U. Harst and M. Reuter. “The ‘Tetrad only’ theory space: Nonperturbative renormalization flow and Asymptotic Safety.” In: *JHEP* 05 (2012), p. 005. DOI: [10.1007/JHEP05\(2012\)005](https://doi.org/10.1007/JHEP05(2012)005). arXiv: [1203.2158](https://arxiv.org/abs/1203.2158) [hep-th].
- [161] A. Eichhorn. “On unimodular quantum gravity.” In: *Class. Quant. Grav.* 30 (2013), p. 115016. DOI: [10.1088/0264-9381/30/11/115016](https://doi.org/10.1088/0264-9381/30/11/115016). arXiv: [1301.0879](https://arxiv.org/abs/1301.0879) [gr-qc].
- [162] A. Eichhorn. “The Renormalization Group flow of unimodular f(R) gravity.” In: *JHEP* 04 (2015), p. 096. DOI: [10.1007/JHEP04\(2015\)096](https://doi.org/10.1007/JHEP04(2015)096). arXiv: [1501.05848](https://arxiv.org/abs/1501.05848) [gr-qc].
- [163] G. P. de Brito et al. “Can quantum fluctuations differentiate between standard and unimodular gravity?” In: *JHEP* 12 (2021), p. 090. DOI: [10.1007/JHEP12\(2021\)090](https://doi.org/10.1007/JHEP12(2021)090). arXiv: [2105.13886](https://arxiv.org/abs/2105.13886) [gr-qc].
- [164] G. P. de Brito, A. D. Pereira, and A. F. Vieira. “Exploring new corners of asymptotically safe unimodular quantum gravity.” In: *Phys. Rev. D* 103.10 (2021), p. 104023. DOI: [10.1103/PhysRevD.103.104023](https://doi.org/10.1103/PhysRevD.103.104023). arXiv: [2012.08904](https://arxiv.org/abs/2012.08904) [hep-th].
- [165] M. Reuter and H. Weyer. “Background Independence and Asymptotic Safety in Conformally Reduced Gravity.” In: *Phys. Rev. D* 79 (2009), p. 105005. DOI: [10.1103/PhysRevD.79.105005](https://doi.org/10.1103/PhysRevD.79.105005). arXiv: [0801.3287](https://arxiv.org/abs/0801.3287) [hep-th].
- [166] P. F. Machado and R. Percacci. “Conformally reduced quantum gravity revisited.” In: *Phys. Rev. D* 80 (2009), p. 024020. DOI: [10.1103/PhysRevD.80.024020](https://doi.org/10.1103/PhysRevD.80.024020). arXiv: [0904.2510](https://arxiv.org/abs/0904.2510) [hep-th].
- [167] J. A. Dietz and T. R. Morris. “Background independent exact renormalization group for conformally reduced gravity.” In: *JHEP* 04 (2015), p. 118. DOI: [10.1007/JHEP04\(2015\)118](https://doi.org/10.1007/JHEP04(2015)118). arXiv: [1502.07396](https://arxiv.org/abs/1502.07396) [hep-th].
- [168] S. Nagy, K. Sailer, and I. Steib. “Renormalization of Lorentzian conformally reduced gravity.” In: *Class. Quant. Grav.* 36.15 (2019), p. 155004. DOI: [10.1088/1361-6382/ab2e20](https://doi.org/10.1088/1361-6382/ab2e20).
- [169] B. Knorr. “Lessons from conformally reduced quantum gravity.” In: *Class. Quant. Grav.* 38.6 (2021), p. 065003. DOI: [10.1088/1361-6382/abd7c2](https://doi.org/10.1088/1361-6382/abd7c2). arXiv: [2010.00492](https://arxiv.org/abs/2010.00492) [hep-th].
- [170] M. Schaden. “Causal Space-Times on a Null Lattice.” In: (Sept. 2015). arXiv: [1509.03095](https://arxiv.org/abs/1509.03095) [gr-qc].
- [171] M. Asaduzzaman, S. Catterall, and J. Unmuth-Yockey. “Tensor network formulation of two dimensional gravity.” In: *Phys. Rev. D* 102.5 (2020), p. 054510. DOI: [10.1103/PhysRevD.102.054510](https://doi.org/10.1103/PhysRevD.102.054510). arXiv: [1905.13061](https://arxiv.org/abs/1905.13061) [hep-lat].
- [172] V. Vitagliano. “The role of nonmetricity in metric-affine theories of gravity.” In: *Class. Quant. Grav.* 31.4 (2014), p. 045006. DOI: [10.1088/0264-9381/31/4/045006](https://doi.org/10.1088/0264-9381/31/4/045006). arXiv: [1308.1642](https://arxiv.org/abs/1308.1642) [gr-qc].

- [173] F. W. Hehl et al. “Metric affine gauge theory of gravity: Field equations, Noether identities, world spinors, and breaking of dilation invariance.” In: *Phys. Rept.* 258 (1995), pp. 1–171. DOI: [10.1016/0370-1573\(94\)00111-F](https://doi.org/10.1016/0370-1573(94)00111-F). arXiv: [gr-qc/9402012](https://arxiv.org/abs/gr-qc/9402012).
- [174] P. Baekler and F. W. Hehl. “Beyond Einstein-Cartan gravity: Quadratic torsion and curvature invariants with even and odd parity including all boundary terms.” In: *Class. Quant. Grav.* 28 (2011), p. 215017. DOI: [10.1088/0264-9381/28/21/215017](https://doi.org/10.1088/0264-9381/28/21/215017). arXiv: [1105.3504](https://arxiv.org/abs/1105.3504) [[gr-qc](#)].
- [175] I. L. Shapiro. “Physical aspects of the space-time torsion.” In: *Phys. Rept.* 357 (2002), p. 113. DOI: [10.1016/S0370-1573\(01\)00030-8](https://doi.org/10.1016/S0370-1573(01)00030-8). arXiv: [hep-th/0103093](https://arxiv.org/abs/hep-th/0103093).
- [176] D. Sauro and O. Zanusso. “The origin of Weyl gauging in metric-affine theories.” In: *Class. Quant. Grav.* 39.18 (2022), p. 185001. DOI: [10.1088/1361-6382/ac82a2](https://doi.org/10.1088/1361-6382/ac82a2). arXiv: [2203.08692](https://arxiv.org/abs/2203.08692) [[hep-th](#)].
- [177] D. Sauro, R. Martini, and O. Zanusso. “Projective transformations in metric-affine and Weylian geometries.” In: (Aug. 2022). arXiv: [2208.10872](https://arxiv.org/abs/2208.10872) [[hep-th](#)].
- [178] J. F. B. G. et al. “On-shell equivalence of general relativity and Holst theories with nonmetricity, torsion, and boundaries.” In: *Phys. Rev. D* 105.6 (2022), p. 064066. DOI: [10.1103/PhysRevD.105.064066](https://doi.org/10.1103/PhysRevD.105.064066). arXiv: [2201.12141](https://arxiv.org/abs/2201.12141) [[gr-qc](#)].
- [179] U. Ellwanger. “Flow equations for N point functions and bound states.” In: *Z. Phys.* C62 (1994). [206(1993)], pp. 503–510. DOI: [10.1007/BF01555911](https://doi.org/10.1007/BF01555911). arXiv: [hep-ph/9308260](https://arxiv.org/abs/hep-ph/9308260) [[hep-ph](#)].
- [180] M. Bonini, M. D’Attanasio, and G. Marchesini. “Perturbative renormalization and infrared finiteness in the Wilson renormalization group: The Massless scalar case.” In: *Nucl. Phys.* B409 (1993), pp. 441–464. DOI: [10.1016/0550-3213\(93\)90588-G](https://doi.org/10.1016/0550-3213(93)90588-G). arXiv: [hep-th/9301114](https://arxiv.org/abs/hep-th/9301114) [[hep-th](#)].
- [181] N. Ohta, R. Percacci, and A. D. Pereira. “Gauges and functional measures in quantum gravity I: Einstein theory.” In: *JHEP* 06 (2016), p. 115. DOI: [10.1007/JHEP06\(2016\)115](https://doi.org/10.1007/JHEP06(2016)115). arXiv: [1605.00454](https://arxiv.org/abs/1605.00454) [[hep-th](#)].
- [182] N. Ohta, R. Percacci, and A. D. Pereira. “Gauges and functional measures in quantum gravity II: Higher derivative gravity.” In: *Eur. Phys. J. C* 77.9 (2017), p. 611. DOI: [10.1140/epjc/s10052-017-5176-z](https://doi.org/10.1140/epjc/s10052-017-5176-z). arXiv: [1610.07991](https://arxiv.org/abs/1610.07991) [[hep-th](#)].
- [183] G. P. De Brito et al. “Asymptotic safety and field parametrization dependence in the $f(R)$ truncation.” In: *Phys. Rev. D* 98.2 (2018), p. 026027. DOI: [10.1103/PhysRevD.98.026027](https://doi.org/10.1103/PhysRevD.98.026027). arXiv: [1805.09656](https://arxiv.org/abs/1805.09656) [[hep-th](#)].
- [184] K. Groh et al. “Higher Derivative Gravity from the Universal Renormalization Group Machine.” In: *PoS EPS-HEP2011* (2011), p. 124. DOI: [10.22323/1.134.0124](https://doi.org/10.22323/1.134.0124). arXiv: [1111.1743](https://arxiv.org/abs/1111.1743) [[hep-th](#)].
- [185] N. Ohta and R. Percacci. “Higher Derivative Gravity and Asymptotic Safety in Diverse Dimensions.” In: *Class. Quant. Grav.* 31 (2014), p. 015024. DOI: [10.1088/0264-9381/31/1/015024](https://doi.org/10.1088/0264-9381/31/1/015024). arXiv: [1308.3398](https://arxiv.org/abs/1308.3398) [[hep-th](#)].
- [186] S. Sen, C. Wetterich, and M. Yamada. “Asymptotic freedom and safety in quantum gravity.” In: *JHEP* 03 (2022), p. 130. DOI: [10.1007/JHEP03\(2022\)130](https://doi.org/10.1007/JHEP03(2022)130). arXiv: [2111.04696](https://arxiv.org/abs/2111.04696) [[hep-th](#)].

- [187] G. P. De Brito et al. “On the impact of Majorana masses in gravity-matter systems.” In: *JHEP* 08 (2019), p. 142. DOI: [10.1007/JHEP08\(2019\)142](https://doi.org/10.1007/JHEP08(2019)142). arXiv: [1905.11114](https://arxiv.org/abs/1905.11114) [hep-th].
- [188] J. H. Kwapisz. “Asymptotic safety, the Higgs boson mass, and beyond the standard model physics.” In: *Phys. Rev. D* 100.11 (2019), p. 115001. DOI: [10.1103/PhysRevD.100.115001](https://doi.org/10.1103/PhysRevD.100.115001). arXiv: [1907.12521](https://arxiv.org/abs/1907.12521) [hep-ph].
- [189] M. Reichert and J. Smirnov. “Dark Matter meets Quantum Gravity.” In: *Phys. Rev. D* 101.6 (2020), p. 063015. DOI: [10.1103/PhysRevD.101.063015](https://doi.org/10.1103/PhysRevD.101.063015). arXiv: [1911.00012](https://arxiv.org/abs/1911.00012) [hep-ph].
- [190] G. P. de Brito, A. Eichhorn, and R. R. L. d. Santos. “The weak-gravity bound and the need for spin in asymptotically safe matter-gravity models.” In: *JHEP* 11 (2021), p. 110. DOI: [10.1007/JHEP11\(2021\)110](https://doi.org/10.1007/JHEP11(2021)110). arXiv: [2107.03839](https://arxiv.org/abs/2107.03839) [gr-qc].
- [191] A. Eichhorn and M. Schiffer. “ $d = 4$ as the critical dimensionality of asymptotically safe interactions.” In: *Phys. Lett. B* 793 (2019), pp. 383–389. DOI: [10.1016/j.physletb.2019.05.005](https://doi.org/10.1016/j.physletb.2019.05.005). arXiv: [1902.06479](https://arxiv.org/abs/1902.06479) [hep-th].
- [192] C. Laporte et al. “Scalar-tensor theories within Asymptotic Safety.” In: *JHEP* 12 (2021), p. 001. DOI: [10.1007/JHEP12\(2021\)001](https://doi.org/10.1007/JHEP12(2021)001). arXiv: [2110.09566](https://arxiv.org/abs/2110.09566) [hep-th].
- [193] A. Eichhorn, J. H. Kwapisz, and M. Schiffer. “Weak-gravity bound in asymptotically safe gravity-gauge systems.” In: *Phys. Rev. D* 105.10 (2022), p. 106022. DOI: [10.1103/PhysRevD.105.106022](https://doi.org/10.1103/PhysRevD.105.106022). arXiv: [2112.09772](https://arxiv.org/abs/2112.09772) [gr-qc].
- [194] P. F. Machado and F. Saueressig. “On the renormalization group flow of $f(R)$ -gravity.” In: *Phys. Rev. D* 77 (2008), p. 124045. DOI: [10.1103/PhysRevD.77.124045](https://doi.org/10.1103/PhysRevD.77.124045). arXiv: [0712.0445](https://arxiv.org/abs/0712.0445) [hep-th].
- [195] A. Eichhorn and F. Versteegen. “Upper bound on the Abelian gauge coupling from asymptotic safety.” In: *JHEP* 01 (2018), p. 030. DOI: [10.1007/JHEP01\(2018\)030](https://doi.org/10.1007/JHEP01(2018)030). arXiv: [1709.07252](https://arxiv.org/abs/1709.07252) [hep-th].
- [196] A. Eichhorn, A. Held, and C. Wetterich. “Quantum-gravity predictions for the fine-structure constant.” In: (2017). arXiv: [1711.02949](https://arxiv.org/abs/1711.02949) [hep-th].
- [197] D. Oriti and H. Pfeiffer. “Spin foam model for pure gauge theory coupled to quantum gravity.” In: *Physical Review D* 66.12 (2002). DOI: [10.1103/physrevd.66.124010](https://doi.org/10.1103/physrevd.66.124010).
- [198] E. Bianchi et al. “Spinfoam fermions.” In: *Classical and Quantum Gravity* 30.23 (2013), p. 235023. DOI: [10.1088/0264-9381/30/23/235023](https://doi.org/10.1088/0264-9381/30/23/235023).
- [199] S. Steinhaus. “Coupled intertwiner dynamics: A toy model for coupling matter to spin foam models.” In: *Phys. Rev. D* 92.6 (2015), p. 064007. DOI: [10.1103/PhysRevD.92.064007](https://doi.org/10.1103/PhysRevD.92.064007). arXiv: [1506.04749](https://arxiv.org/abs/1506.04749) [gr-qc].
- [200] L. Glaser. “The Ising model coupled to 2d orders.” In: *Class. Quant. Grav.* 35.8 (2018), p. 084001. DOI: [10.1088/1361-6382/aab139](https://doi.org/10.1088/1361-6382/aab139). arXiv: [1802.02519](https://arxiv.org/abs/1802.02519) [gr-qc].
- [201] J. Ambjørn et al. “Matter-driven phase transition in lattice quantum gravity.” In: (Feb. 2021). arXiv: [2103.00198](https://arxiv.org/abs/2103.00198) [hep-th].
- [202] G. Pradisi and A. Salvio. “(In)equivalence of Metric-Affine and Metric Effective Field Theories.” In: (June 2022). arXiv: [2206.15041](https://arxiv.org/abs/2206.15041) [hep-th].
- [203] R. Küspert. “Master thesis.” Jena 2020.

- [204] F. Synatschke et al. “Flow Equation for Supersymmetric Quantum Mechanics.” In: *JHEP* 03 (2009), p. 028. DOI: [10.1088/1126-6708/2009/03/028](https://doi.org/10.1088/1126-6708/2009/03/028). arXiv: [0809.4396](https://arxiv.org/abs/0809.4396) [[hep-th](#)].
- [205] H. Gies, F. Synatschke, and A. Wipf. “Supersymmetry breaking as a quantum phase transition.” In: *Phys. Rev. D* 80 (2009), p. 101701. DOI: [10.1103/PhysRevD.80.101701](https://doi.org/10.1103/PhysRevD.80.101701). arXiv: [0906.5492](https://arxiv.org/abs/0906.5492) [[hep-th](#)].
- [206] F. Synatschke, H. Gies, and A. Wipf. “Phase Diagram and Fixed-Point Structure of two dimensional N=1 Wess-Zumino Models.” In: *Phys. Rev. D* 80 (2009), p. 085007. DOI: [10.1103/PhysRevD.80.085007](https://doi.org/10.1103/PhysRevD.80.085007). arXiv: [0907.4229](https://arxiv.org/abs/0907.4229) [[hep-th](#)].
- [207] M. Heilmann et al. “Phases of supersymmetric O(N) theories.” In: *Phys. Rev. D* 86 (2012), p. 105006. DOI: [10.1103/PhysRevD.86.105006](https://doi.org/10.1103/PhysRevD.86.105006). arXiv: [1208.5389](https://arxiv.org/abs/1208.5389) [[hep-th](#)].
- [208] H. Gies et al. “A functional perspective on emergent supersymmetry.” In: (2017). arXiv: [1705.08312](https://arxiv.org/abs/1705.08312) [[hep-th](#)].

Abdol Sabor Salek

Curriculum Vitae

Personal Details

Gender	male
Date of Birth	01.01.1994
Place of Birth	Kabul, Afghanistan
Citizenship	German

Education

- Oct. 2019 – today **Ph.D. in Physics**, *Friedrich Schiller University*, Jena.
PhD Thesis in Quantum Gravity (Supervisor: Prof. Dr. Holger Gies), funded by the Research Training Group 2522
- Nov. 2021 – Dec. 2021 **Research Stay**, *University of Southern Denmark*, Odense (Denmark).
Research stay during Ph.D. in the Research Group of Prof. Dr. Astrid Eichhorn
- Oct. 2016 – Sep. 2019 **M.Sc. in Physics**, *Goethe University*, Frankfurt (Main), *1.0 (with Distinction)*.
Master Thesis in Theoretical Elementary Particle Physics (Supervisor: Prof. Dr. Dirk Rischke), Minor: Astronomy
- Sabbatical.**
– Sabbatical during M.Sc. from Feb. 2017 to Sep. 2018 for personal reasons –
- Oct. 2013 – Sep. 2016 **B.Sc. in Physics**, *Goethe University*, Frankfurt (Main), *1.3 (Very Good)*.
Bachelor Thesis in Theoretical Condensed Matter Physics (Supervisor: Prof. Dr. Peter Kopietz), Minor: Astronomy
- Aug. 2004 – June 2013 **Abitur**, *Heinrich-von-Kleist-Schule*, Eschborn, *1.5 (Very Good)*.
Advanced Subjects: Mathematics and Physics

Professional Experience

- Oct. 2022 – today **Consultant**, *d-fine GmbH*, Frankfurt (Main).
Management Consultant (IT, Finance, Data Science)
- Oct. 2019 – Sep. 2022 **Research Assistant**, *Friedrich Schiller University*, Jena.
PhD Student & Research Assistant at the Theoretical Physics Institute

- Aug. 2008 – Sep. 2019 **Sales Assistant**, *SWAT e. K.*, Bad Homburg.
Helping out in the Family Store of my Parents
- Oct. 2016 – Sep. 2019 **Teaching Assistant**, *Goethe University*, Frankfurt (Main).
Teaching Assistant for tutorials in Theoretical Physics
- Nov. 2018 – Dec. 2018 **Intern**, *Deutsche Bank A.G.*, Frankfurt (Main).
Intern in the Risk and Return Engineering Team

Languages

Pashto	native
Persian	native
German	native
English	fluent
French	basic

Teaching Experience

- SuSe 2021 (Jena) Quantum Field Theory (Prof. Dr. Holger Gies)
SuSe 2021 (Jena) Theoretical Mechanics (Prof. Dr. Holger Gies)
WiSe 2020/21 (Jena) Particles and Fields (Prof. Dr. Holger Gies)
SuSe 2020 (Jena) Theoretical Mechanics (Prof. Dr. Holger Gies)
SuSe 2019 (Frankfurt) Quantum Mechanics (Prof. Dr. Walter Hofstetter)
WiSe 2018/19 (Frankfurt) Electrodynamics (Prof. Dr. Marc Wagner)
WiSe 2017/18 (Frankfurt) Classical Mechanics (Prof. Dr. Walter Hofstetter)
SuSe 2017 (Frankfurt) Quantum Mechanics (Prof. Dr. Roser Valenti)
WiSe 2016/17 (Frankfurt) Statistical Mechanics (Prof. Dr. Walter Hofstetter)

Talks & Posters

- Sep. 2020 **RTG Combo ***, Leipzig (Germany).
Talk: "Curvature bound from gravitational catalysis in thermal backgrounds"
- Oct. 2020 **Quantum Spacetime and the Renormalization Group ***, Odense (Denmark).
Poster: "Curvature bound from gravitational catalysis in thermal backgrounds"
- Nov. 2020 **Exact Renormalization Group 2020 ***, Kyoto (Japan).
Talk: "Curvature bound from gravitational catalysis in thermal backgrounds"
- May 2021 **Asymptotic Safety Online Seminar**, Online.
Talk: "Curvature bound from gravitational catalysis in thermal backgrounds"

- Sep. 2021 **RTG Combo ***, Leipzig (Germany).
Talk: "Asymptotically safe Einstein-Palatini gravity"
- Nov. 2021 **Quantum Gravity Group Seminar**, Odense (Denmark).
Talk: "Asymptotically safe Einstein-Palatini gravity"
- July 2022 **Exact Renormalization Group 2022**, Berlin (Germany).
Poster: "Asymptotically safe Hilbert-Palatini gravity"

*The participation in the events marked with * was online due to the COVID-19 pandemic.*

Publications

- [1] Holger Gies and Abdol Sabor Salek. Curvature bound from gravitational catalysis in thermal backgrounds. *Phys. Rev. D*, 103(12):125027, 2021. arXiv:2103.05542, doi:10.1103/PhysRevD.103.125027.
- [2] Holger Gies and Abdol Sabor Salek. Asymptotically safe Hilbert–Palatini gravity in an on-shell reduction scheme. *Eur. Phys. J. C*, 83(2):173, 2023. arXiv:2209.10435, doi:10.1140/epjc/s10052-023-11324-1.

Ehrenwörtliche Erklärung

Ich erkläre hiermit ehrenwörtlich, dass ich die vorliegende Arbeit selbständig, ohne unzulässige Hilfe Dritter und ohne Benutzung anderer als der angegebenen Hilfsmittel und Literatur angefertigt habe.

Die aus anderen Quellen direkt oder indirekt übernommenen Daten und Konzepte sind unter Angabe der Quelle gekennzeichnet. Bei der Auswahl und Auswertung folgenden Materials haben mir die nachstehend aufgeführten Personen in der jeweils beschriebenen Weise entgeltlich/unentgeltlich geholfen:

1. Holger Gies bei den in Kapiteln 5, 6 und 7 präsentierten Ergebnissen, basierend auf [23] und [24].

Weitere Personen waren an der inhaltlich-materiellen Erstellung der vorliegenden Arbeit nicht beteiligt. Insbesondere habe ich hierfür nicht die entgeltliche Hilfe von Vermittlungs- bzw. Beratungsdiensten (Promotionsberater oder andere Personen) in Anspruch genommen.

Niemand hat von mir unmittelbar oder mittelbar geldwerte Leistungen für Arbeiten erhalten, die im Zusammenhang mit dem Inhalt der vorgelegten Dissertation stehen.

Die Arbeit wurde bisher weder im In- noch im Ausland in gleicher oder ähnlicher Form einer anderen Prüfungsbehörde vorgelegt.

Die geltende Promotionsordnung der Physikalisch-Astronomischen Fakultät ist mir bekannt.

Ich versichere ehrenwörtlich, dass ich nach bestem Wissen die reine Wahrheit gesagt und nichts verschwiegen habe.

Ort, Datum

Unterschrift d. Verfassers

